

ANKARA YILDIRIM BEYAZIT UNIVERSITY
GRADUATE SCHOOL OF NATURAL AND APPLIED SCIENCES



**DESIGN AND DEVELOPMENT OF A NOVEL PHOTOVOLTAIC
SYSTEM WITH REFLECTORS AND A SUN TRACKER**

M.Sc. Thesis by

Mustafa Latif OBANKAYA

Department of Electrical and Electronics Engineering

August 2017

ANKARA

**DESIGN AND DEVELOPMENT OF A NOVEL
PHOTOVOLTAIC SYSTEM WITH REFLECTORS
AND A SUN TRACKER**

A Thesis Submitted to the

Graduate School of Natural and Applied Sciences of

Ankara Yıldırım Beyazıt University

**In Partial Fulfillment of the Requirements for the Master of Science in
Electrical and Electronics Engineering, Department of Electrical and
Electronics Engineering**

by

Mustafa Latif ÇOBANKAYA

August 2017

ANKARA

M.Sc. THESIS EXAMINATION RESULT FORM

We have read the thesis entitled “**DESIGN AND DEVELOPMENT OF A NOVEL PHOTOVOLTAIC SYSTEM WITH REFLECTORS AND A SUN TRACKER**” completed by **MUSTAFA LATİF ÇOBANKAYA** under supervision of **PROF. DR. ŞERAFETTİN EREL** and we certify that in our opinion it is fully adequate, in scope and in quality, as a thesis for the degree of Master of Science.

Prof. Dr. Şerafettin EREL

Supervisor

Yrd. Doç. Dr. Mustafa Yağcı

Jury Member

Yrd. Doç. Dr. Serdar ÖZYURT

Jury Member

Prof. Dr. Fatih V. ÇELEBİ

Director

Graduate School of Natural and Applied Sciences

ETHICAL DECLARATION

I hereby declare that, in this thesis which has been prepared in accordance with the Thesis Writing Manual of Graduate School of Natural and Applied Sciences,

- All data, information and documents are obtained in the framework of academic and ethical rules,
- All information, documents and assessments are presented in accordance with scientific ethics and morals,
- All the materials that have been utilized are fully cited and referenced,
- No change has been made on the utilized materials,
- All the works presented are original,

and in any contrary case of above statements, I accept to renounce all my legal rights.

ACKNOWLEDGMENTS

I would like to express my gratitude to my supervisor, Prof. Dr. Şerafettin EREL for his continuous support and motivation during my study. His knowledge, invaluable experiences and priceless advices constructed the milestones of my thesis study. It was a pleasure to work with him.

I express my sincere love and special thanks to my mother and father, to my wife and brothers for their sincere prayers, supports, courage and patience for me.

Lastly, the greatest gratitude of my heart and all my praise belong to my Compassionate Creator for all his bounties.

2017, 25 August

Mustafa Latif ÇOBANKAYA

DESIGN AND DEVELOPMENT OF A NOVEL PHOTOVOLTAIC SYSTEM WITH REFLECTORS AND A SUN TRACKER

ABSTRACT

In this thesis study, as a new method, design and development of a double surface photovoltaic system with reflection property was aimed. In the direction of this purpose, the thesis study was completed within three stages as design, development, and performance measurements.

The double surface panel system was designed completely as the first stage of the thesis study. A single axis sun tracking system, a reflector system for the back panel, two solar panels placed back to back, and suitable platforms were planned.

In the development stage, two opto-electronically controlled reflectors with the ability to rotate around their own axes were used to illuminate the back solar panel. Thus, the system was optimized in the way that equal amount of light fluxes irradiates the front and back panels. The system was supported by the optoelectronic based single axis sun tracker to increase working performance.

Measurements of the developed system were done in laboratory settings and on open field as real time. The results showed that the back solar panel produces sufficient amount of electricity and the system works under proper angular conditions.

It is concluded that the system developed as a prototype might be used in industrial applications.

Keywords: Solar cell, dual surface solar panel, solar tracking system, photovoltaic system.

YANSITMALI VE GÜNEŞ İZLEYİCİLİ YENİ BİR FOTOVOLTAİK SİSTEMİN TASARIMI VE GELİŞTİRİLMESİ

ÖZ

Bu tez çalışmasında, yeni bir yöntem olarak çift yüzeyli, yansıtmalı fotovoltaik bir sistemin tasarımı ve geliştirilmesi hedeflenmiştir. Bu hedef doğrultusunda, tez çalışması tasarım, geliştirme ve performans ölçümleri olarak üç temel aşamada tamamlanmıştır.

Tezin ilk aşaması olarak çift yüzeyli güneş panel sisteminin tasarımı tamamlanmıştır. Tasarımda tek eksenli bir güneş izleme sistemi, arka panel için bir yansıtıcı sistem, sırt sırta yerleştirilen iki güneş paneli ve uygun platformlar planlanmıştır.

Geliştirme aşamasında arka yüzeydeki güneş panelini aydınlatmak için optoelektronik olarak kontrol edilen iki adet kendi eksenini etrafında dönebilen reflektör kullanılmıştır. Böylece ön ve arka yüzeydeki güneş panellerine eşit miktarda ışık akısı düşecek şekilde sistem optimize edilmiştir. Çalışma performansını artırmak için optoelektronik temelli, tek eksenli güneş izleyicisi yardımıyla sistem desteklenmiştir.

Geliştirilen sistemin laboratuvar şartlarında ve açık alanda gerçek zamanlı olarak ölçümleri yapılmıştır. Sonuçlar, uygun açılarda arka güneş panelinin yeterli miktarda elektrik ürettiğini ve sistemin çalıştığını göstermektedir.

Prototip olarak geliştirilen çift yüzeyli sistemin endüstriyel alandaki uygulamalarda kullanılabileceği sonucuna varılmıştır.

Anahtar Kelimeler: Güneş hücresi, çift yüzeyli güneş paneli, güneş takip sistemi, fotovoltaik sistem.

CONTENTS

M.Sc. THESIS EXAMINATION RESULT FORM	ii
ETHICAL DECLARATION	iii
ACKNOWLEDGMENTS	iv
ABSTRACT	v
ÖZ.....	vi
NOMENCLATURE.....	ix
LIST OF TABLES	x
LIST OF FIGURES	xii
CHAPTER 1	1
INTRODUCTION.....	1
1.1 Photovoltaic Systems and Solar Cells	1
1.1.1 Silicon Solar Cells	11
1.1.1.1 Monocrystalline Silicon Solar Cells.....	11
1.1.1.2 Polycrystalline Silicon Solar Cells	12
1.1.1.3 Amorphous Silicon Solar Cells	13
1.1.2 Other Solar Cell Types	13
1.2 Maximum Power Point Tracking	15
1.2.1 Maximum Power Point	15
1.2.2 Fill Factor.....	16
1.3 Sun Tracking Systems	17
1.3.1 Passive Tracking Systems.....	21
1.3.2 Active Tracking Systems	23
1.3.2.1 Electro-Optical (Real Time) Tracking Systems	24
1.3.2.2 Timing Based Tracking Systems.....	29
1.3.2.3 Auxiliary Bifacial Solar Cell Based Tracking Systems	33
1.3.2.4 Combinations of Three Types of Tracking Systems	35
1.4 Storage of Surplus Electricity.....	37
CHAPTER 2	38
EXPERIMENTAL PROCEDURE.....	38
2.1 Equipment Used in the Experiment.....	38

2.1.1	Reflectors	40
2.1.2	Solar Panels.....	41
2.1.3	Pulley Systems	42
2.1.4	Geared Motor for Solar Tracking	43
2.1.5	Geared Motor for the Motion of the Reflectors	44
2.1.6	12V-Battery	45
2.1.7	Single Axis Solar Tracker Circuits	45
2.1.8	Lux Meter	50
2.1.9	Light Source.....	52
2.2	Measurements Done in the Experiment	53
CHAPTER 3		55
EXPERIMENTAL RESULTS.....		55
3.1	Laboratory Measurements	55
3.1.1	Laboratory MPP Measurement Values in Tables	55
3.1.2	Laboratory MPP Measurement Results	62
3.1.3	Laboratory Simulation Measurement Values in Tables	69
3.1.4	Laboratory Simulation Measurement Results.....	72
3.2	Real Time Measurements	77
3.2.1	Real Time MPP Measurement Values in Tables	78
3.2.2	Real Time MPP Measurement Results	80
3.2.3	Real Time Hour-Based Measurement Values in Tables.....	82
3.2.4	Real Time Hour-Based Measurement Results.....	86
CHAPTER 4		93
DISCUSSION AND CONCLUSION		93
REFERENCES.....		95
CURRICULUM VITAE.....		118

NOMENCLATURE

Acronyms

AC	Alternating Current
A/D	Analog-to-Digital
BOS	Balance of System
CIGS	Copper-Indium-Gallium-Selenium
CIS	Copper Indium Diselenide
CSE	Concentrated Solar Energy
DC	Direct Current
DSSC	Dye-Sensitized Solar Cell
EEPROM	Electrically Erasable Programmable Read-Only Memory
FF	Fill Factor
FL	Fuzzy Logic
LDR	Light Dependent Resistor
MPP	Maximum Power Point
MPPT	Maximum Power Point Tracking
OPAMP	Operational Amplifier
PC	Personal Computer
PIC	Programmable Interface Controller
PLA	Programmable Logic Array
PLC	Programmable Logic Controller
PTC	Parabolic Trough Collector
PV	Photovoltaic
SBC	Schlumberger Business Consulting
STC	Solar Thermal Collectors
VR	Virtual Reality

LIST OF TABLES

Table 1.1 PV modules solar-to-electrical power conversion efficiencies	4
Table 1.2 Solar cell types and their recorded properties	14
Table 2.1 Reflection ratio of the reflectors.....	40
Table 2.2 Visible light spectrum	51
Table 3.1 Lab MPP measurement values of back-side panel for 50cm distance	56
Table 3.2 Lab MPP measurement values of front-side panel for 50cm distance	57
Table 3.3 Lab MPP measurement values of back-side panel for 70cm distance	58
Table 3.4 Lab MPP measurement values of front-side panel for 70cm distance	59
Table 3.5 Lab MPP measurement values of back-side panel for 1m distance	60
Table 3.6 Lab MPP measurement values of front-side panel for 1m distance.....	61
Table 3.7 Lab measurement results of back-side panel: Tracking system with 30° of tilt angle.....	69
Table 3.8 Lab measurement results of front-side panel: Tracking system with 30° of tilt angle.....	70
Table 3.9 Lab measurement results of back-side panel: Tracking system with 45° of tilt angle.....	70
Table 3.10 Lab measurement results of front-side panel: Tracking system with 45° of tilt angle.....	71
Table 3.11 Lab measurement results of back-side panel: Fixed system with 30° of tilt angle	71
Table 3.12 Lab measurement results of front-side panel: Fixed system with 30° of tilt angle	72
Table 3.13 Real time MPP measurement values of back-side panel.....	78
Table 3.14 Real time MPP measurement values of front-side panel	79
Table 3.15 Real time measurement values of back-side panel: Fixed system with 30° tilt angle.....	82
Table 3.16 Real time measurement values of front-side panel: Fixed system with 30° tilt angle.....	83
Table 3.17 Real time measurement values of back-side panel: Tracking system with 30° tilt angle	83
Table 3.18 Real time measurement values of front-side panel: Tracking system with 30° tilt angle	84
Table 3.19 Real time measurement values of back-side panel: Fixed system with 45° tilt angle.....	84
Table 3.20 Real time measurement values of front-side panel: Fixed system with 45° tilt angle.....	85

Table 3.21 Real time measurement values of back-side panel: Tracking system with 45° tilt angle85

Table 3.22 Real time measurement values of front-side panel: Tracking system with 45° tilt angle86



LIST OF FIGURES

Figure 1.1 Global solar radiance	2
Figure 1.2 Average cost of crystalline silicon PV cells per watt between 1977 and 2015	3
Figure 1.3 Total obtained global energy by PV systems	5
Figure 1.4 Predicted PV electricity generation in the future	5
Figure 1.5 Solar radiation spectrum	6
Figure 1.6 A typical PV system	8
Figure 1.7 PV cell types based on used material	9
Figure 1.8 Production of PV cell types over years	10
Figure 1.9 Monocrystalline (left) and polycrystalline (right) solar cells	12
Figure 1.10 Example of an I-V curve	15
Figure 1.11 I–V photovoltaic characteristic for four different irradiation levels.....	16
Figure 1.12 Fill factor calculated by P_{MAX}/P_T	17
Figure 1.13 Effect of sun tracking systems on efficiency	19
Figure 1.14 Direct insolation area vs angle of incidence	20
Figure 1.15 Solar irradiation types reaching a PV system	20
Figure 1.16 Effect of the sunlight incidence on output power of a solar panel	21
Figure 1.17 A passive solar tracker using two identical cylindrical tubes filled with a fluid under partial pressure	22
Figure 1.18 Sunlight pointing methods for getting more precise results	24
Figure 1.19 Experimental total solar radiation vs. time	27
Figure 1.20 Three tracking systems simulated by Alate et al.	31
Figure 1.21 Schematic representation of solar angles used in the study	31
Figure 1.22 Scheme of the space tracker on a satellite	33
Figure 1.23 Polar axis tracker built by Poulek & Libra	34
Figure 2.1 The completed photovoltaic system	39
Figure 2.2 Back and front sides of the solar panels	41
Figure 2.3 The pulley system for solar tracking	42
Figure 2.4 The pulley system for controlling the reflectors	43
Figure 2.5 The geared motor used for the sun tracking with Its wheel	43
Figure 2.6 The motor used for angular control of the reflectors	44
Figure 2.7 12V 1.3Ah/20hr battery used as a power supply in the experiment.....	45

Figure 2.8 Rotational angle, θ of the sun tracking system in cylindrical (θ) and spherical (φ) coordinate systems	46
Figure 2.9 Schematic diagram of the solar tracker	47
Figure 2.10 LDRs positioned for accurate following of the sun	47
Figure 2.11 LDRs for control of the reflectors.....	48
Figure 2.12 The solar tracker used for controlling angular positions of the reflectors	49
Figure 2.13 The solar tracker used for following the sun during daytimes	49
Figure 2.14 The lux meter used in the experiment.....	50
Figure 2.15 Spectral sensitivity of the lux meter	51
Figure 2.16 The light source used in the experiment	52
Figure 2.17 Measurements done on the solar panel system in laboratory	53
Figure 2.18 Real time measurements	54
Figure 3.1 I-V graphs of front panel for 50, 70 and 100 cm distances	62
Figure 3.2 P-V graphs of front panel for 50, 70 and 100 cm distances.....	62
Figure 3.3 I-V graphs of back panel for 50, 70 and 100 cm distances.....	63
Figure 3.4 P-V graphs of back panel for 50, 70 and 100 cm distances.....	65
Figure 3.5 I-V graphs of front and back panels for 50 cm distance	65
Figure 3.6 P-V graphs of front and back panels for 50 cm distance	66
Figure 3.7 I-V graphs of front and back panels for 70 cm distance	66
Figure 3.8 P-V graphs of front and back panels for 70 cm distance	67
Figure 3.9 I-V graphs of front and back panels for 100 cm distance	68
Figure 3.10 P-V graphs of front and back panels for 100 cm distance	68
Figure 3.11 P- θ graphs of front panel for 30° tilted-tracking, 45° tracking and 30° fixed systems.....	73
Figure 3.12 P- θ graphs of back panel for 30° tilted-tracking, 45° tracking and 30° fixed systems	74
Figure 3.13 P- θ graphs of front and back panels for 30° tilted-fixed system	75
Figure 3.14 P- θ graphs of front and back panels for 30° tilted-tracking system.....	75
Figure 3.15 P- θ graphs of front and back panels for 45° tilted-tracking system.....	76
Figure 3.16 Power-Light flux graph of front panel for 30° tilted-tracking system...	76
Figure 3.17 Power-Light flux graph of back panel for 30° tilted-tracking system...	77
Figure 3.18 I-V graphs of front and back panels	80
Figure 3.19 P-V graphs of front and back panels	81

Figure 3.20 Power-Hour graphs of front and back panels for 30°-tilted tracking system	87
Figure 3.21 Power-Hour graphs of front and back panels for 30°-tilted fixed system	87
Figure 3.22 Partial shading seen on back solar panel	88
Figure 3.23 Reflector system with proper angle (left) and without proper angle (right)	89
Figure 3.24 Power-Hour graphs of front and back panels for 45°-tilted tracking system	89
Figure 3.25 Power-Hour graphs of front and back panels for 45°-tilted fixed system	90
Figure 3.26 Power-Hour graphs of tracking vs. fixed systems of front panel for 30°-tilted case.....	90
Figure 3.27 Power-Hour graphs of tracking vs. fixed systems of front panel for 45°-tilted case.....	91
Figure 3.28 Power-Hour graphs of 30°-tilted vs. 45°-tilted tracking systems of front panel	92
Figure 3.29 Power-Hour graphs of 30°-tilted vs. 45°-tilted fixed systems of front panel	92

CHAPTER 1

INTRODUCTION

Renewable energy systems are developing fast in recent years. As being environment friendly, renewable systems are preferred by various energy producers. As renewable energy systems, solar systems, wind power systems, tidal power systems, geothermal energy systems are considered. The most important type among these renewable energy systems is solar energy systems.

Photovoltaic (PV) systems are used in many different areas. They are used in space applications, electricity production, hydrogen production, solar dryers, space heating and water heating systems. Most of established systems are used in electricity production [1]. Some of these applications are used as hybrid systems of solar thermal systems and electrical photovoltaic (PV) systems such as, space heating systems, water heating systems, and solar dryers.

1.1 Photovoltaic Systems and Solar Cells

The earth takes every year 124 exa (10^{18}) Watts of average power or 3,850 zetta (10^{24}) Joules of solar energy. Moreover, this is only the energy reaching to the surface [2]. This huge power shall be utilized by humanity through solar cells. Figure 1.1 shows the global solar energy potential. For the countries which have high values of sunshine duration, solar energy systems are more profitable.

Solar systems produce two types of energy: Heat and Electricity. Solar heating systems vary from water heaters [3-8] to cookers [9-12], from driers [13-16], air-conditioning [17-21] and chimneys [22-24] to ponds [25-28] and solar architectures [29-31].

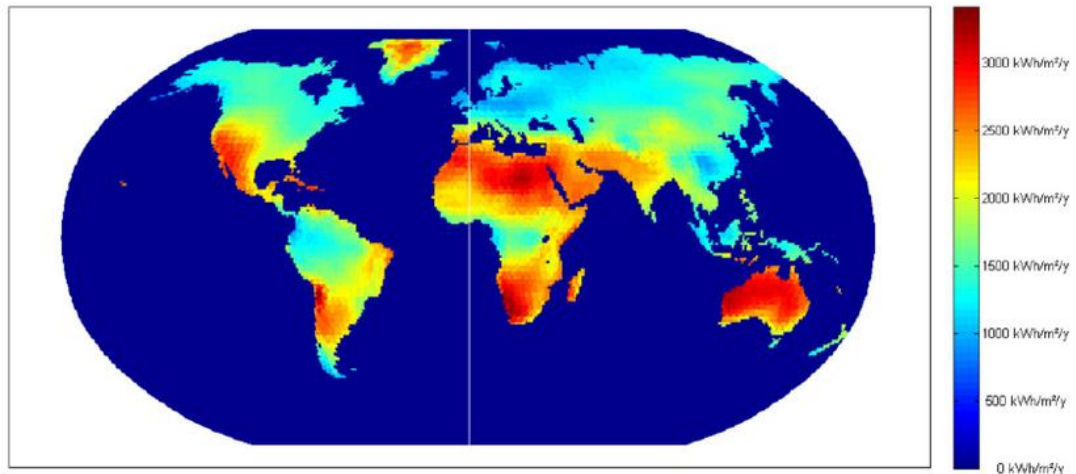


Figure 1.1 Global solar radiance [32]

Photovoltaic systems produce electrical energy from the sunlight. Therefore, they are called photo-voltaic energy systems. Other types of solar energy sources are solar thermal systems and hybrid systems of these two types.

As an important part of solar energy systems, photovoltaic systems are investigated in terms of the categories of being environment friendly (green and clean), sustainability, and efficiency in the following pages.

Being green and clean: Being green and clean, in other words being environment friendly is an important property today because dangers and effects of global warming have been increasing over years. Regarding the increasing dangerous results of global warming, green energy sources have become more important and more admirable for the world today.

During the operation of solar systems, no air pollution and no harmful environmental effects occur. However, this does not mean any pollution effects do not occur during the life cycle of solar cells [33]. The production and assembly of solar cells, balance of system (BOS) production, solar cell system installation and retrofitting, system disposal and recycling have some pollution effects [34]. Still, these steps are needed only once and huge amounts of pollution are not seen; therefore, they are ignorable. Thus, comparing other energy production techniques, solar systems are much cleaner and environment friendly. They are much preferable from this aspect.

Sustainability: Considering energy shortage coming from conventional energy sources, as an important sustainable energy type, solar systems come into mind.

In the past, solar systems were not commonly used and did not spread over the world. The main reason for slow development of solar systems was high investment cost. Especially in early times of solar cells, it was too high for investment but the costs had a fast reduction. The cost of a solar cell has pretty much reduced from 1980s to 1990s [35] and to the present, and are continuing to decrease. Figure 1.2 shows the reduction on silicon PV cells from 1977 to 2015.

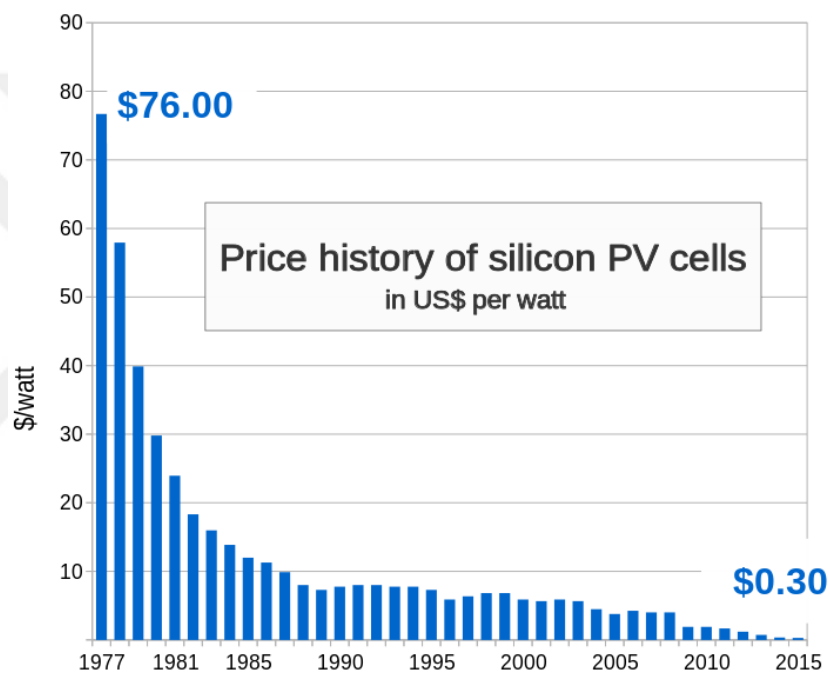


Figure 1.2 Average cost of crystalline silicon PV cells per watt between 1977 and 2015 [36].

The most appropriate places for photovoltaic systems seem to be isolated places like Sahara Desert and other deserts, archipelagos, remote areas, mountainous locations, rural areas etc. [37]. In these areas, solar systems operate for many years and yield high amounts of profit.

Efficiency: Efficiency of conversion of solar energy to electrical energy changes according to the material used in PV cells and technology. Nevertheless, one of the main obstacles towards development of solar cells is efficiency since it is generally less than or about 20% in practical installations.

There is some historical development about efficiencies of solar cell types. For instance, efficiency of polycrystalline silicon solar cells was 8% in 1980, then increased to 12% in 1984, it increased to 13% in 1985 and increased to more than 30% in 1990s in laboratory studies [38, 39]. These results, of course, laboratory results and therefore, cannot give the exact information about real life applications. Table 1.1 compares and gives better information to see the real-life implementations and laboratory studies together.

Table 1.1 PV modules solar-to-electrical power conversion efficiencies [40]

PV Module Type	Practice Module Efficiency (%)	Lab Efficiency (%)
Dye-sensitized solar cells	3-5	11
Amorphous silicon (multijunction)	6-8	13.2
Cadmium Telluride (CdTe) thin film	8-10	16.5
Copper-Indium-Gallium-Selenium (CIGS)	9-11	19.5
Polycrystalline silicon	12-15	20.3
Monocrystalline silicon	14-16	21.6
High performance monocrystalline silicon	16-18	24.7
Triple-junction (GaInP/GaAs/Ge) cell	---	39.0

As it is seen from Table 1.1, most of the laboratory results have almost twofold efficiencies of the installed solar systems. The main target is to increase the efficiencies in real life systems and they are less than 20% in most of the applications.

One can easily understand that the low efficiency condition is one of the factors which prevent widespread use of solar cells. Nevertheless, production and usage of solar cells has been spreading over years under favor of the other positive properties which were mentioned.

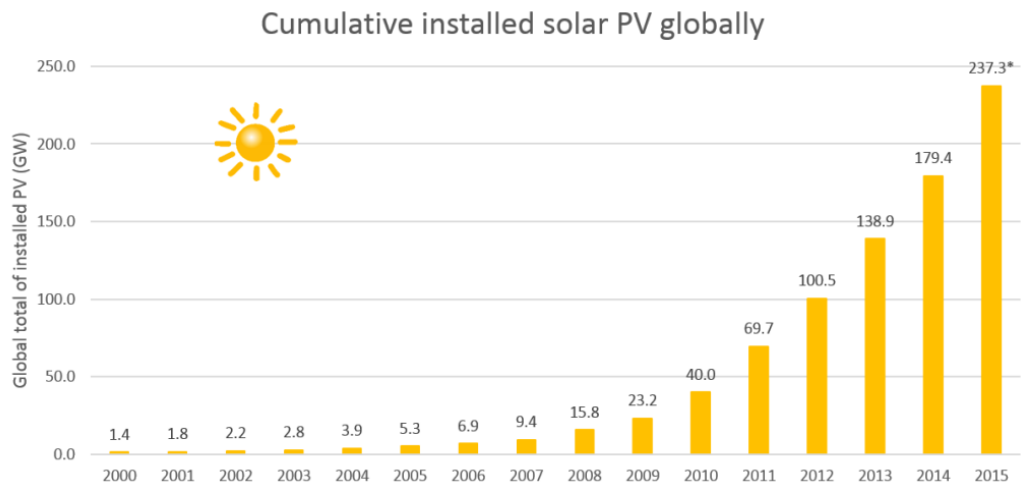


Figure 1.3 Total obtained global energy by PV systems [41]

The information in Figure 1.3 is total global installation of the solar systems. Even annual installation has been increasing year by year in a semi-logarithmic-similar scale. The total installed solar systems can be considered as a complete semi-logarithmic scale. In the future, it is predicted that both cumulative solar production and percentage share of PV systems in global electricity generation will increase more. As it is shown in Figure 1.4, while the percentage of PV electricity generation over global produced electricity is less than 1% today, it will be more than 10% by 2050 in this realistic prediction.

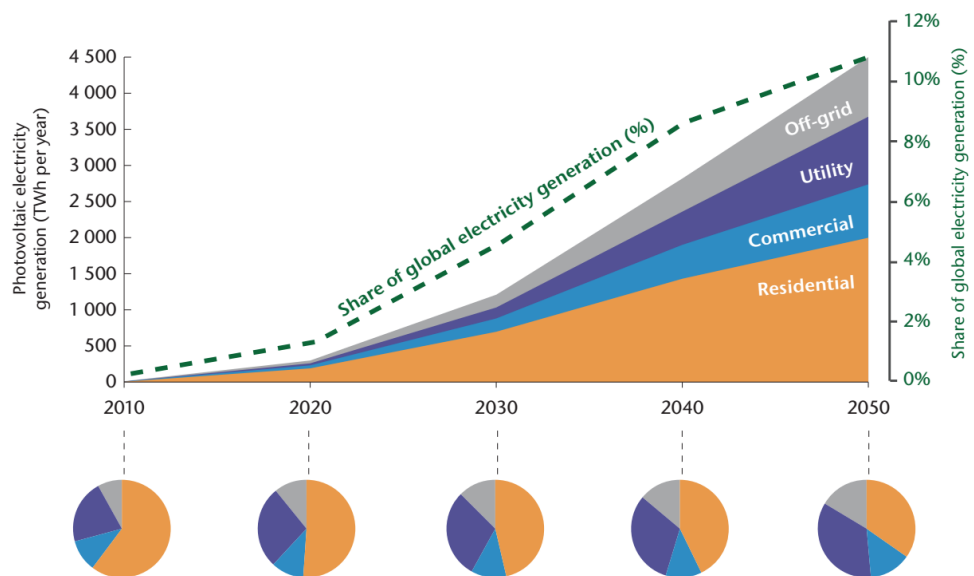


Figure 1.4 Predicted PV electricity generation in the future [42]

Within the photovoltaic energy systems, the most common type is residential installed system. Since they do not require a land, investment costs reduce and they are more preferred than the other types. The other important PV energy systems types are off-grid systems, utility systems and commercially established systems by solar companies. Off-grid systems are not connected to electricity distribution networks. They are used for supplying electricity of small local places. Utility systems are also commonly used. They are used in some of road lamps, traffic lights and lighting systems in various places.

Working principles of solar cells are categorized mainly into two: The principles in solar-thermal cells and PV cells. The working principles of solar thermal cells include heating of a fluid. Then, the thermal energy inside the fluid is converted to other energy types, like mechanical or electrical energies or is not converted but directly used as a heating source. On the other side, PV cells convert the solar energy directly to electricity through semiconductors.

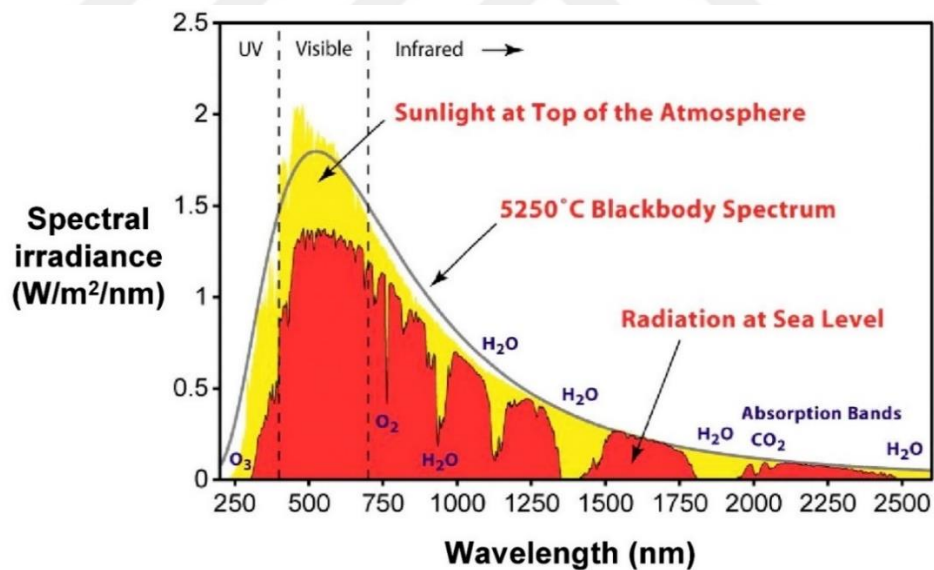


Figure 1.5 Solar radiation spectrum [43]

Solar radiation intensifies at visible light spectrum as seen in Figure 1.5. Also, there is a small part in ultraviolet and a wide part in infrared spectrums. Therefore, the solar cells used for electricity production are chosen to be proper with this sunlight spectrum. In other words, band gap of the solar cell must be appropriate with the

sunlight for electricity production. If the band gap is small, the efficiency is decreases and the extra light energy is converted to heat energy; therefore, extensive heating may occur in solar cells. On the other hand, if the bang gap is higher than the sufficient level, again efficiency decreases because the energy of the sunlight becomes not enough to activate electrons for electricity production. As a result, a good band gap selection is one of the factors affecting operation of solar cells. Generally, silicon is one of the preferred semiconductors for the operation since it has 1.1eV of band gap which is appropriate to the sunlight energy.

About solar thermal cells, there are some beneficial reviews to utilize [44-52]. In [44], a good and short summary is given about solar cell types which are stationary and tracking solar heaters. Also, performance enhancement techniques of solar collectors are explained within three main stages which are geometrical arrangements, solar selective coatings and nanofluids.

Categorization of the solar cells may vary according to the references or criteria. Referring a study [53], solar energy utilizers can be categorized into four, as 1- Photovoltaic cells, 2-Solar thermal collectors (STC), 3-Concentrated solar energy (CSE), and 4-Hybrid collectors. Under this categorization, PV cells directly convert solar energy to electrical energy. Solar thermal collectors conventionally produce thermal energy. Concentrated solar energy devices firstly concentrate solar energy, then produce thermal or electrical energy. The systems established in this third category include concentrated photovoltaic cells, power generation via concentrated solar thermal cells, thermoelectric generators, thermionic devices and thermophotovoltaic devices. Through these devices, electrical or thermal energy is produced and the only distinctive feature is being concentrated. As the fourth category, the hybrid systems show up. Photovoltaic thermal and concentrated photovoltaic thermal systems are the known ones. Hybrid systems produce both thermal and electrical energy.

In Figure 1.6 below, a review of PV system is shown:

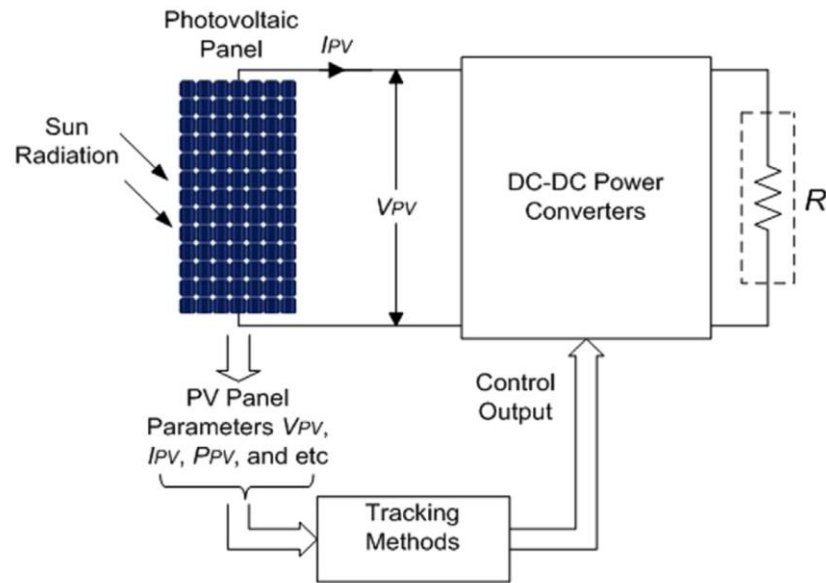


Figure 1.6 A typical PV system [54]

As seen in Figure 1.6, in a photovoltaic system, there exist generally photovoltaic panels, batteries, charging controllers, inverters, DC-DC power converter system, load controllers, circuit breakers and a tracking system which is sometimes used to increase exergy of the system [55]. Photovoltaic panel is the place where electricity is produced by semiconductor materials. Voltage of the produced electricity is reduced or increased to the desired level in DC-DC converter block. Also, in a grid-connected system there is DC-AC power converter. The power converter converts DC electricity produced by the PV system to AC voltage value of the relative grid network. If there is a sun tracker in the PV system, the tracker follows the sun in order to increase the perpendicular area of PV panels; and thereby more electrical energy is produced from the same panel.

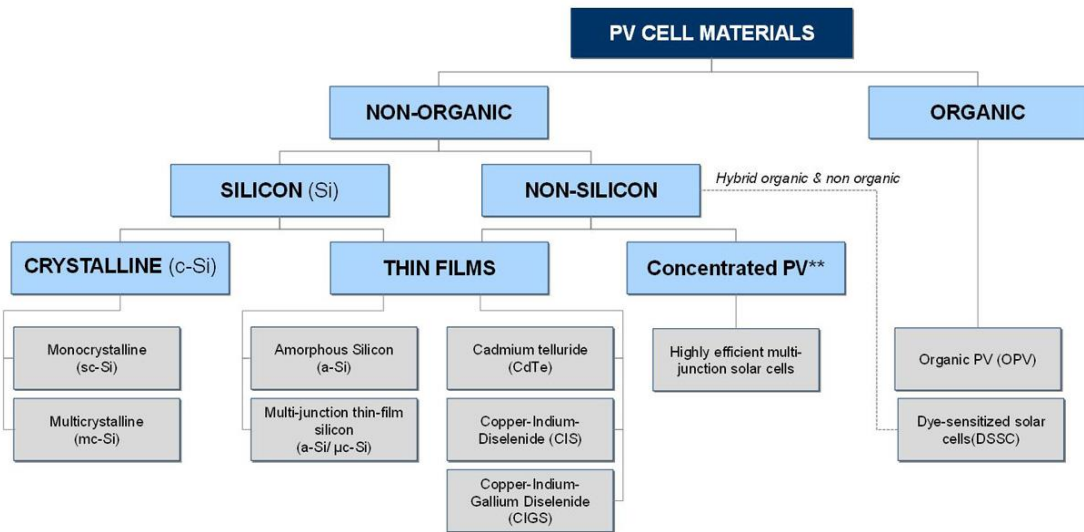


Figure 1.7 PV cell types based on used material [56]

According to SBC Energy Institute, PV cell materials can be categorized as shown in Figure 1.7. Material can be non-organic or organic in a basic scale. In organic materials, dye-sensitized solar cells (DSSC) shows up as the most important element. As inorganic materials, the most important material is silicon. There are monocrystalline and multi-crystalline (polycrystalline) silicon as conventional types; also, amorphous silicon and multi-junction silicon solar cells as thin film technologies. Other than silicon, cadmium telluride (CdTe), Copper-Indium-Diselenide (CIS), Copper-Indium-Gallium-Diselenide (CIGS) and gallium arsenide (GaAs) solar cells show up. In addition, there are various more types of materials which are being studied.

As it is understood, there are many types of solar cells. From the practical point of view, production in types of semiconductor material is also important to understand installed types of PV cells better. Figure 1.8 is helpful below to understand solar cell production over years according to the types of solar cells.

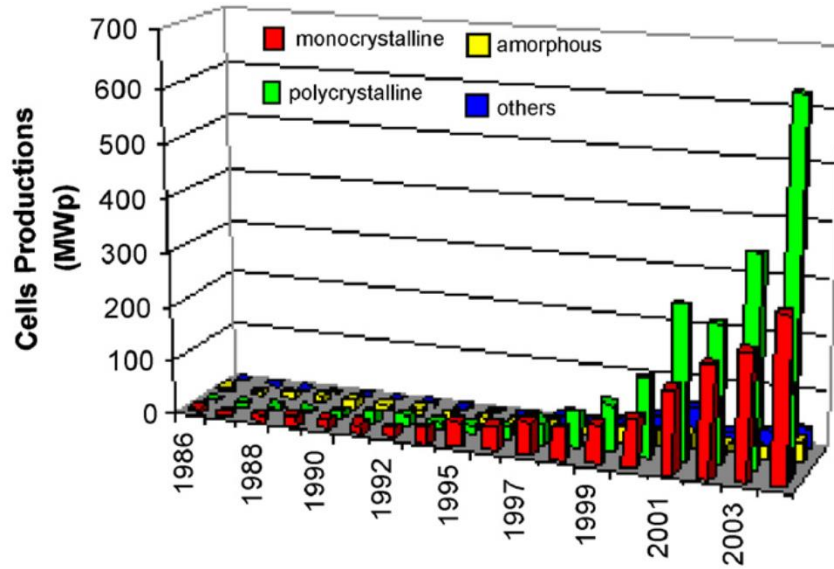


Figure 1.8 Production of PV cell types over years [57]

An important issue here, is the used material for producing solar cells. The most preferred material is silicon based materials. There are some criteria about choosing material. On one hand efficiency is important, and on the other hand ecological and biological effects of the material and economic conditions are important. Considering all these criteria, silicon seems to be the most useful material for industrial area and it has been the most commonly used one. Looking at the materials which have good properties regarding some of the criteria, Arsenic (As) and Cadmium (Cd) have high efficiencies, but they are highly toxic, and therefore dangerous when it comes to usage of broad areas on the earth. Compounds of these two materials should not be used in broad areas. Gallium arsenide (GaAs) solar cells have high efficiency comparing others, on the other hand it is expensive than some others for usage of broad applications and it is toxic as well. Another common candidate is Cadmium telluride (CdTe), but it has Cd inside and Te is not an easily found element on the earth [58]. Therefore, the best and easiest choice for the material in solar cells is silicon. It is cheap, its efficiency is sufficient, and it can be found easily almost everywhere. Because of these reasons, in this thesis study, only silicon based solar cell types are explained in the following chapters.

1.1.1 Silicon Solar Cells

Silicon solar cells are most widely used types among all the solar cells. The main reason for vast usage of silicon is cheapness. Cheapness is the result of being found everywhere and being easy to be manufactured.

There are some silicon solar cell types. Monocrystalline, polycrystalline, amorphous, and other thin film silicon cells are among them. These types are explained in the next sections. As it is seen in Figure 1.8, number of silicon cells and other types are not even comparable to each other. Almost all vast production systems prefer silicon-type solar cells.

There are some other advantages of silicon solar cells. Durability, no harm to environment, and heat resistance. Silicon cells are stable and can be used for many years. They have long life span. Especially crystalline silicon solar cells are one of the best in longevity; as an example, some crystalline silicon modules deployed in 1970s are still in operation [59]. As the second, they are not harmful or toxic to environment. Lastly, their heat resistance is relatively good comparing some other solar cell types. As the temperature increase, all types of solar cells are affected in a negative way. While some other solar cell types are affected badly, silicon solar cells stay more in acceptable values [60].

1.1.1.1 Monocrystalline Silicon Solar Cells

Monocrystalline silicon cells are commonly used for many years. The reason is that its efficiency is sufficient, it is found everywhere and its manufacture method is cheap. Therefore, many companies and producers prefer monocrystalline silicon solar cells. For production of monocrystalline silicon cells, Czochralski method is used as it is the best and the cheapest method [61, 62].

Monocrystalline solar cells have about 35 mA of current and voltage of 0.55 V per cm² area under best irradiation values of sunlight, namely about 1000 W/m². On the other hand, these values are for small solar cells; whole modules have always lower values

when they are gathered together. The efficiency is reported about 20-24% for general usage of monocrystalline silicon photovoltaic systems in real life [60,63-65].

On the other hand, monocrystalline silicon cells are more expensive than polycrystalline and amorphous silicon solar cells [66].

1.1.1.2 Polycrystalline Silicon Solar Cells

Production of polycrystalline silicon solar cells is even simpler than monocrystalline ones. Therefore, cheapness is one reason for preferring polycrystalline silicon solar cells and it is the main advantage over monocrystalline silicon solar cells. On the other hand, the efficiency of polycrystalline silicon cells is less than monocrystalline and it is about 15% in practice [67, 68]. This low efficiency has been an inhibitor for polycrystalline silicon technologies [69].

Production of polycrystalline cells is done by firstly melting silicon and solidifying it to compose crystals in various directions. By this way, a rectangular ingot with multi-crystals is produced. Then, the ingot is cut into slices and wafers are obtained [70, 71]. Evergreen Solar has developed this manufacture technology [67, 72] and it is commonly used by semiconductor producer companies. Also, there are some other metallurgical and chemical technologies for production of polycrystalline silicon [73, 74].

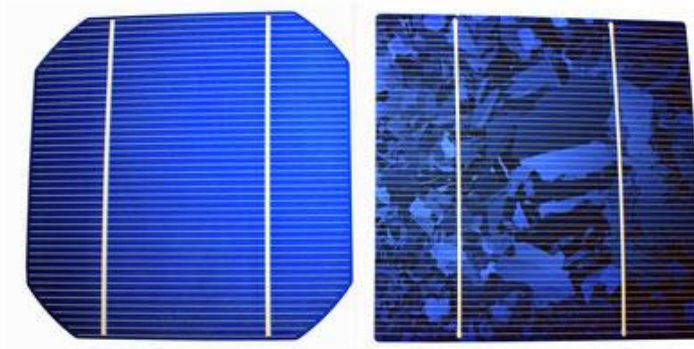


Figure 1.9 Monocrystalline (left) and polycrystalline (right) solar cells [75].

Figure 1.9 is a symbolic scheme to give information about crystal structures of mono- and poly-crystalline silicon solar cells. As seen from the figure, monocrystalline solar cells have only one direction crystal structures, whereas polycrystalline silicon solar cells have many different crystal structures in many different directions in nanoscale.

1.1.1.3 Amorphous Silicon Solar Cells

Amorphous silicon (a-Si) technology is one of the second-generation silicon solar cell technology. It is among earliest developed thin film technologies [76]. Diverging from crystalline silicon solar cells, another way of atomic packing was found and applied. In this technology, silicon atoms are randomly located, and therefore no crystalline structure is obtained [77]. This random structure of silicon atoms results a higher band gap of 1.7 eV, whereas crystalline silicon structure has a band gap of about 1.1 eV. Under favor of this high band gap, amorphous silicon solar cells absorb the light spectrum with higher energy better than crystalline silicon solar cells. However, although this advantageous property, amorphous silicon solar modules have less efficiency than crystalline silicon solar cell modules because it cannot utilize lower energy spectrum of the sunlight. Also, because of being thin film cells, amorphous silicon cells have less operating longevity comparing to crystalline silicon cells. On the other hand, the main advantage of amorphous silicon cells is cheaper production opportunity comparing with other two crystalline silicon solar cells. While efficiency of monocrystalline solar cells is about 25% maximum, polycrystalline cell efficiency is 20%. On the other hand, efficiency of amorphous silicon solar cell is about 10% [78].

1.1.2 Other Solar Cell Types

The crystalline (poly and mono) silicon solar cells are the first-generation solar modules. The second and third generation solar cell types are given as following:

Second-Generation [79];

- Amorphous
- Thin film
- CuIn(S)Se₂
- CdTe

Third-Generation [79];

- Organic Dye Sensitized Photovoltaic Module
- Plastic Photovoltaic Module (molecular and polymeric)
- High Efficiency Poly-Junction Batteries
- Hot Electron Converters
- Quantum Dot Photovoltaic Cells

Also, there are more solar cell types with different production methods. Since those methods and types are not in the scope of the study, they are not mentioned in detail. Green et al. prepared an up-to-date list of some solar cell types and their properties. The list is given in Table 1.2.

Table 1.2 Solar cell types and their recorded properties [78]

Classification	Efficiency	Area	V _{oc}	J _{sc}	Fill Factor	Test Centre	Description
	(%)	(cm ²)	(V)	(mA/cm ²)	(%)	(date)	
Si (crystalline cell)	26.7 ± 0.5	79.0 (da)	0.738	42.65	84.9	AIST (3/17)	Kaneka, n-type rear IBC
Si (multicrystalline cell)	21.9 ± 0.4	4.0003 (t)	0.6726	40.76	79.7	FhG-ISE (2/17)	FhG-ISE, n-type
Si (thin transfer submodule)	21.2 ± 0.4	239.7 (ap)	0.687c	38.50	80.3	NREL (4/14)	Solexel (35 μm thick)
Si (thin film minimodule)	10.5 ± 0.3	94.0 (ap)	0.492c	29.70	72.1	FhG-ISE (8/07)e	CSG Solar (<2 μm on glass)
III-V cells							
GaAs (thin film cell)	28.8 ± 0.9	0.9927 (ap)	1.122	29.68	86.5	NREL (5/12)	Alta Devices
GaAs (multicrystalline)	18.4 ± 0.5	4.011 (t)	0.994	23.020	79.7	NREL (11/95)	RTI, Ge substrate
InP (crystalline cell)	24.2 ± 0.5	1.008 (ap)	0.939	31.15	82.6	NREL (9/12)	NREL
Thin film chalcogenide							
CIGS (cell)	21.7 ± 0.5	1.044 (da)	0.718	40.70	74.3	AIST (1/17)	Solar Frontier
CdTe (cell)	21.0 ± 0.4	1.0623 (ap)	0.8759	30.25	79.4	Newport (8/14)	First Solar, on glass
CZTS (cell)	10.0 ± 0.2	1.113 (da)	0.7083	21.77	65.1	NREL (3/17)	UNSW
Amorphous/microcrystalline							
Si (amorphous cell)	10.2 ± 0.3	1.001 (da)	0.896	16.36	69.8	AIST (7/14)	AIST
Si (microcrystalline cell)	11.9 ± 0.3	1.044 (da)	0.550	28.72	75.0	AIST (2/17)	AIST
Perovskite							
Perovskite (cell)	19.7 ± 0.6	0.9917 (da)	1.104	24.67	72.3	Newport (3/16)	KRICT/UNIST
Perovskite (minimodule)	16.0 ± 0.4	16.29 (ap)	1.029c	19.51	76.1	Newport (4/17)	Microquanta, 6 serial cells
Dye sensitised							
Dye (cell)	11.9 ± 0.4	1.005 (da)	0.744	22.47	71.2	AIST (9/12)	Sharp
Dye (minimodule)	10.7 ± 0.4	26.55 (da)	0.754c	20.19	69.9	AIST (2/15)	Sharp, 7 serial cells
Dye (submodule)	8.8 ± 0.3	398.8 (da)	0.697c	18.42	68.7	AIST (9/12)	Sharp, 26 serial cells
Organic							
Organic (cell)	11.2 ± 0.3	0.992 (da)	0.780	19.30	74.2	AIST (10/15)	Toshiba
Organic (minimodule)	9.7 ± 0.3	26.14 (da)	0.806	16.47	73.2	AIST (2/15)	Toshiba (8 series cells)

1.2 Maximum Power Point Tracking

Maximum power point tracking (MPPT) is trying to find the optimum power output point for a solar system. MPPT has been researched for some years in order to increase output power of photovoltaic systems [80-85].

Photovoltaic cells convert photon energy to DC electrical energy. Since they use photo-voltaic effect and convert the energy from photons to electricity, they are called photovoltaic cells.

Photovoltaic cells, as explained in Chapter 1.1, can be considered as a type of solar cells. They produce electrical energy from light by utilizing photovoltaic effect.

1.2.1 Maximum Power Point

The power delivered by the solar cell is maximized by operating the cell at the voltage V_{mpp} and current I_{mpp} that gives the largest product, visualized by the shaded rectangle in Figure 1.10. By choosing a material with smaller band gap, the short circuit current I_{sc} will increase. The open circuit voltage V_{oc} will, to a certain point, increase with increasing band gap [86].

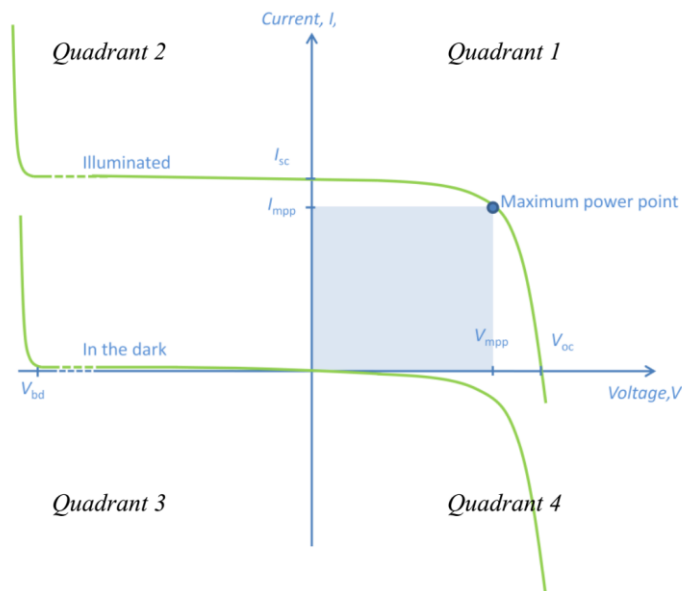


Figure 1.10 Example of an I-V curve [86].

The maximum power point MPP of a system takes place somewhere between the open circuit voltage and short circuit current. The output power is the multiplication of voltage and current of the system and MPP is the point that I-V graph takes maximum value for power. In other words, MPP is the point that multiplication of voltage and current of the cell takes its maximum value. That value is also the maximum output power of the cell. The output current becomes higher, but the output voltage reduces faster upside of MPP, and vice versa.

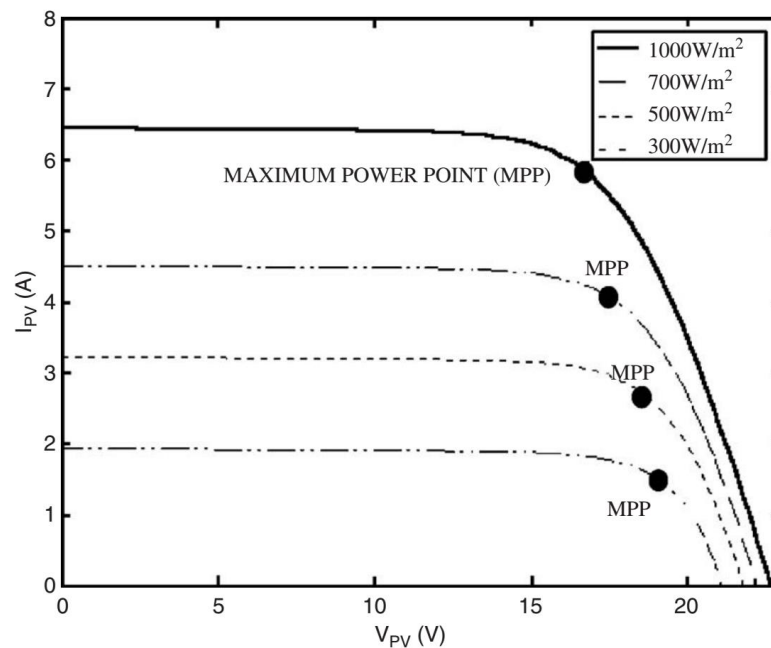


Figure 1.11 I–V photovoltaic characteristic for four different irradiation levels [87]

Maximum power points are shown for different solar radiation levels in Figure 1.11. As the light flux increases, maximum output power also increases in a PV system. It is expected that the output power for 1000 W/m² illumination is twofold of the power for 500 W/m² in Figure 1.11.

1.2.2 Fill Factor

Fill factor (FF) is the term used for expressing output efficiency of the system. It defines the maximum power could be obtained from a solar cell. It is expressed as a percentage ratio. Fill factor can be defined by the ratio of multiplication of V_{MPP} and I_{MPP} to multiplication of V_{OC} and I_{SC} [88]. V_{mpp} and I_{mpp} are the voltage and current

values at the maximum power point. V_{OC} is open circuit voltage and I_{SC} is short circuit current of the system.

In Figure 1.12, fill factor is visually shown. It is the ratio of P_{MAX} -rectangular area over P_T -rectangular area. Generally, FF becomes over 60% for an acceptable PV system. The FF values under 60% are generally considered to be insufficient.

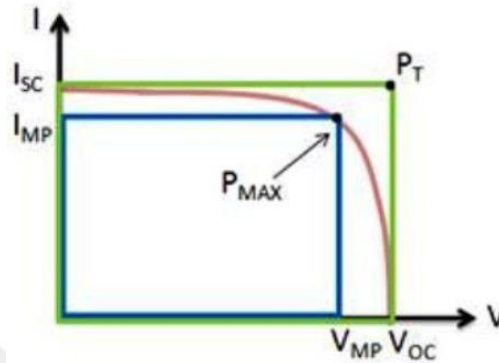


Figure 1.12 Fill factor calculated by P_{MAX}/P_T [89]

There are some factors which have influence on FF. Such as, series resistance of the solar cell (R_s), parallel or shunt resistance of the solar cell (R_{sh}), recombination current in the space charge region of the cell, and reverse saturation current [90]. When FF is too low in a system, generally these factors are checked and changed so that the system has a higher value of fill factor.

1.3 Sun Tracking Systems

Sun tracking systems are used for maximizing efficiency of PV systems [91]. The main aim of these systems is to catch the coming sun light at near to 90° with the PV cell plane. Efficiency is inversely proportional to obliquity factor which is cosine of the angle between the coming sun light and the solar panel plane [92].

The first tracker was built by Finster in 1962 and it was a mechanical system [93]. After him, Saavedra have developed a system which was controlled electronically and utilized Eppley pyrhelimeter [94]. Starting from these dates, sun tracking systems

have been widely researched because the energy gain provided by sun tracking might reach important percentages. Energy gain vary from 20% to 80% according to type of tracking system and some other factors like geographical location, seasons, and shading effects [95-101]. On the other hand, generally the systems which provide more energy increase are more expensive [102, 103]. Therefore, economically thinking, sometimes even fixed solar panels might be more cost effective [104].

When solar panels convert the sunlight energy to electrical energy, one of the main factors affecting the efficiency of energy is “angle of incidence”. The efficiency increases when angle of incidence closes to zero degree. The best angle is 0° for the maximum efficiency.

During a day, the angle of coming sunlight to the earth changes. Moreover, during the seasons, a second change of incident angle shows up due to the axial tilt of the earth. Over a year, totally two times 23.5° which is the axial tilt value of the earth, 47° of incident angle change occurs in south-north direction. This axial tilt angle, more accurately, is expressed as $\theta=23.441^\circ$ [80, 105]. Therefore, without a tracking system, 0° of incident angle to the sunlight is only possible between the geographical latitudes of 23.5° north and 23.5° south during a year and it occurs only twice a year. The places which have higher latitude values cannot reach zero angle to the sunlight. Therefore, sun tracking systems are very helpful in order to catch zero incident angle to the sunlight. Moreover, through tracking the sun, having zero degrees of angle is possible for many hours in a day.

The main aim of sun trackers is to catch minimum (0°) angle between the coming sunlight and the normal of solar panel plane. In this concept, there are two types of sun tracking systems: Single axis trackers and double axis tracking systems. Double axis tracking systems provide more freedom while single axis tracking systems can only rotate on a single direction. On the other hand, double axis tracker systems are generally more expensive. Therefore, economic factors are always effective on deciding whether single axis tracker is better or double axis tracker is better when a photovoltaic system is installed.

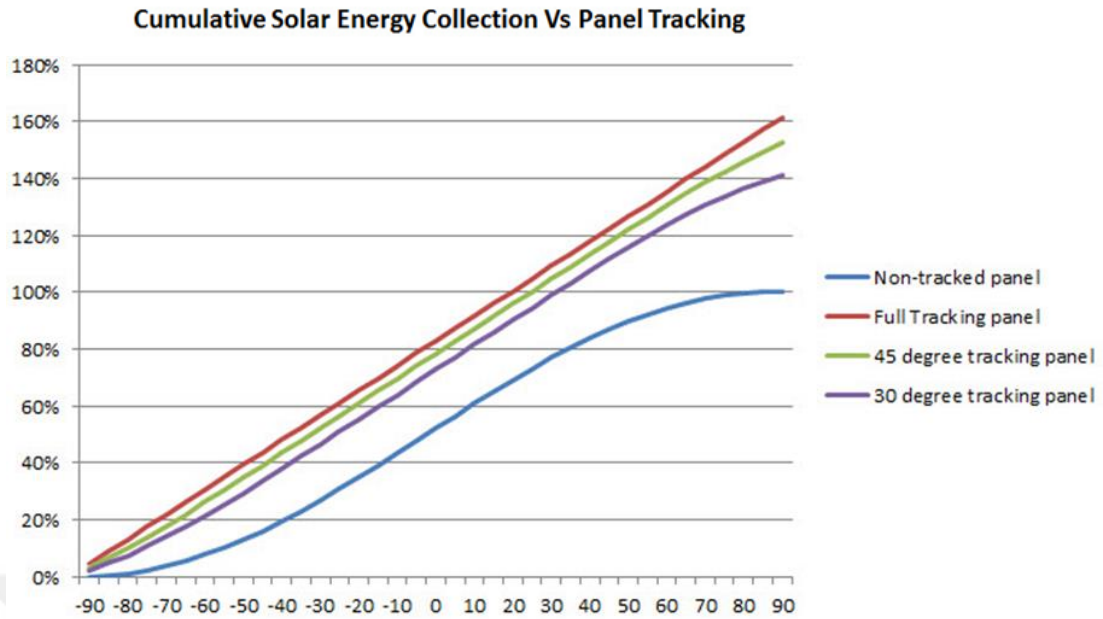


Figure 1.13 Effect of sun tracking systems on efficiency [106]

Figure 1.13 demonstrates effects of the sun tracking systems which are full tracking, 45° of tracking and 30° of tracking. The system without a tracker has less output energy as seen from the figure.

Another aspect of sun tracking is insolation area. Changing the sunlight incident angle affects directly the insolation area. An important reason of the change on efficiency is this factor. Figure 1.14 virtually explains the insolation area changes depending on incident angle of solar panels. As seen on the figure, assuming the system which has zero degree of incident angle to the sunlight produces 1000 W, when the incident angle becomes 45°, the produced energy by the same system drops to about 700 W from the direct sunlight. If the incident angle is increased to 70°, the produced energy drops to 342 W, and no output is taken if the angle becomes 90°. However, this calculation includes another assumption that all the produced energy is from direct irradiation of the sunlight.

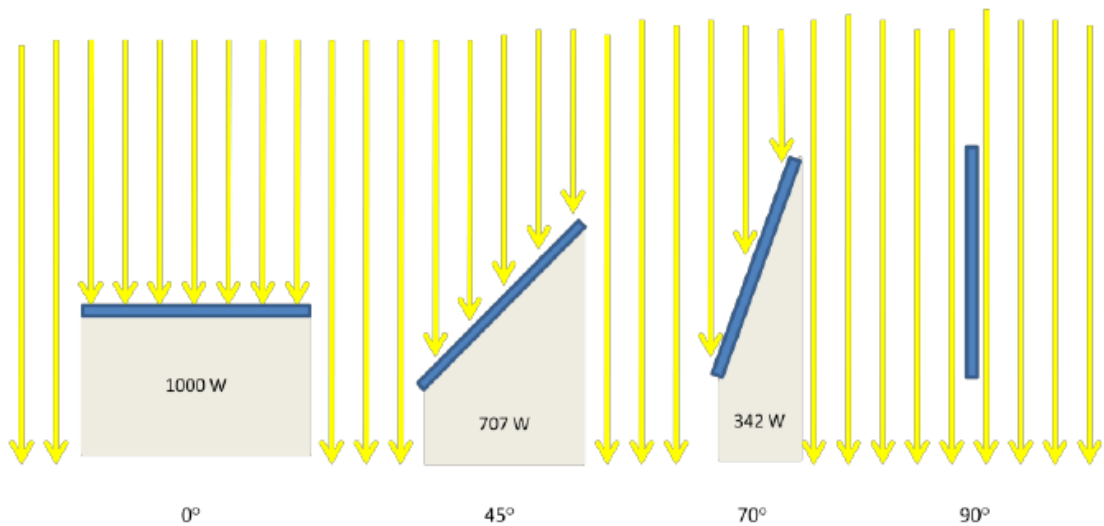


Figure 1.14 Direct insolation area vs angle of incidence [80]

On the other hand, solar radiation reaching to solar panels is not only direct radiation. Diffuse radiation and ground-reflected radiation are the other two types of radiations. Therefore, even when the incident angle is 90° , the output of solar panels is not reduced to zero in real life. Moreover, shading conditions are also an important issue and there have been a number of studies done about shading conditions [107-116].

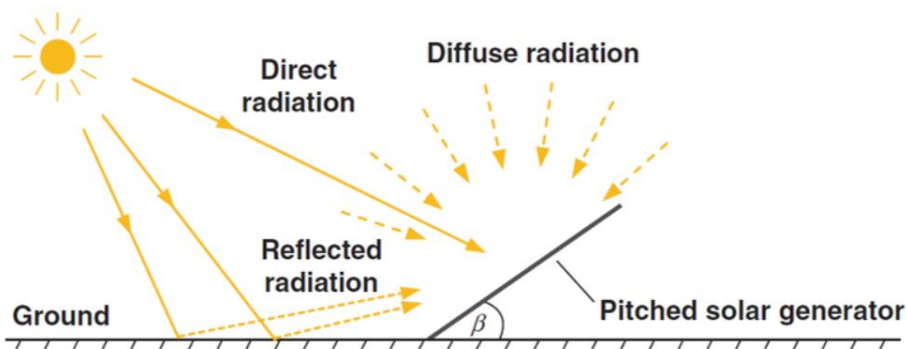


Figure 1.15 Solar irradiation types reaching a PV system [117]

As shown in Figure 1.15, other than direct radiation, reflected radiation from the ground and diffused radiation on the atmosphere are the other light sources for photovoltaic systems. Therefore, even for 90° of incident angles, the output power does not reduce to zero. This fact is demonstrated as a graph in Figure 1.16.

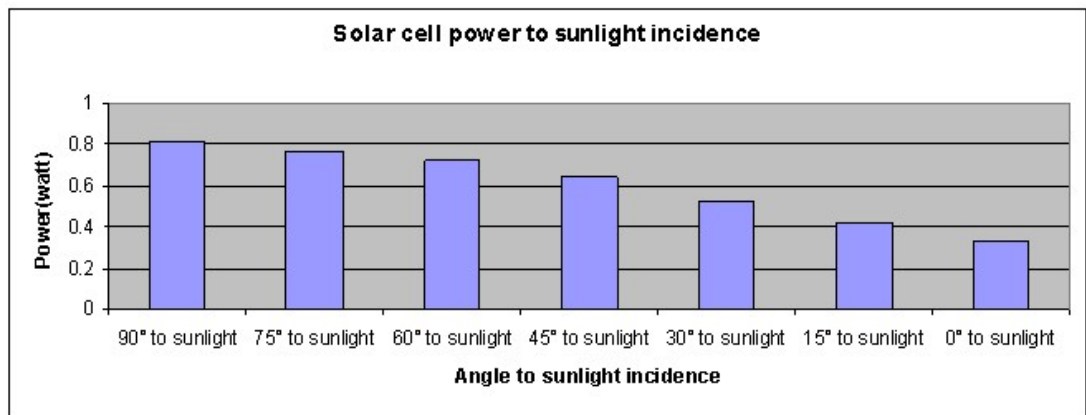


Figure 1.16 Effect of the sunlight incidence on output power of a solar panel [118]

The main elements of a solar tracking system are a tracking device and a tracking algorithm; control system, sensing devices, positioning and driving mechanisms [119, 120].

As an example of how much beneficial a sun tracker system can be, in a study, measurements done at a place on 30° north latitude showed that even one axis tracking systems can gain more energy from 15% up to 35% compared to the fixed PV system with the same characteristics [91].

In practice, available sun tracking systems can be categorized into two, as passive and active tracking systems.

1.3.1 Passive Tracking Systems

Passive tracking systems are generally mechanical systems which are based on thermal expansion of a matter. Sometimes shape memory alloys are also used, as shown in Figure 1.17.

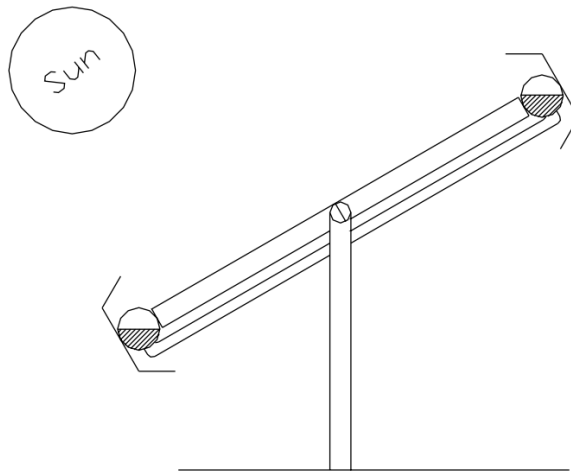


Figure 1.17 A passive solar tracker using two identical cylindrical tubes filled with a fluid under partial pressure [121]

Clifford and Eastwood [121] used the passive tracking system shown in Figure 1.17. They have increased the efficiency of their PV system up to 23%. Their passive solar tracker design includes two bimetallic strips made of aluminum and steel. These strips are positioned on a wooden frame and are partially shaded so that they do not take sun light when the angle is not proper. Since one side of the system takes more sunlight when the panel plane is not perpendicular, the PV system plane slowly comes to the balance angle through the expansion of bimetallic strip.

Another study with a passive tracking system was done earlier. Poulek has installed a PV system with a single axis passive sun tracking system which has included a shape memory alloy actuator. However, the passive tracking system was not very stable and easily deformed under 70°C [122].

Passive sun tracking systems are generally less complex than active tracking systems. In the past, their performance was comparable to active tracking systems [123, 124]. However, efficiency of passive systems is not comparable to active systems today due to fast development of active trackers, and they do not work properly at low temperatures [125]. Therefore, they are not preferred today and there are few research projects done on this subject.

1.3.2 Active Tracking Systems

Active tracking systems follow the sunlight actively. As mentioned in the previous sections, they have the following elements inside: tracking device and tracking algorithm, control system, sensing devices, positioning and driving mechanisms [119, 120].

There are two types of tracking algorithms: Astronomical based algorithms and real time controlled algorithms. Astronomical based algorithms use known astronomical measurements and angles. They decide angles of PV system according to pre-saved data related to the positions of the sun and the position of photovoltaic system. The pre-saved data includes the position formula of the sun with respect to date and time; or sometimes includes directly angles of the sun with respect to date and time. Also, the angle of the ground which the PV system is installed on must be considered.

As for real time controlled algorithms, they find the best sunlight angle real time through electrical comparing devices. These circuits compare the sun light according to the coming light power for at least two different incident angles. After finding the best angle, the PV system faces towards the sun.

As conventional active sun tracking system algorithms, hill-climbing (HC) [126], incremental conductance (IncCond) [127,128], perturbation and observation (P&O) [129], fuzzy-logic (FL) [130], artificial neural network (ANN) [131,132], voltage based [133] and current based [134,135] algorithms are studied. However, these conventional tracker algorithms are not efficient enough under shading conditions. There are some other algorithms developed for shading conditions, like particle swarm optimization (PSO) algorithm [136-141], cuckoo search (CS) method [142-145], and Fibonacci line search scheme [146-149].

The studies done have shown that tracking systems, especially active ones improve the efficiency and output energy of the photovoltaic system from 20% even up to 80% [150-153].

There are three main ways of tracking the sun actively. Electro-optical (real time) tracking, timing based tracking and auxiliary bifacial solar cell based tracking systems.

Therefore, active tracking systems are detailed and explained within three different titles; electro-optical (real time) tracking systems, timing based tracking systems and auxiliary bifacial solar cell based systems. Also, combinations of these systems are used in practical applications.

1.3.2.1 *Electro-Optical (Real Time) Tracking Systems*

In this type of tracking systems, illumination of sensors utilized and the solar panels are oriented to the sunlight direction. There become at least two sensors for tracking and according to illumination of sensors, the panel rotates towards the needed direction for maximizing output power. When both (or all) sensors take the same amount of sunlight, the system is at balance and no movement is seen. Also, to obtain more precise sunlight alignment, some other engineering methods are added to the sensors, such as collimator and shading element as shown in Figure 1.18.

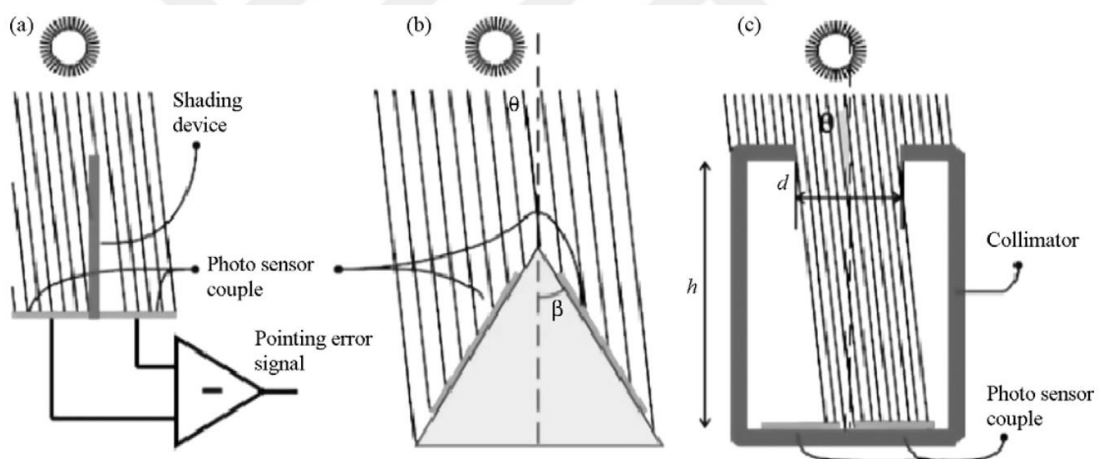


Figure 1.18 Sunlight pointing methods for getting more precise results [154]

Shading device (a) and collimator (c) increase accuracy of the sunlight direction. Also, giving angular positions (b) to sensors provides more certain tracking. However, collimator and shading device have better results because diffused light is prevented in those cases, while diffuse radiation occurs in case (b) of the figure.

There have been many research studies on real time-based active tracking systems. To understand different methods, some examples are included chronologically:

Zogbi et al. developed a double axis sun tracking system using some electronic circuits. Since it was a two-axis system, four sensors were used. The sensors were placed on four quadrants which were set up by two intersecting rectangular planes. The system included comparator circuits for the sunlight, a power amplifier and two motors to move and drive the solar panel. They determined a threshold value and if any exceed is seen from a sensor, related motor is activated and the system moves accordingly. Also, they added the feature that the system automatically turns into east after the sunset to catch the sunlight in next morning. This prototype was successful and was working even under variable light intensity [155].

Another study was done based on shadow method by Rumala. Sensors were placed on a ground under two back-to-back fixated semi cylinder pairs. One semi-cylinder pair was for east and west check, the other was for north and south check of coming light. In this system, the tracker remained on sunset position during the night and when the first sunlight is seen by east sensor, the system moved and faced the coming sunlight [156].

A few years later, a low cost two-axis sun tracking system was developed by Lynch et al. There were two sensors in the system and one of them was a four-cell pyramid which was placed on the tracker plane. The other sensor was for sunlight detection. A powerful gearbox motor was used for orienting the panel towards the sunlight. The system was able to work up to 0.1° sensitivity. This was considered to be minimizing wonder on partially overcast weathers by the researchers [157].

A single-axis sun tracker based on a microcontroller was designed by Konar et al. to utilize in photovoltaic systems. The design was concluded as successful on saving an important amount of power and as independent from geographical locations and temporal changes [158]. Koyuncu and Balasubramanian developed a two-axis tracker with a microprocessor. They added two limit angles to the solar panel for east and west sides. The results of the study proved that the maximum output power from the system is obtained if the solar panel is normal to the coming sunlight [159].

There was a thesis study done by Hamilton on two-axis solar tracker system based on a microcontroller. The microcontroller worked digitally on amplifying, comparing the

sensor values, and deciding which side to turn. There were two step motors for two axes and a four-sided pyramid sensor. C language was used in the microprocessor. The system was tested under real sunlight and under laboratory conditions with 16 different positions of a light source. The results demonstrated that the maximum output power was obtained all the time with the sun tracking system, while it was obtained only for noon times without tracking [160].

On a water heating solar system, a closed loop sun tracking system with electro optical sensors and a microcontroller was constructed. In addition, some other parameters of the system were controlled like wind velocity, temperature of the environment and pressure. The system was confirmed through long term tests in different circumstances by the owners of the study, Zeroual et al. [161].

A single-axis sun tracking system was developed by Kalogirou. The tracker consisted of a control system with three different-responsibility light sensors, a relay, a timer, and a complex circuit. The first sensor checked direct sunlight to the plane, the second sensor was a cloud sensor and the last one was used as a diffused daylight sensor. Any of these three sensors could stimulate the motor for starting the motion towards the sun in east-west direction. The tracking system was very accurate on following the sunlight that it was 0.2° for 100 Wm^{-2} illumination and it was even 0.05° for 600 Wm^{-2} [162].

Khalifa and Al-Mutawalli studied the performance of a two-axis sun tracking system used in a compound parabolic concentrator. The system could follow and update its angle for every 3-4 minutes in east-west direction and for every 4-5 minutes in south-north direction. The tracker spent only 0.5 Wh of energy. A number of tests were made for understanding and determining the performance gain of the tracker. During tests, the fixed collector had an angle of 33° which was the best angle for that location. Considering effect of seasons, it was concluded that the tracking system might increase output energy of the system up to 75% [163].

In the study done by Abouzeid, using XILINX software, another program was loaded to an electronically erasable programmable read-only memory (EEPROM). The power for orienting the sun was controlled by a programmable logic array (PLA) chip. The

chip gave a fixed power to a reluctance four-phase stepper motor for turning 7.5° or 15° . Therefore, this system worked for 7.5° and its multiples. When the sunlight leaves enough from being normal to solar plane, two position sensing cells send error to the chip and the stepper motor was started to move accordingly. Also, the motor was self-breaking via a group of switches inside the power amplifier [164].

Abdallah and Nijmeh developed a two-axis sun tracking system. In their system, they defined two angles for two motions; the first one was the azimuth angle and the second one was the zenith angle. Two motors were used for motion, one was on north-south direction and the other one was for rotation about vertical axis to the ground. A PLC was used for control of the tracking system. The tracker used only about 3% of the saved energy by itself. The tracker provided daily 41% of more energy than a fixed and same featured one with 32° of angle to the normal of ground [165]. Daily energy gain of the sun tracking system from morning hours to the evening can be understood, as an example, from Figure 1.19 which demonstrates sunlight energy taken by solar panels with the two-axis tracking system (line) and without it (dashed line). Energy gain takes high values especially during the morning and afternoon hours. Only at noon times the gain becomes relatively small.

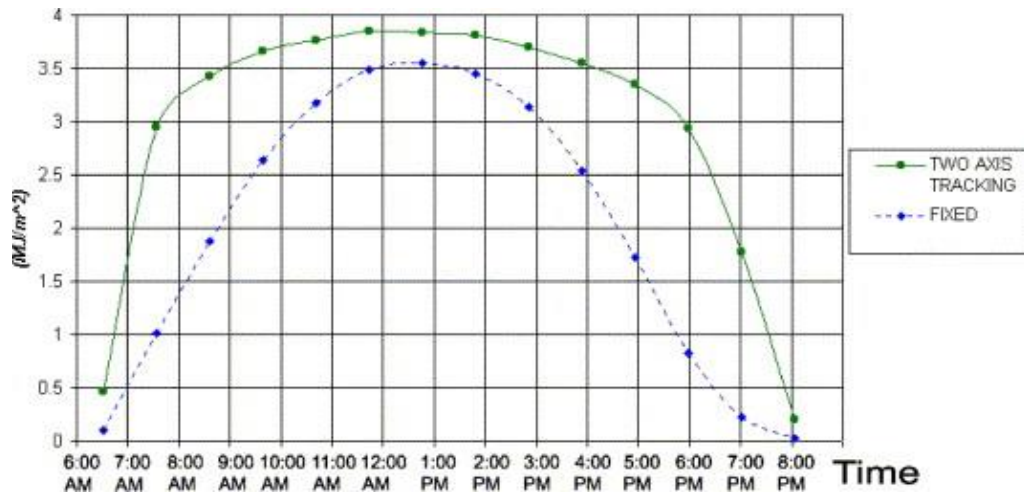


Figure 1.19 Experimental total solar radiation vs. time (07/05/2001) [165]

As it is seen on Figure 1.19, the difference between tracker and fixed systems is not high during midday hours. On the other hand, the difference takes higher values as the

sun takes away positions from the top, namely morning and evening hours. Another study determines these differences as following; fixed systems took 99.98% of the maximum energy when the angle is 1° to sunlight; while it drops to 98.5% for 10° of angle [125]. As it gets higher angle differences from the sunlight, dropping values exceed 40%.

In some other studies, robotic arms with PIC microcontroller built in PIC Basic PRO were used and gained 30% of efficiency [166]; a programmable logic device (Xilinx XC95108) written in Assembly and C++ was used regarding its cost effectivity [167]; a light sensor, a microcontroller and an A/D converter were utilized and resulted with 27% of energy gain comparing the fixed one [168]; in a single axis sun tracker, a PIC microcontroller was used and commented that using sun trackers for small solar panels may cause high energy losses [169] whereas another study done by Aiuchi et al. offers to use sun trackers in smaller systems [170]; a two-axis sun tracker with nine light dependent resistors (LDRs) to decide rotation and three LDRs for inclination arrangement was built with the feature of being cheap on sensing [171]; in a dish type solar concentrator, a two axes sun tracking system with an electronic circuit which took sensor signals from a group of photo resistors and utilizes relays to rotate the dish was used [172]. Also, a 1 kW closed loop sun tracking system was designed in Ioffe Institute PV Laboratories with continuous rotation of motors which were activated every 5-8 seconds for motion and rotation. A main sensor and an additional sensor was used to detect light [173].

Abdallah designed and developed four different sun tracking systems: A two-axis tracker, a vertical single axis tracker, an east-west single axis tracker and a north-south single axis tracker. He used a fixed solar system to investigate efficiency gains of the four tracker systems. The tracker systems spent less than 2% of produced energy. Comparing the fixed system, the trackers have obtained more energy up to about 44%, 38%, 35% and 16% for the two axes tracker, east-west tracker, vertical tracker, and north-south tracker, respectively [174].

A photovoltaic and thermally working low concentrator solar system was built by Rosell et al. The system had two-axis sun tracker working with two DC linear actuator and reed sensors. Concentrating ratio was about 11, namely 11 times of solar

irradiation was obtained on panels. The sun tracker worked with a PLC control system. Comparing an optimally tilted and fixed concentrator, the system obtained 50% of energy gain [175].

Huang and Sun designed and constructed a single axis sun tracking system with three fixed angles for morning, noon, and afternoon. Even for this three-stage sun following system, nearly 25% of yearly energy gain was provided comparing to that of fixed one [176].

1.3.2.2 Timing Based Tracking Systems

The second common type of solar tracking systems is timing based solar trackers. These trackers calculate the sun's position and orient towards it. For the calculation of position, some formulations or algorithms, date, time, and geographical information are used.

As an example of the studies done, in the times of 70s, Edwards set up a computer based sun tracker for parabolic collectors. Using the controller computers, 10,000 solar collectors followed the sun during day hours. The data speed was only 500 bits per second at that time and it was sufficient [177].

Davies designed an original tracking system using equatorial and ecliptic axes. In the system, the sun was considered as a fixed point. Therefore, the opposite angular velocity of the earth was accepted as the angular velocity of the tracker. For free motion of the tracker, a ball joint was used to pivot the panel. Also, the tracking error was only $\pm 2^\circ$. Since the tracker have a constant angular velocity, it did not need any complicated electronic circuit and a basic constant speed motor was employed [178].

In another study done on a solar concentrator system, Al-Jumaily and Al-Kaysi used a linear Fresnel lens to concentrate the sunlight. By using a two-axis sun follower, they managed to keep the solar incident light perpendicular to the collector all the time and got a constant efficiency of 64% out of more than 200 experiments [179].

Nuwayhid et al. built a two-axis tracking system in a solar concentrator. The true angles for tracking the sun were determined by using solar altitude and azimuth angles. These angles are in sinusoidal form and vary as a function of time. A PC were used to compute the position of the sun. Motors in the system were connected to the PC. As a result, sun tracker increased the temperature of the working fluid to the range of 200-600 °C, whereas the fixed system managed to increase only in the range of 80-200 °C. On the other hand, due to simpler design and lower cost of fixed systems, they seem still attractive [180].

Blanco et al. developed a new algorithm named PSA algorithm. They compared beforehand, four different algorithms and found Michalsky algorithm to be the most efficient. Their newly developed PSA algorithm had better results in their experiments. It had lower standard deviation of 14, 22 and 28% in azimuth, zenith angle and direction vector of the sun, respectively when it was compared with Michalsky algorithm. Also, range of errors were lower by 8, 24 and 35% for azimuth, zenith distance and direction vector of the sun, respectively [181].

As a timing based algorithm, Alata et al. completed a simulation study. In the study, angular locations of the sun were formulated and three different types of sun tracker designs were completed. The systems are similar to three different types of robotic arms. They are shown in Figure 1.20.

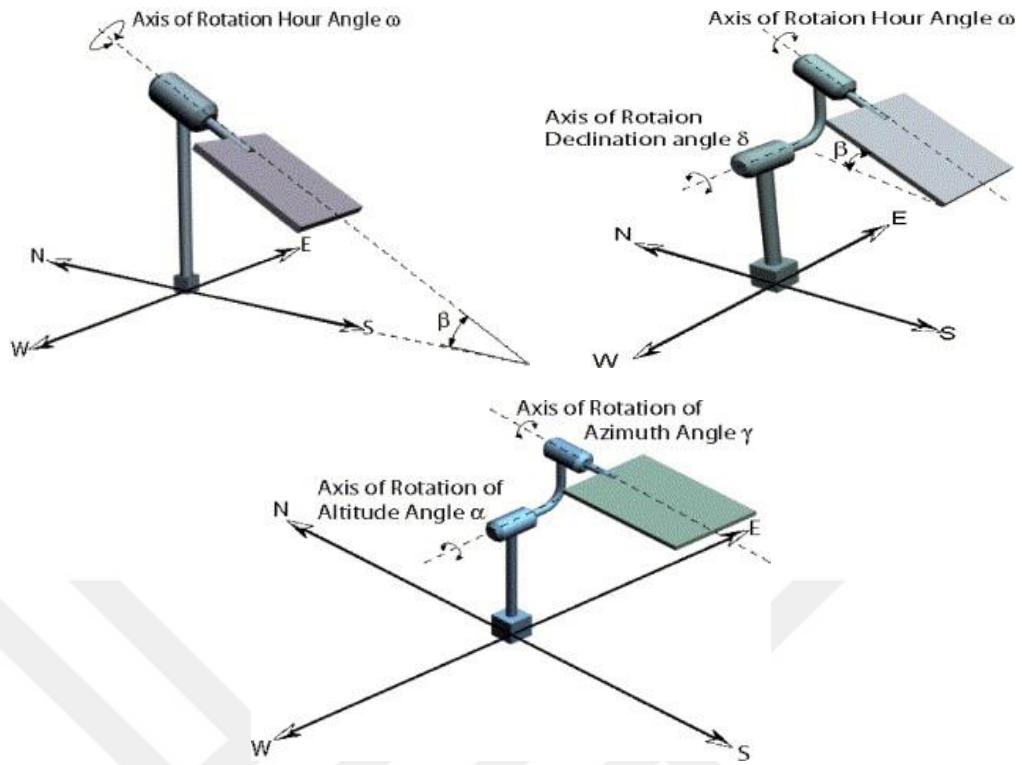


Figure 1.20 Three tracking systems simulated by Alate et al. 1. Left Top: One-axis sun tracking system, 2. Right Top: Two-axis equatorial sun tracking system; 3. Bottom: Two-axis azimuth/elevation sun tracking system [182].

The performance of the three trackers were compared and discussed. Through a virtual reality (VR) mode, 3D simulation of the whole system was achieved. In their formulas, azimuth, altitude, and declination were determined by using only the day number in a year and the hour in a day. Figure 1.21 shows the angles used by this sun tracker system [182].

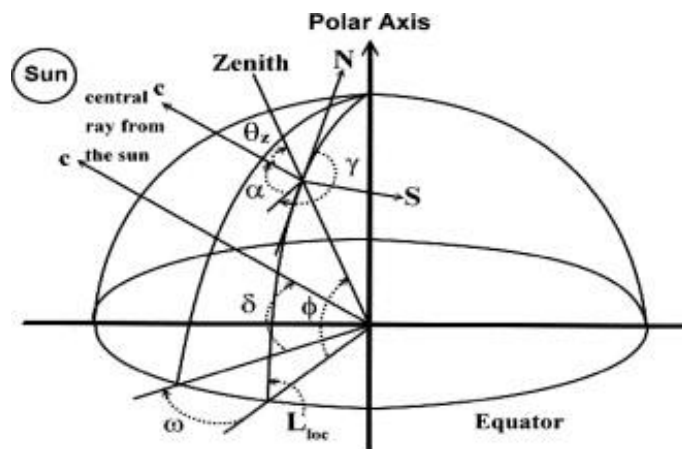


Figure 1.21 Schematic representation of solar angles used in the study [182]

Not for a PV system, but to measure global and direct spectral solar irradiation in the earth (in the related location) within 330-1100 nm of wavelength range, a sun tracking system was designed and developed by Canada et al. The system was specially designed for the needs of the team. The movement of the tracker was provided by a motor and a gear speed reducer with two axes of motion; one is in the azimuth plane and the second is in the principal solar plane. There were two sensors on a fixed aluminum plane in the system. The needed program codes were written in C++ for the relative movement to the sun, to control the motor, for the rest position in nights, and for working processes of the sensors. Also, utilizing Bouguer-Lambert-Beer law, the system could measure the atmospheric thickness and aerosol optical depth within the relative wavelength range [183].

Aliman et al. constructed a sun tracking system for higher efficiency. There were several mirrors in the system, one was master mirror and others were slave mirrors and they were used to concentrate the sun light. The tracker had two movement axes, a rotational axis towards the target and an elevation axis parallel to the master reflector. The mirror plane turns horizontally and vertically to follow the sun. The study team used date and time as inputs and calculated the needed angle as the output and moved the follower accordingly [184].

A 1 m² single axis solar tracker was constructed by Abdallah et al. for a solar still. They control the follower with PLC. The day was divided to four intervals by PLC for the speed of motor in the system. By that way, they managed to spend only 3% of total collected energy for the tracker. After their measurements, 40% of increase in efficiency during the morning hours and 22% of increase for the afternoon hours had achieved [185].

Khlaichom et al. built a two-axis sun tracker with genetic algorithm (GA) method. The sensor in the system was also a solar cell. It converted the sunlight to voltage difference. The tracker had relatively small sensitivity of $\pm 10^\circ$ in two axes. Results showed that genetic algorithm had an advantageous increase of about 7% in efficiency [186].

1.3.2.3 Auxiliary Bifacial Solar Cell Based Tracking Systems

Auxiliary bifacial solar cells are generally directly connected to a magnet DC motor and are fixed also on a rotary axle. In this way, bifacial solar cells both follow the sun and produce electricity.

In a study done in the past, an auxiliary bifacial solar cell based solar follower was constructed. The follower updated the angle every 5 minutes and with a sensitivity of $\pm 5^\circ$. The system was also a concentrating solar panel. Being bifacial, increased the efficiency by 15-25% comparing with mono-facial followers. This meant also that comparing to a fixed system, auxiliary bifacial solar cell based system increases the produced energy about 50% comparing with the fixed ones [187].

Poulek et al. constructed a simple and reliable solar tracker based on auxiliary bifacial solar cells. Any electronic circuits, codes, microprocessors, batteries were not needed for the tracking system. The system could be used in terrestrial areas and in space and down to -40° of temperature. In the system, the bifacial solar cells were about 1% of total solar cell area. Bifacial solar cells were connected to a motor and via motor, the whole system followed the sun with sensitivity of $\pm 5^\circ$. According to the results, the system achieved to produce more than 95% of an ideal system with the same properties. In addition, the system had 360° of freedom while the similar systems had only 120° [188]. Figure 1.22 shows an example of this system for a satellite:

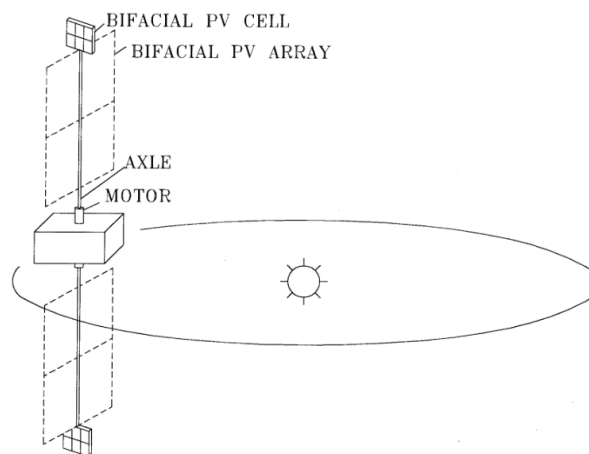


Figure 1.22 Scheme of the space tracker on a satellite [188]

Karimov et al. developed a single axis solar tracker for their PV system. The inclination angle was manually adjustable and during the day hours, the tracker followed the sun. There were four parts of solar panels. The panels were divided into two group and the angle between two parts within the same group was 170° . Through a bridge which was similar to the Wheatstone bridge, they managed that when the output voltages of the pairs are different from each other, motor starts to turn towards the sun. Their results showed that the output energy in the morning and the evening were not different from each other, unlike the fixed ones. Also, the tracker provided 30% of more efficiency [189].

Poulek and Libra designed an auxiliary bifacial solar tracking system. Solar cells were used for both tracking and providing energy. Figure 1.23 demonstrates their constructed solar tracker. When the sensors, namely the auxiliary bifacial solar cells had the same output, the system was in balance and there was no motion. When any difference existed, the system started to rotate about a single axis. The sensitivity to the sunlight was 10% which was a medium level of accuracy. Bifacial solar cell area was 2% of the total solar panels. The output energy was increased about 40% [190].

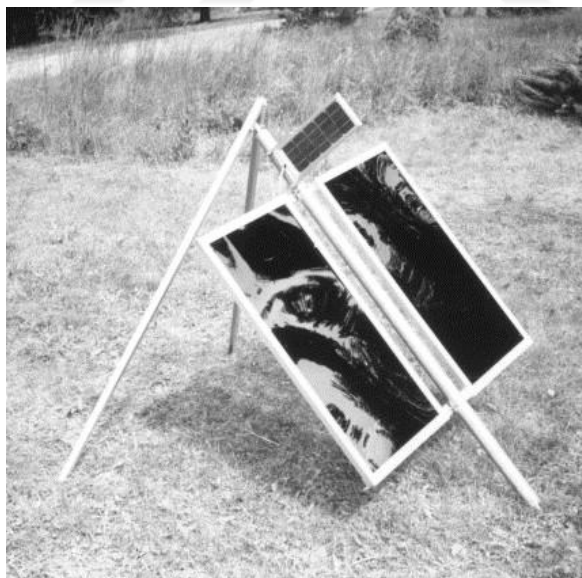


Figure 1.23 Polar axis tracker built by Poulek & Libra [190].

1.3.2.4 Combinations of Three Types of Tracking Systems

Since new engineering approaches have been continuously developed, combinations of different engineering approaches are always to be regarded. In the field of solar tracking system, there are various combinations and various new approaches of the three different systems which are mentioned in the previous sections.

In the study done by Hession and Bonwick in early years of solar trackers, a combination of real time (electro optical) and timing based single axis solar tracking system was established. In sunny days, the system used six sensors for wide angle determining and two more sensors for precise angle sensing to follow the sun. On the other hand, during cloudy days, the system worked by using a timing based algorithm and a clock type drive mechanism [191].

Saxena and Dutta completed a full design and construction of a two-axis sun tracker. The tracker followed the sun in azimuth and altitude planes. There were two modes in the system, open loop and closed loop mode. In open loop mode, the system was an electro-optical type follower of the sun, whereas in closed loop mode, it began its “cloudy” time based mode [192].

In another study, a comparison of a mathematical method and a real-time measurement method was done by Durisch et al. Temperature, normal incidence, voltage and current of the system and wind speed were all measured via the sensors in the system. As a result, only 0.02% of difference was detected between two different methods [193].

A microcontroller and a timing based single axis tracking system was designed by Ajay and Nagaraju. The tracking system was used in a concentrating collector. The system had a $\pm 1^\circ$ of sensitivity in sunny conditions. On the other hand, when the sunlight intensity was low, the system turned to timing based type and resolution dropped a little [194].

As a good example, combination of two different systems was achieved by Luque Heredia et al. for a photovoltaic concentrator. The tracker had a hybrid system of an ephemeris computational system and a sensor based real time system. Ephemeris

computation used geographical coordinates and time as inputs. The tracker system achieved to catch and follow the sun [195].

Georgiev et al. developed a two-axis sun tracking system with 0.05° of sensitivity to the position of the sun. The system had three different modes which are the clock mode which used date and time for tracking, the sun mode which follows the sun actively via real time sensors, and the remote mode. The irradiance of the sun was measured via three automatic pyrheliometers and a manual pyrheliometer during working hours [196].

Roth et al. developed a two axes sun tracking system. In the system, Eppley pyrheliometers and a Kipp and Zonen pyrheliometer to measure and follow the sun. A 16F877 series microprocessor and a PC were also used for calculations and management of the system. There were two different modes. In the clock mode, the system computed the position of the sun by using date and time. During a day, data were gathered and analyzed. The results were used in the next day to have better following properties. As the second mode, the sun mode was used. In this mode, the system followed the sun actively via real time sensors. Also, when solar irradiation dropped below 140 W/m^2 , the system turned to passive mode and no output was given. The results of the study showed that this equipment had a comparable efficiency to the Swiss sun tracker, and it was 75 times cheaper than the Swiss tracker [197,198].

Bakos designed and developed a two axes sun tracker for a parabolic trough collector (PTC). The tracker had a hybrid system of conventional photoresistors. It had two following axes on east-west and north-south directions. As a result, the system had about 47% of more efficiency in comparison to the fixed one which was optimally tilted with 40° [199].

Another example of hybrid following system was designed by Rubio et al. They used also two modes, one was solar movement model which was a timing based algorithm and the second mode was the classical electro-optical system. Results showed that this system had 55% of more output electrical power than a fixed one [200].

As it is seen from the studies done, a good engineering approach for the hybrid systems of the three types of the tracking systems is to have a sunny mode and a cloudy mode. In sunny mode, active tracking via electro-optical equipment or auxiliary bifacial based equipment are preferable. In cloudy mode, commonly preferred type is to use date, time and geographical location as inputs; in other words, timing based algorithms are better for cloudy days regarding performance. As for cost, it varies depending on needs, complexity of the system, the equipment used and preferred engineering approach.

1.4 Storage of Surplus Electricity

Storage of electricity is a commonly researched and a hard problem to solve since the technology is limited for storing high amount of energies for a long time. There are different ways to store electrical energy. These can be categorized into seven: 1- gravitational potential energy in a pumped hydraulic scheme, 2- compressing gas, 3- batteries (used in most PV cells), 4- in feed stock of a fuel cell, 5- flywheel, 6- inductor and 7- capacitor [201]. Energy storage techniques are explained in detail by [202-207].

CHAPTER 2

EXPERIMENTAL PROCEDURE

In the experimental process, a prototype of double-surface PV system with sun tracker and reflectors was established. The main aim of the experiment was to design and develop this double faced PV system with two reflectors.

In the system, positions of reflectors, proper dimensions of solar panels and reflectors, number of reflectors, the sun tracking system and working principles of it, angular motion and degree of freedom of the tracker, distance between the reflectors and panels, the reflector control system with pulleys, manually configurable tilt angle of the system were designed. After the design, the whole system was built and constructed. During the construction, the practical difficulties were handled and dealt; such as power of the motors, voltage level of the system, power of the batteries, and diameters of pulleys and wheels.

In this chapter, firstly the equipment used in thesis study is explained. Some working principles of the components of the PV system are described and explained in Chapter 2.1. As the equipment is described, properties and usage targets of the components are also mentioned so that the aims of the tools can be understood better. In Chapter 2.2, some information is given about measurements of the system.

2.1 Equipment Used in the Experiment

In the experiment, two reflectors, two solar panels, two solar tracker circuits, two pulley systems, a gear motor with 5 rpm of circular motion, a gear motor with 150 rpm of rotational movement, and a lux meter were used. This equipment is explained in detail in the following sub-sections.

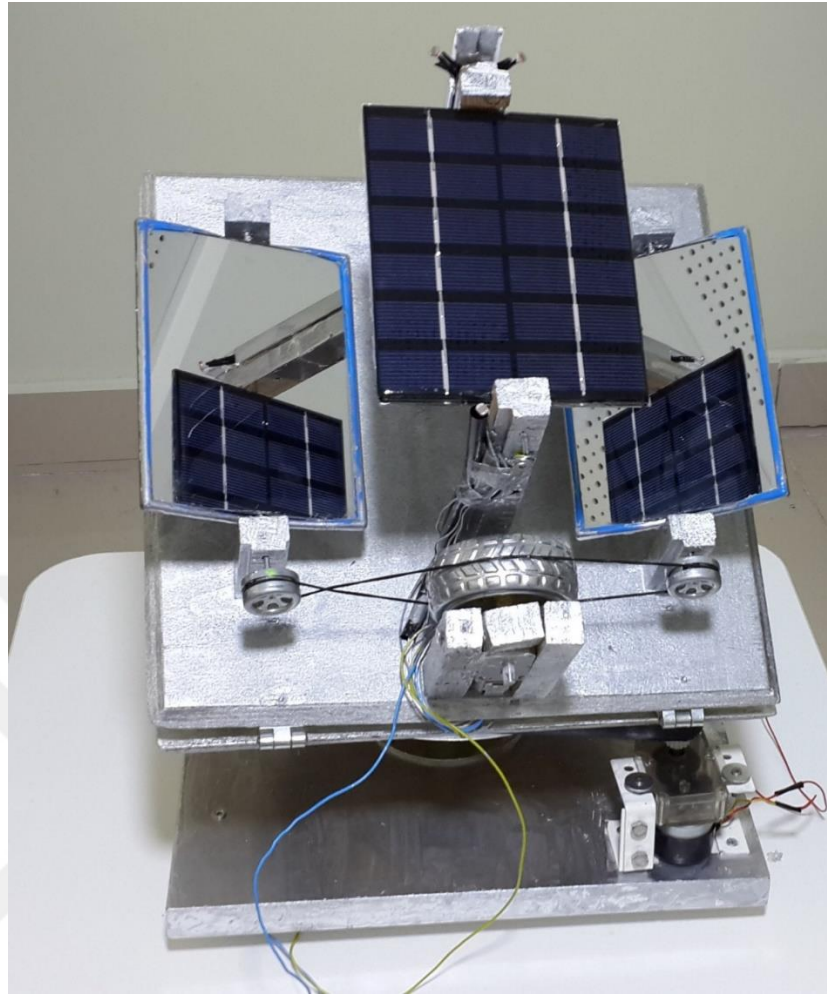


Figure 2.1 The completed photovoltaic system

The system is demonstrated in Figure 2.1. The front solar panel in the system takes the light directly, whereas the back solar panel takes it through two reflectors.

A pulley system links the reflectors to a motor which controls the reflectors. The motor is connected to a comparator circuit which compares light fluxes of front and back panel and decides to which direction the reflectors rotate. If the front and back panels are at balance, no rotation is done by the motor. Another motor is used for sun tracking system; it is seen on right bottom of the figure. There is a second pulley system which is not seen in the figure. It is placed and attached under the platform of the solar panels. The second motor rotates the whole system to track the sun. Another comparator circuit is connected to the second motor and controls the motion of it. To understand the details of the system, components are explained separately.

2.1.1 Reflectors

Two reflectors were used in the experiment. The aim of the reflectors was to reflect the coming light to the back-side solar panel. On the other hand, the incoming light directly reached to the front-side solar panel.

Dimensions of both reflectors are 9.5x13.5 cm. The main reason for choosing these dimensions was to have the reflectors similar sized to the solar panels. Solar panels have 11x13.6 cm dimensions.

Reflection ratios of the reflectors used in the system are about 80% as average. The reflection ratio was measured through the lux meter. To measure reflection ratio, firstly the light flux of the light source was measured from a distance. Then, using the reflectors, the reflected light flux was measured for the same distance. By this way the ratio was obtained. One important issue in this measurement is to have the same total distances from the light source to the flux meter for the two cases, namely with and without reflectors.

The exact measurement results of the reflection rate for the reflectors are given in Table 2.1 below:

Table 2.1 Reflection ratio of the reflectors

Distance (cm)	Flux with Reflector (lx)	Flux with No Reflector (lx)	Reflection Ratio (%)
50	241	310	77
100	94	116	81

According to the measurements, the average value for reflection rates of the reflectors used in the experiment is 79%. A specific light source was used for the reflection rate measurements.

2.1.2 Solar Panels

In the experiment, two amorphous and identical solar panels were used. One was the front panel and the other one was the back panel. Since the experiment was a prototype, small-sized solar panels were sufficient for the measurements.

The efficiency of amorphous silicon is the smallest one among silicon-based solar cells. On the other hand, it is generally acceptable values and the experiment did not need very high efficiencies. Since amorphous silicon is cheaper and it has a sufficient amount of efficiency, it was preferred for the experiment.

Figure 2.2 demonstrates the solar panels. Each solar panel has six-line and four-columns of solar cells and totally 24 solar cells.

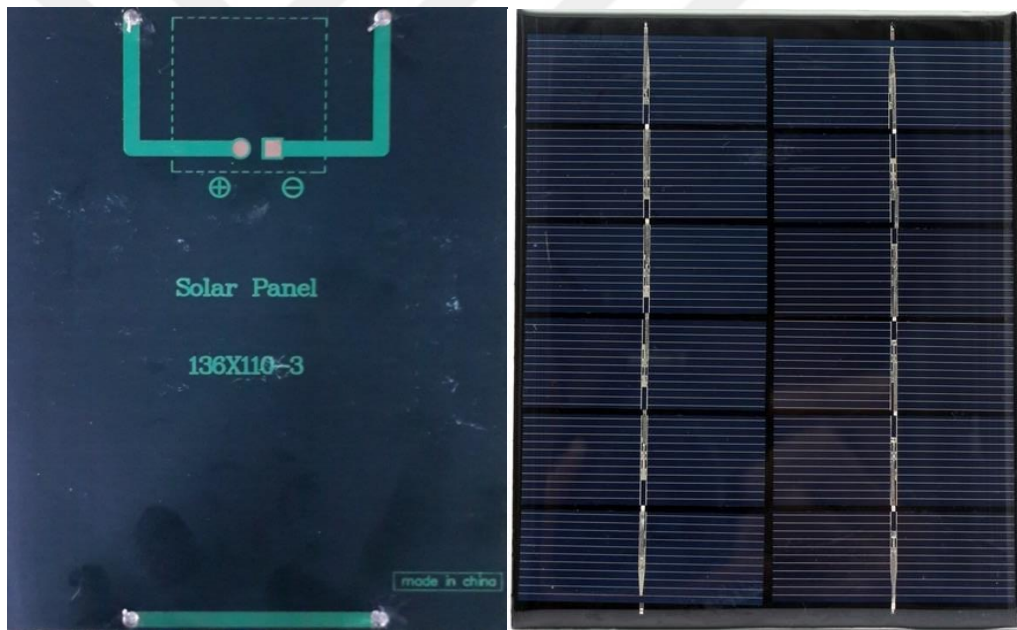


Figure 2.2 Back and front sides of the solar panels

The properties of solar panels are given below [208]:

Company: LEORY

Max Power: 2 W

Output Voltage: 6 V-DC

Max Supply Current: 0.33 A

Dimensions: 110x136x3mm

2.1.3 Pulley Systems

The pulley system shown in Figure 2.3 was used for following the sunlight in the experiment. The system consists of a pulley, a wheel, and a belt.

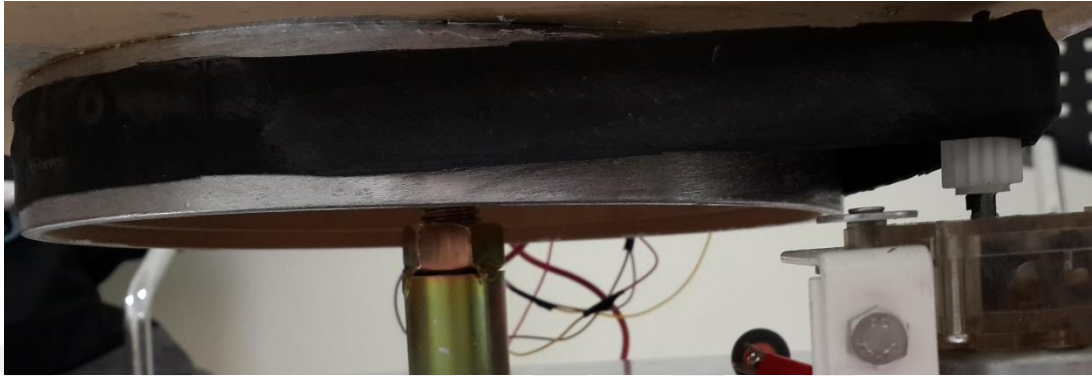


Figure 2.3 The pulley system for solar tracking

Radius of the pulley is 10 cm, and radius of the wheel is 1.5 cm. Therefore, an important power gain was obtained through this pulley system. The ratio of force gain is $10 / 1.5 = 6.67$. So, the torque of the motor was multiplied with almost 7. Since the PV system and its ground woods were about 3kg in total, this power gain became beneficial. Through this power gained-pulley system, the 5rpm motor easily turned the system and followed the sun during daytimes.

One advantage of this pulley system is slow and balanced rotation. The motor connected to this pulley system is 5 rpm; and ratio of the radii of the big pulley and wheel is about 7. Therefore, rotation velocity of the PV system as following the sun becomes even less than 1 rpm. This small value of the rotation provides a balanced, well-controlled sun track.

The second pulley system was used for controlling the reflectors. Three wheels, two shafts and a rubber were used in the pulley system. Two identical and small wheels were connected to the reflectors through the shafts. A bigger wheel was connected to the 150-rpm motor. Radii of the small wheels are 1.3 cm and radius of the bigger wheel is 3.9 cm. Therefore, a power loss occurs in this pulley system. Torque of the motor is

divided by 3 because of this pulley system. Nevertheless, the motor was powerful enough to rotate the reflectors with the help of 12 V-battery.



Figure 2.4 The pulley system for controlling the reflectors

The pulley system had to rotate two reflectors in opposite directions. Therefore, a straight connection (right in Figure 2.4) was done from the bigger wheel to one of the reflectors, while a cross connection (left in Figure 2.4) was used for the other one.

A disadvantage of this reflector-controlling pulley system is fast rotation. The bigger wheel which is connected to the motor has 3 times greater radius; therefore, the angular velocity of the reflectors became high. Even, the system was able to catch a sufficient angle for the reflectors.

2.1.4 Geared Motor for Solar Tracking

The rotational speed of the geared motor is 5 rpm. Its strength is 30 kg-cm torque. A low speed-motor is enough due to slow rotational motion of the sun. Also, the motor moved about 3kg-system. Therefore, the specified motor was preferred.

Specifications of the motor is given below*:

Working Voltage: 12 V DC

Torque: 30 kg-cm (at 12 V)

Angular Velocity: 5 Rpm (at 12 V)

Current: 60 mA (at 12 V)

*These specifications were obtained from the seller.

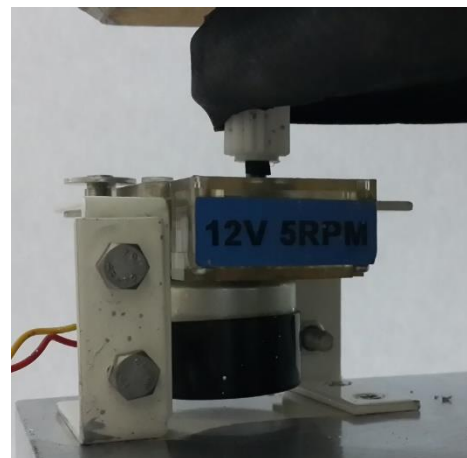


Figure 2.5 Geared motor used for sun tracking

2.1.5 Geared Motor for the Motion of the Reflectors

There were two motors used in the experiment set up. The first one was explained in the previous section. The second motor was connected to the controller circuit of the reflectors. The aim of that circuit was to have equal amounts of energy production from both surfaces.



Figure 2.6 The motor and wheel used for angular control of the reflectors [209]

The motor connected to that circuit was used for rotational motion of the reflectors via the pulley system mentioned in Section 2.1.3. It provided angular position of the reflectors so that the both faces of the photovoltaic system take equal amounts of sunlight. Characteristics of the motor is given below [209]:

Working Voltage: 6-12 V DC

Torque: 1 kg-cm (at 12 V)

Angular Velocity: 150 Rpm (at 12 V)

Current: 300 mA (at 12 V)

Since the strength of the motor does not have to be high, 1 kg-cm torque was sufficient for the experiment. On the other hand, the pulley system connected to this motor has some power loss due to the diameter rates of wheels.

2.1.6 12V-Battery

12-Volt battery was used as the power source of the sun tracker and reflector controller system. The controller circuits of both systems and the motors were suitable for 12V power supply. Figure 2.7 shows the used battery for the experiment. The main constraints as choosing battery were being 12V, enough power and cheapness. Thus, the battery shown in the figure was chosen.



Figure 2.7 12V battery used as a power supply in the experiment

Technical properties of the battery were obtained from the seller and are given below:

Voltage: 12V

Energy: 1.3Ah/20hr

Company: OR-TEC

Specifications: Valve regulated rechargeable battery

2.1.7 Single Axis Solar Tracker Circuits

Two basic solar tracker circuits were used in the experiment. The first tracker was for comparing the light fluxes on the two solar panels. The first solar panel was faced towards the sun; and the other one was placed back to back with the first panel. By this way, a simple dual surface solar panel system was built. Therefore, the first solar tracker compared the light fluxes coming to two solar panels and turned the reflectors in order to provide equal amount of light fluxes to the solar panels. Also, to be more accurate, “reflector controller” is used in the following sections.

The second solar tracker was used for following the sun during a day. Sun tracking was achieved through this second tracker and the pulley system under the ground of the solar panels. Starting from the morning, the system followed the sun via the second tracker with one dimensional freedom. The freedom was a rotational motion on a vertical axis to the earth. The rotational axis can be explained through cylindrical and/or spherical coordinates. The azimuthal angle, θ is the angle changing during the day in this system. Referring cylindrical coordinates, the z-axis is vertical to the earth, and the solar tracker turns the system around that z-axis; therefore, becomes θ in cylindrical coordinates. Also, referring spherical coordinates, the same angle is explained through the same concept but with a different name, ϕ . Therefore, the angle becomes ϕ (φ) in spherical coordinates. In addition, the notations of the angles in spherical and cylindrical coordinate systems change depending on the references [210, 211].

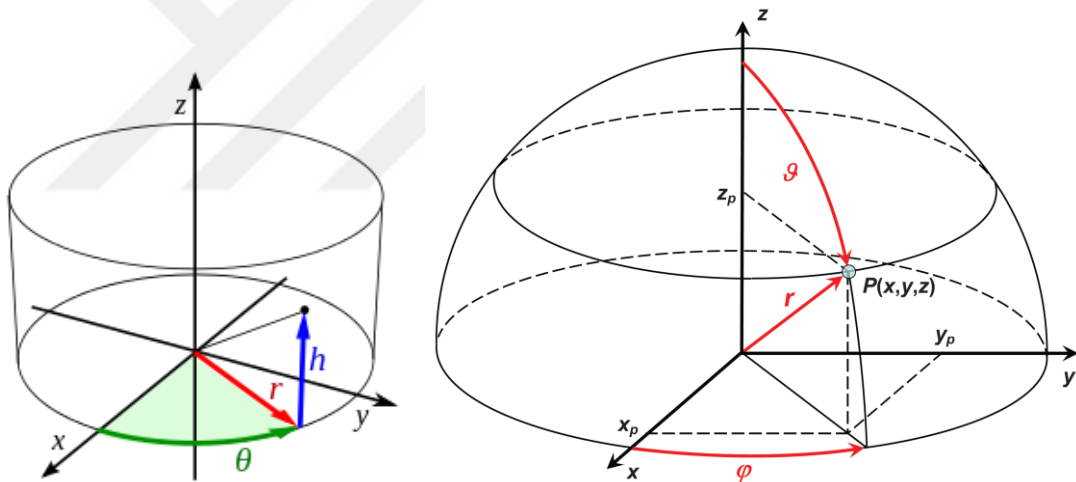


Figure 2.8 Rotational angle, θ of the sun tracking system in cylindrical (θ) and spherical (φ) coordinate systems [212, 213]

The two main reasons for choosing that type of solar trackers are simplicity and cheapness.

The solar trackers were simple circuits working with 2 LDRs, an OPAMP, and 4 transistors mainly. The figure below shows the schematic diagram of each solar tracker.

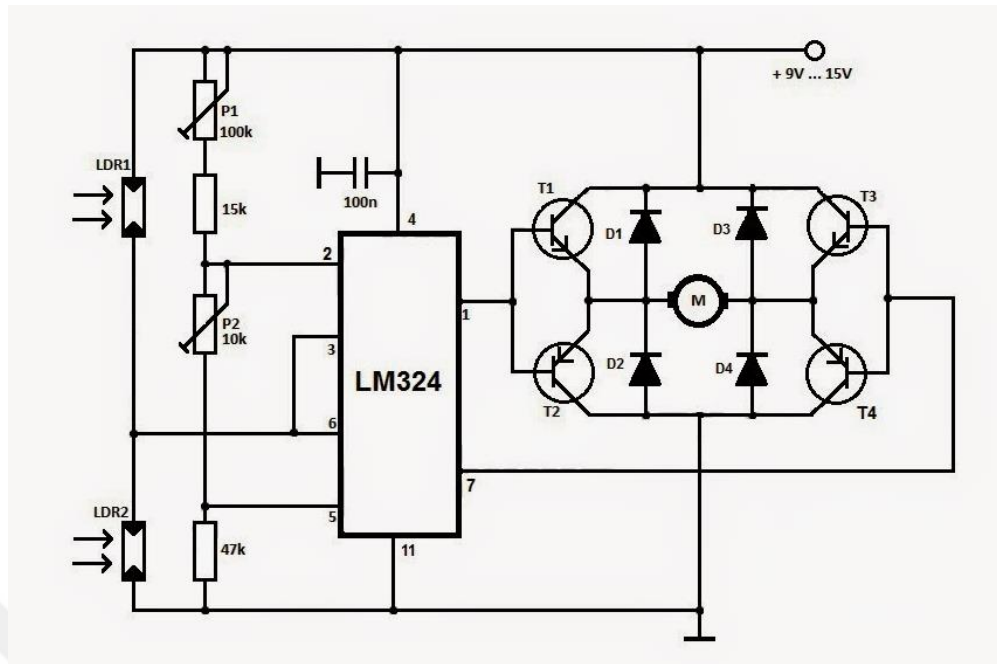


Figure 2.9 Schematic diagram of the solar tracker [214, 215]

All the electronic circuits worked with a 12 volt-battery in the experiment. Technically, the used circuit components of solar trackers are listed below:

- **Light Dependent Resistors (LDRs):** A Light Dependent Resistor is a photoresistor which changes its resistance depending on the light coming on its front face. Since the resistance of an LDR change depending on light, they are used as photo sensors. In this study, they are used for comparing light fluxes.

In the solar tracker system, LDRs were placed with 90° between them and 45° to the normal of the ground of the solar panel system as shown in Figure 2.10.

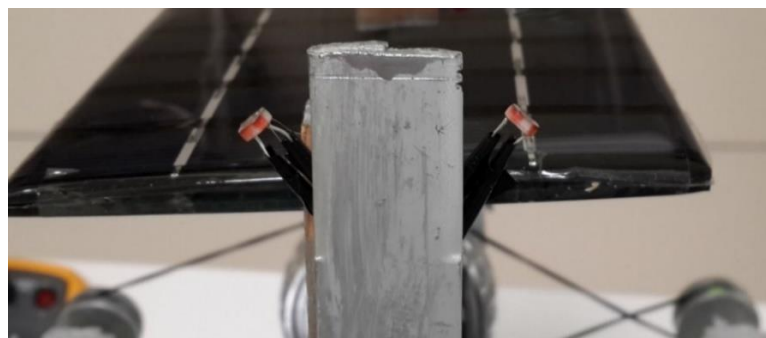


Figure 2.10 LDRs positioned for accurate following of the sun

In reflector control system, the LDRs were positioned back-to-back as shown in Figure 2.11. By this way, the upcoming light densities to the upper and lower solar panels were checked through these LDRs. The upper LDR took light directly from the light source or the sun; while the bottom LDR faced the light coming through the reflectors.



Figure 2.11 LDRs for control of the reflectors

- **OPAMP:** LM324 was used for amplifying the LDR voltage variations. LDR's resistance change directly affects voltage of it. Therefore, when resistance changes, voltage also change. LM324 is a quadruple OPAMP. It has 4 OPAMPs inside. In the solar tracker, two of them were used [216].
- **Transistors:** Four transistors were used. BD139 (n-p-n), BD140 (p-n-p), BD239 (n-p-n) and BD240 (p-n-p) are the power transistors. BD139 is the complementary of BD140 and BD239 is the complementary of BD240 [217].
- **Motor:** One motor was used for each solar tracker circuit. The motor used in the solar tracking system is 5 rpm and 12 V geared motor. Its torque is 30 kg-cm. The other motor was used in the reflector control system. It is 150 rpm and 12 V. Its torque is 1 kg-cm. The motors connected to the solar trackers were explained in the previous sections in detail.
- **Diode:** Four 1N4001 model diodes were used in a solar tracker circuit. These diodes were connected to the transistors in order to regulate output voltage and power.

- **Variable Resistors:** A 10 k Ω and a 100 k Ω variable resistors were used for regulations of sensitivity and working region of the solar trackers.
- **Resistors and a capacitor:** Resistors (47 k Ω and 15 k Ω) were for input lines of the OPAMPs in LM324. The capacitor (100 nF) was used as a bypass capacitor.

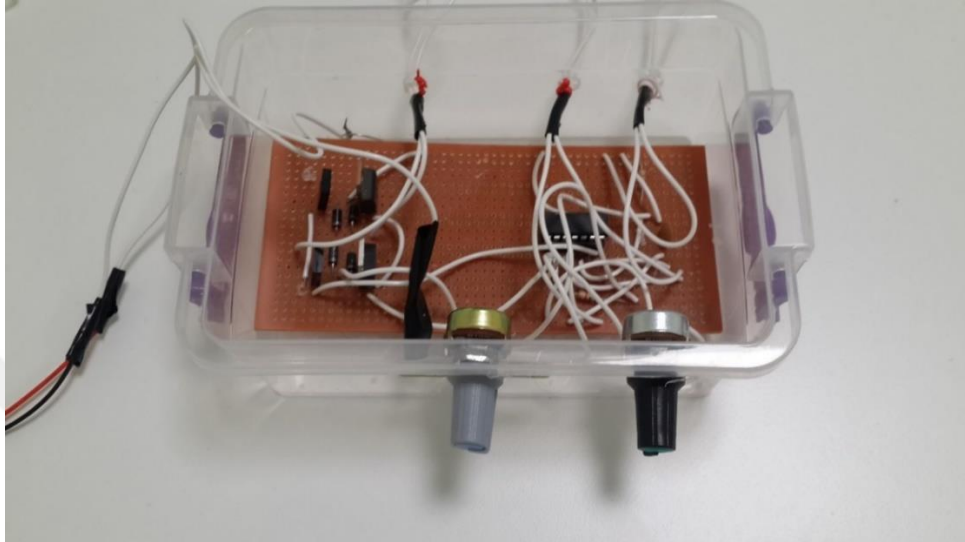


Figure 2.12 The solar tracker used for controlling angular positions of the reflectors

Figure 2.12 and Figure 2.13 demonstrates the reflector controller circuit and solar tracker control circuit, respectively.

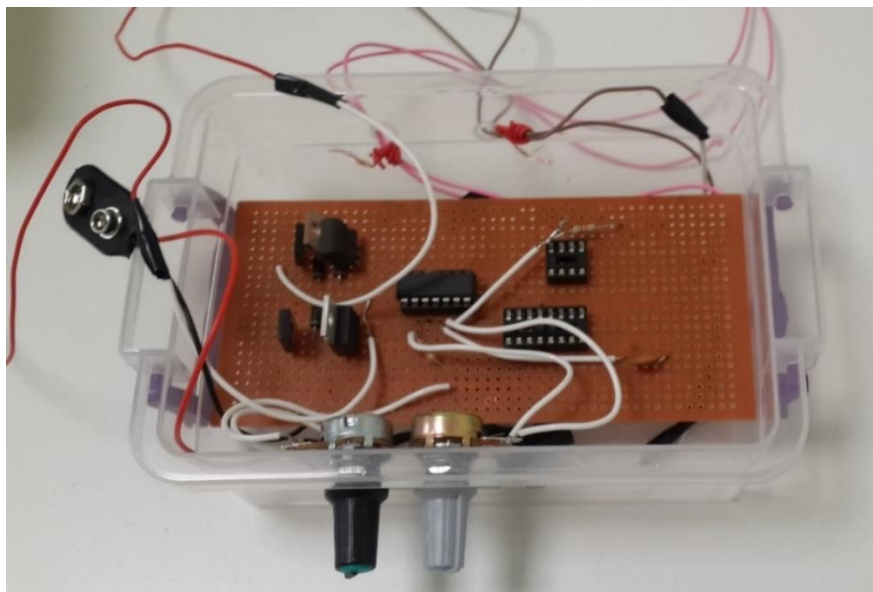


Figure 2.13 The solar tracker used for following the sun during daytimes

2.1.8 Lux Meter

The used lux meter model is LX-1010B. Its specifications are given below [218]:

- Range: 0-50000 lx
- Accuracy: (23±5°C): ±(5%+2d)
- Display: 18mm (0.7") LCD
- Sampling time: 0.4 seconds
- Operating Temperature: 0° to 40°C
- Operating Humidity: 0 to 80% RH

Since the specifications of this lux meter were sufficient of this study, this lux meter was used for the measurements of light flux in the study.



Figure 2.14 The lux meter used in the experiment

Also, spectrum of the lux meter is important for true measurements. Since the solar panel of the study works mostly under visible light, the lux meter must be sensitive in the relative range. Therefore, an according lux meter must be used. The lux meter used in the study has relatively good spectrum for the experiment. It is sensitive for the visible region which is in the interval of 380-750 nm. The visible spectrum is given in Table 2.2. Also, the spectral sensitivity is given in Figure 2.15.

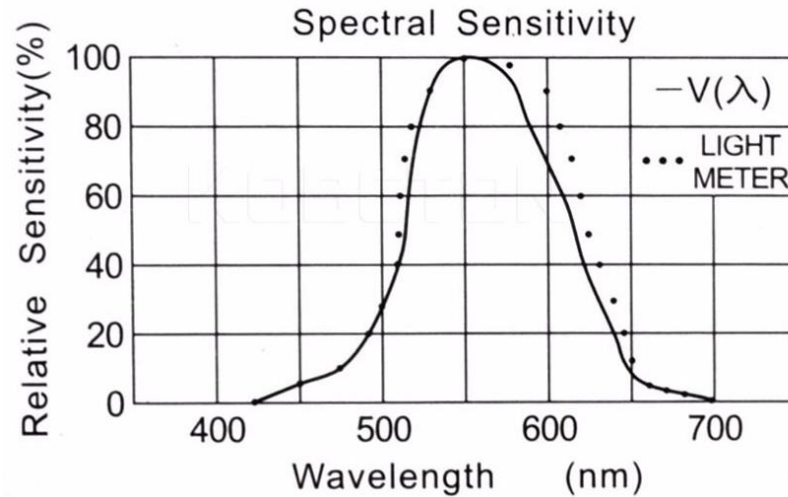


Figure 2.15 Spectral sensitivity of the lux meter [219].

As seen from the figure above and the table below, spectrum of the lux meter is proper to the visible light spectrum. Since the solar panels used have the same spectrum for working conditions, the lux meter is suitable for the experiment.

Table 2.2 Visible light spectrum [220]

Color	Wavelength (nm)
Violet	380-450
Blue	450-495
Green	495-570
Yellow	570-590
Orange	590-620
Red	620-750

W/m^2 and lux (lx) are the units which are used for radiometric and photometric measurements, respectively.

2.1.9 Light Source

The light source was used for laboratory simulation measurements. The source is 3600 lm, cool daylight and a partially isotropic source. It is isotropic for front side which was used in the study. Its diameter is 10 cm.



The stick which holds the light source was made such that its height is changeable. The height of the light source from its bottom could take the values from 90 cm to 130 cm. There are 11 different values with about 4 cm increase between each height.

Efficiency of the solar panels might be found approximately in the unit of W/m^2 . The dimensions of the solar panels are 13 x 11 mm. Thus, the area of a panel becomes about 0.015 m^2 . In August in which the measurements done, the average of daily maximum solar radiation might be taken as about 800 W/m^2 [221].

There is a goniometer attached to the light source. This goniometer was used for measuring angle of the light source with respect to the ground.

Figure 2.16 The light source used in the experiment

2.2 Measurements Done in the Experiment

All the measurements were done with two multimeters, separately used for front and back solar panels. Voltage values were measured and current values were found by dividing voltage values to resistor values. Also, power values were calculated through multiplying voltage and current values.

Two types of measurements were done in this study: Laboratory simulation measurements and real time measurements.

Laboratory measurements were done to simulate real time conditions. A partially isotropic light source was used for these measurements. Imitating the virtual angular motion of the sun in daytimes, different angles were given to the light source in laboratories. Also, MPP measurements were done for 50 cm, 70 cm and 100 cm distances of the light source away from the front solar panel. Sun tracking system and fixed system cases were studied with different angles. An exemplary picture is given in Figure 2.17, taken during the laboratory measurements.

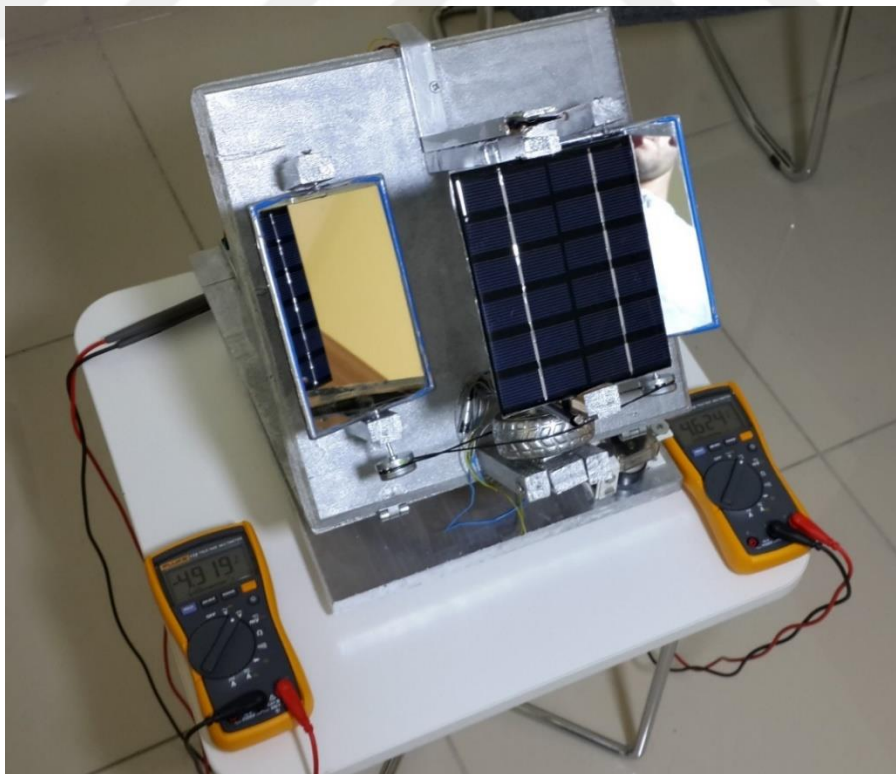


Figure 2.17 Measurements done on the solar panel system in laboratory

Real time measurements were done in the yard of Ankara Yıldırım Beyazıt University. During daytimes, hourly measurements were done starting from 06 am till 7 pm. In real time measurements, 30° tracking system, 45° tracking system, 30° fixed system and 30° fixed system cases were studied. There are some reasons for choosing these cases. Firstly, 30° is a suitable angle for Ankara placed on 40° latitude. Since the measurements were done in August, the best angles are around 20°-35°. Thus, 30° was chosen. On the other hand, 45° was chosen to see effect of tilt angle of the system on output power of solar cells. Also, tracking systems and fixed systems were studied to show effects of sun tracking on solar panels. Figure 2.18 was taken during real time measurements in Yıldırım Beyazıt University.

In addition, MPP measurements were done through trying different number of resistors between 0.5 Ω to 31 k Ω . The resistor values were chosen watchfully to obtain distinctive current-voltage and power-voltage graphs.

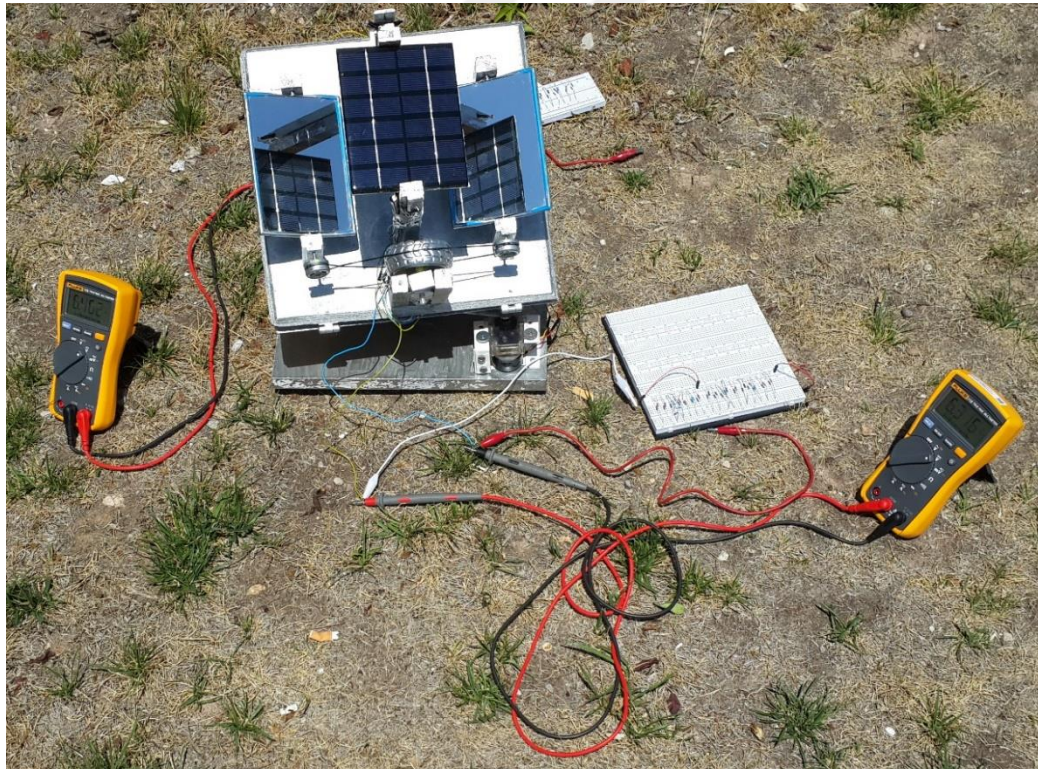


Figure 2.18 Real time measurements

CHAPTER 3

EXPERIMENTAL RESULTS

During the evaluation of results, in addition to power ratio, efficiencies, MPPs, and fill factors of front and back panels are evaluated. In addition, tracking and fixed system differences and effects of them to measurement results, tilt (zenith) angle differences and effects of them to the result are evaluated.

One important criterion of this experimental set up is the “power ratio” between the back panel and the front panel. The power ratio is obtained by dividing back panel output power to front panel output power. The main aim of the system is to have high power ratio. In other words, if the back panel provides output power values near to the ones of the front panel, the system is considered to be successful.

3.1 Laboratory Measurements

Laboratory measurements were done in Yıldırım Beyazıt University 15 Temmuz Şehitleri Campus laboratories. In laboratory measurements, a partially isotropic 3600-lumen light source was used.

The main aim of laboratory measurements is to simulate real time conditions.

In this chapter, all the results given in tables, then their graphs are given and relative comments are done. All the graphs in this chapter were sketched in MATLAB.

3.1.1 Laboratory MPP Measurement Values in Tables

In Table 3.1, 3.2, 3.3, 3.4, 3.5 and 3.6, the results of MPP measurements done in laboratories are given. For each resistor connected to the system, related voltage, current and power values are given. MPP measurements were done separately for front

and back panels for the distances of 50 cm, 70 cm and 100 cm from the front solar panel.

Table 3.1 Lab MPP measurement values of back-side panel for 50 cm distance

Connected Resistor (Ω)	Voltage (Volts)	Current (mA)	Power (mW)
∞ (Open Circuit)	5.10	0	0
31000	5.06	0.16	0.83
22000	5.00	0.23	1.14
9000	4.85	0.54	2.61
4200	4.30	1.02	4.40
3600	4.00	1.11	4.44
2700	3.24	1.20	3.88
1000	1.25	1.25	1.56
390	0.50	1.28	0.64
300	0.40	1.33	0.53
220	0.29	1.31	0.38
200	0.26	1.30	0.34
100	0.14	1.40	0.20
56	0.072	1.28	0.093
47	0.060	1.28	0.077
27	0.035	1.30	0.045
15	0.020	1.33	0.027
2.3	0.003	1.30	0.004
1	0.001	1.00	0.001
0.5	0.001	2.00	0.002
0 (Short Circuit)	0	1.50	0
Light Flux: 1110 lx			

Table 3.2 Lab MPP measurement values of front-side panel for 50 cm distance

Connected Resistor (Ω)	Voltage (Volts)	Current (mA)	Power (mW)
∞ (Open Circuit)	5.62	0	0
31000	5.50	0.18	0.98
22000	5.47	0.25	1.36
9000	5.40	0.60	3.24
4200	5.20	1.24	6.44
3600	5.12	1.42	7.28
2700	4.95	1.83	9.08
1900	4.38	2.31	10.10
1400	3.76	2.69	10.10
1000	2.76	2.76	7.62
390	1.1	2.82	3.10
300	0.83	2.77	2.30
220	0.61	2.77	1.69
200	0.55	2.75	1.51
100	0.28	2.80	0.78
56	0.16	2.85	0.46
47	0.13	2.76	0.36
27	0.075	2.77	0.21
15	0.042	2.80	0.12
2.3	0.006	2.60	0.016
1	0.002	2.00	0.004
0.5	0.001	2.00	0.002
0 (Short Circuit)	0	2.80	0
Light Flux: 2360 lx			

Table 3.3 Lab MPP measurement values of back-side panel for 70 cm distance

Connected Resistor (Ω)	Voltage (Volts)	Current (mA)	Power (mW)
∞ (Open Circuit)	4.9	0	0
31000	4.8	0.16	0.74
22000	4.74	0.22	1.02
13200	4.55	0.35	1.57
9000	4.45	0.50	2.20
4200	3.25	0.77	2.52
3600	2.78	0.77	2.15
2700	2.12	0.79	1.67
1000	0.82	0.82	0.67
390	0.33	0.85	0.28
300	0.26	0.87	0.23
220	0.19	0.86	0.16
200	0.17	0.85	0.15
100	0.09	0.90	0.08
56	0.045	0.80	0.04
47	0.040	0.85	0.03
27	0.023	0.85	0.02
15	0.013	0.87	0.011
2.3	0.002	0.87	0.001
1	0.001	1.00	0.001
0.5	0	0	0
0 (Short Circuit)	0	1	0
Light Flux: 790 lx			

Table 3.4 Lab MPP measurement values of front-side panel for 70 cm distance

Connected Resistor (Ω)	Voltage (Volts)	Current (mA)	Power (mW)
∞ (Open Circuit)	5.2	0	0
31000	5.16	0.17	0.86
22000	5.13	0.23	1.20
9000	4.98	0.55	2.76
4200	4.53	1.08	4.89
3600	4.29	1.19	5.11
2700	3.6	1.33	4.80
1000	1.50	1.50	2.25
390	0.59	1.51	0.89
300	0.45	1.50	0.68
220	0.33	1.50	0.50
200	0.30	1.50	0.45
100	0.16	1.60	0.26
56	0.085	1.52	0.13
47	0.072	1.53	0.11
27	0.041	1.52	0.06
15	0.023	1.53	0.04
2.3	0.003	1.30	0.004
1	0.001	1.00	0.001
0.5	0.001	2.00	0.002
0 (Short Circuit)	0	1.7	0
Light Flux: 1265 lx			

Table 3.5 Lab MPP measurement values of back-side panel for 1 m distance

Connected Resistor (Ω)	Voltage (Volts)	Current (mA)	Power (mW)
∞ (Open Circuit)	4.4	0	0
31000	4.35	0.14	0.61
22000	4.29	0.20	0.84
9000	3.68	0.41	1.51
4200	2.15	0.51	1.10
3600	1.83	0.51	0.93
2700	1.39	0.51	0.72
1000	0.53	0.53	0.28
390	0.21	0.54	0.11
300	0.17	0.57	0.10
220	0.12	0.55	0.07
200	0.11	0.55	0.06
100	0.058	0.58	0.03
56	0.030	0.54	0.02
47	0.026	0.55	0.01
27	0.015	0.56	0.008
15	0.008	0.53	0.004
2.3	0.001	0.43	0
1	0	0	0
0.5	0	0	0
0 (Short Circuit)	0	0.5	0
Light Flux: 460 lx			

Table 3.6 Lab MPP measurement values of front-side panel for 1 m distance

Connected Resistor (Ω)	Voltage (Volts)	Current (mA)	Power (mW)
∞ (Open Circuit)	4.80	0	0
31000	4.71	0.15	0.72
22000	4.63	0.21	0.97
9000	4.23	0.47	1.99
7100	4.07	0.57	2.33
6400	3.89	0.61	2.37
5400	3.48	0.65	2.26
4200	3.00	0.71	2.14
3600	2.59	0.72	1.86
2700	1.98	0.73	1.45
1000	0.75	0.75	0.56
390	0.29	0.74	0.22
300	0.23	0.77	0.18
220	0.17	0.77	0.13
200	0.15	0.75	0.11
100	0.081	0.81	0.07
56	0.043	0.77	0.04
47	0.036	0.77	0.03
27	0.021	0.78	0.02
15	0.011	0.73	0.01
2.3	0.002	0.87	0.002
1	0.001	1	0.001
0.5	0	0	0
0 (Short Circuit)	0	1	0
Light Flux: 630 lx			

3.1.2 Laboratory MPP Measurement Results

In Figures 3.1, 3.2, 3.3 and 3.4, circle-marked lines are for 50 cm distance; square-marked lines refer 70 cm distance measurements and diamond-marked lines are used for 100 cm distance measurements.

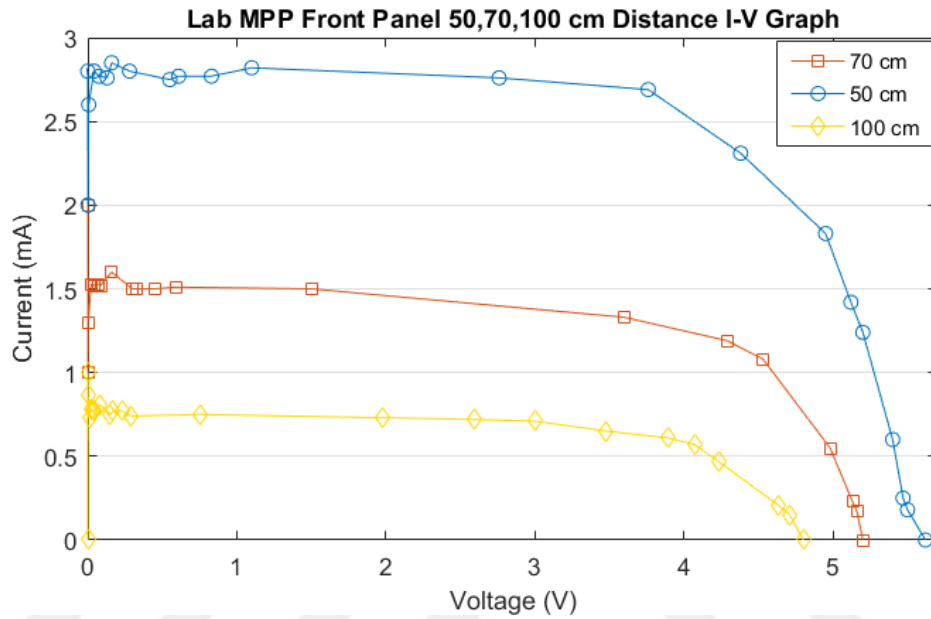


Figure 3.1 I-V graphs of front panel for 50, 70 and 100 cm distances

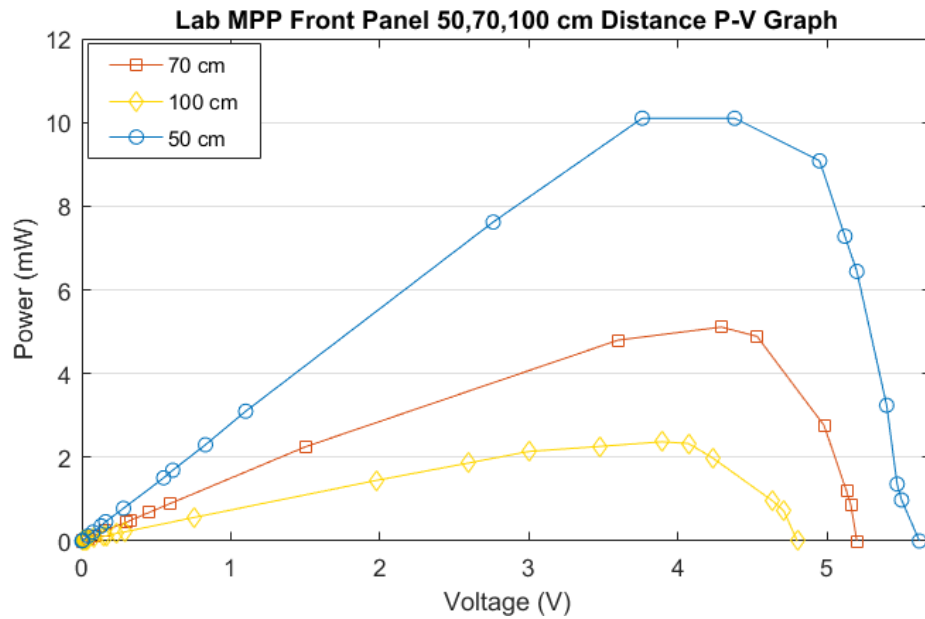


Figure 3.2 P-V graphs of front panel for 50, 70 and 100 cm distances

In Figures 3.1 and 3.2, MPP measurement graphs of the front solar panel are given. I-V graph is given in Figure 3.1 and P-V graph is given in Figure 3.2.

In I-V graph of the front solar panel, MPP for 50 cm distance is at $V_{MPP} = 4.4$ V and $I_{MPP} = 2.3$ mA. $I_{SC} = 2.80$ mA and $V_{OC} = 5.6$ V. So, the fill factor of the system is about 65% for 50 cm distance. In the same way, for 70 cm distance, $V_{MPP} = 4.29$ V, $I_{MPP} = 1.19$ mA, $I_{SC} = 2$ mA and $V_{OC} = 5.2$ V. The fill factor is 58%. For 100 cm distance of the light source, $V_{MPP} = 3.89$ V, $I_{MPP} = 0.61$ mA, $I_{SC} = 1$ mA and $V_{OC} = 4.8$ V. The fill factor is about 50% for 100 cm distance. Thus, having the fill factor higher than 50% is sufficient for the solar system.

MPP is at 1.9 k Ω for 50 cm distance with about 10 mW of power; at 3.6 k Ω for 70 cm distance with about 5 mW and at 6.4 k Ω for 100 cm distance with 2.4 mW of output power. As it is seen from this information, the output power is inversely proportional with square of distance. The reason is that light flux is inversely proportional with the square of distance and the output power is proportional with the light flux. Also, it can be understood that as the incoming power increases, the related resistor value for MPP decreases.

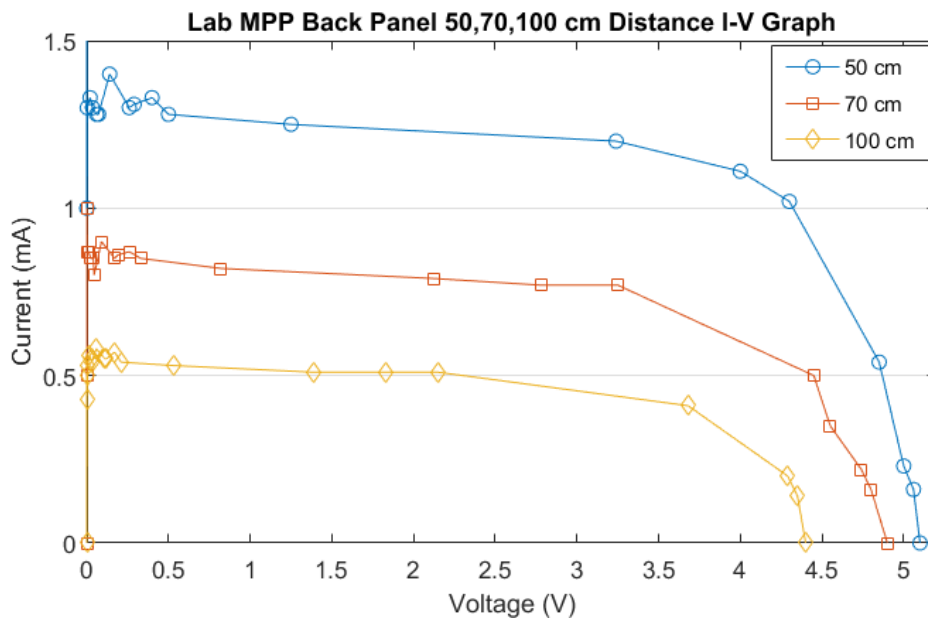


Figure 3.3 I-V graphs of back panel for 50, 70 and 100 cm distances

In Figures 3.3 and 3.4, MPP measurement graphs of the back panel are given. I-V graph is given in Figure 3.3 and P-V graph is given in Figure 3.4.

In I-V graph of the back panel, MPP for 50 cm distance is at $V_{MPP} = 4$ V and $I_{MPP} = 1.11$ mA. $I_{SC} = 1.50$ mA and $V_{OC} = 5.10$ V. So, the fill factor of the system is 58% for 50 cm distance. In the same way, for 70 cm distance, $V_{MPP} = 3.25$ V, $I_{MPP} = 0.77$ mA, $I_{SC} = 1$ mA and $V_{OC} = 4.9$ V. The fill factor is 51%. For 100 cm distance of the light source, $V_{MPP} = 3.68$ V, $I_{MPP} = 0.41$ mA, $I_{SC} = 0.5$ mA and $V_{OC} = 4.4$ V. The fill factor is 69% for 100 cm distance. Thus, in general the fill factors are higher than 50%. On the other hand, they are near to 50%; therefore, some fill factor increasing studies may be needed to have higher efficiencies for back solar panel.

MPP is at 3.6 k Ω for 50 cm distance with 4.44 mW of power; it is at 4.2 k Ω for 70 cm distance with 2.52 mW and at 9 k Ω for 100 cm distance with 1.51 mW of output power. On the back panel, light fluxes are 1110, 790, and 460 for 50, 70 and 100 cm distances, respectively.

Another note is that while the output powers are decreasing inversely proportional to squares of the distances for front panel case [222]; they are not inversely proportional with squares of distances for back panel cases. For example, in front panel case, output power of 100 cm distance case is one quarter of the output of 50 cm case which is the inverse ratio of square of the distance. On the other hand, in back panel case, this ratio becomes about one third. The reason of this condition is that; since there are reflectors in the system, the road which the light passes through is more than the distance. There is an extra 40 cm distance for the light to go to the back panel because the light goes firstly to the reflectors, then it goes to the back panel. For instance, in 50 cm distance-case, the real distance for the back panel is not 50 cm but it is $50+40 = 90$ cm. Similar to this case, the distance is 110 cm for 70 cm-case and it is 140 cm for 1 m-case. Having the new distance values, namely 90, 110 and 140 cm respectively, it is seen that the output power becomes inversely proportional with squares of these new distance values.

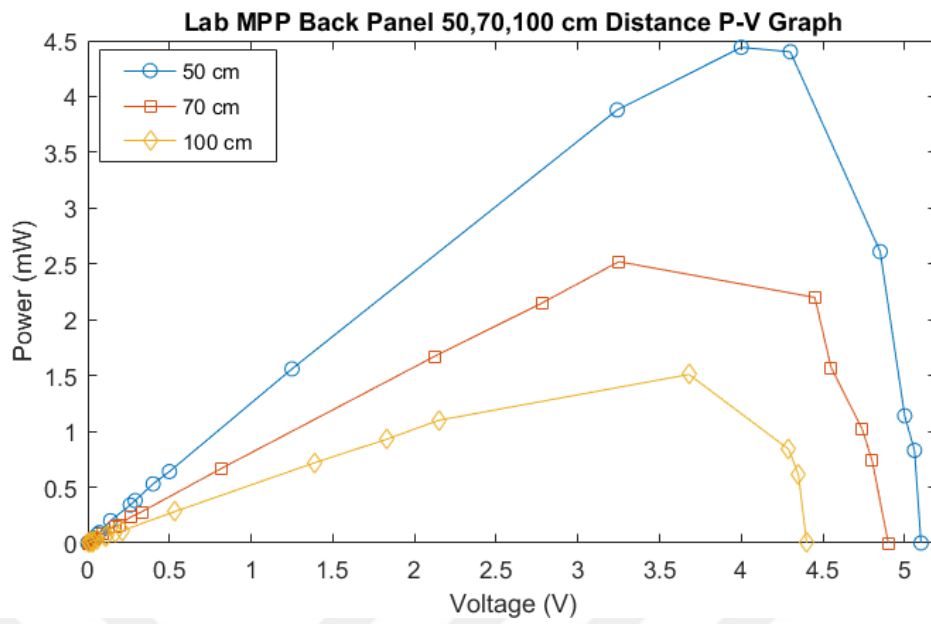


Figure 3.4 P-V graphs of back panel for 50, 70 and 100 cm distances

In Figures 3.5 to 3.10, circle-marked lines refer to front panel measurements and square-marked lines refer to back panel measurements.

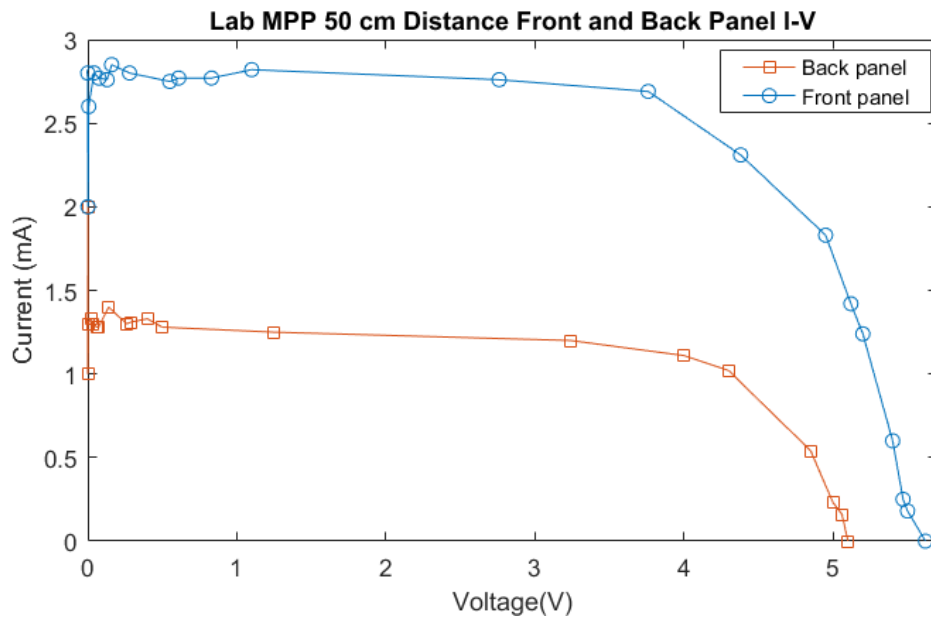


Figure 3.5 I-V graphs of front and back panels for 50 cm distance

Figures 3.5 and 3.6 are I-V and P-V graphs, respectively, of front and back panels for 50 cm-distance measurements. While the maximum power of front panel is about 10 mW, it is about 4.4 mW for the back panel. Thus, the power ratio of back panel to front panel is about 45%.

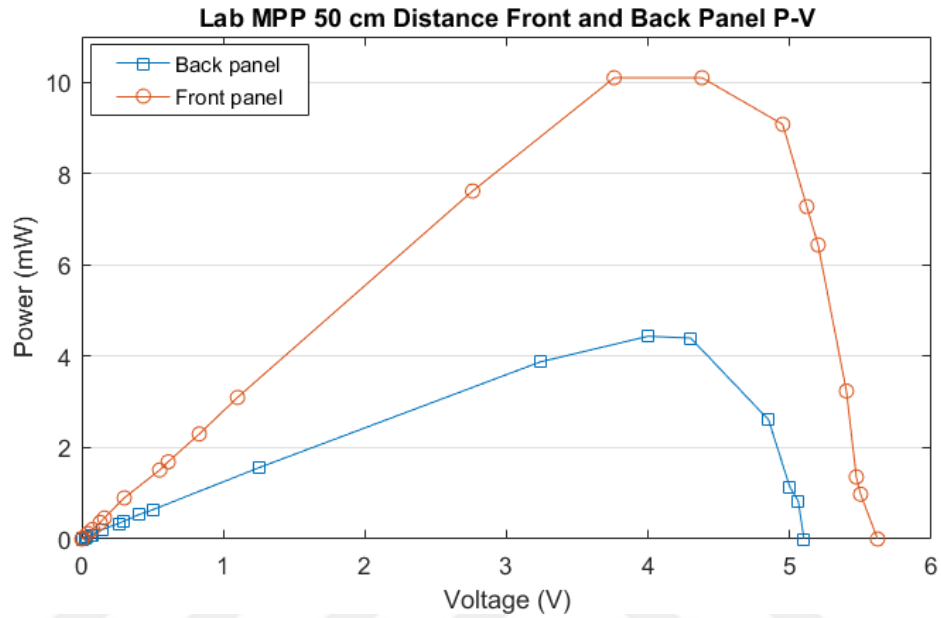


Figure 3.6 P-V graphs of front and back panels for 50 cm distance

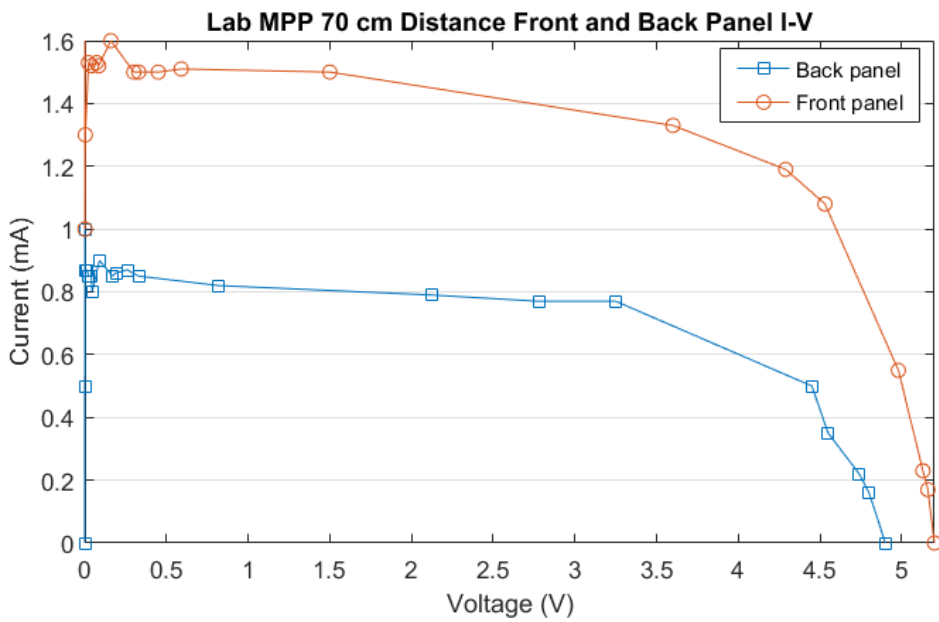


Figure 3.7 I-V graphs of front and back panels for 70 cm distance

The ratio between back panel and front panel was found as 45% from Figure 3.6. On the other hand, looking at the Figures 3.8 and 3.10, it is seen that the ratio increases. In 70 cm distance-case shown by Figure 3.8, maximum power values are about 2.5 and 5 mW. The ratio increases to 50%. In 100 cm distance-case, maximum power values are 2.3 and 1.5 mW. The ratio increases to 64% in the experiment. The underlying reason is that; since the light coming to the back panel travels firstly to the reflectors and then to the back panel, light flux is reduced more and this condition affected more by nearer distances. So, the most affected case is 50 cm-distance case and the least affected is 100 cm-case. On the other hand, in real time measurements, the sunlight is used. Thus, this kind of a loss is not seen.

Also, for better understanding, I-V graphs for 70 and 100 cm-distances are also given in Figure 3.7 and Figure 3.9 respectively.

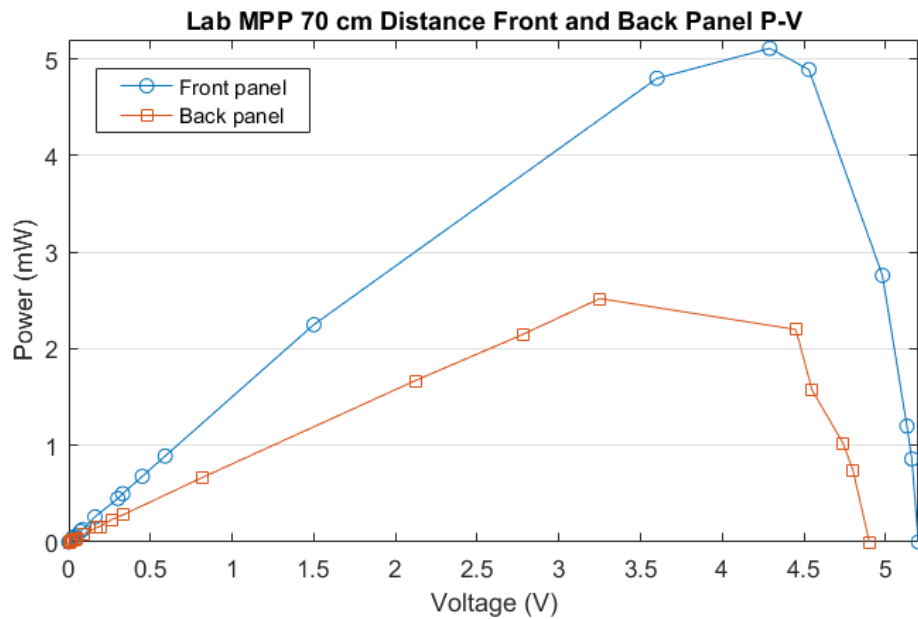


Figure 3.8 P-V graphs of front and back panels for 70 cm distance

Looking at Figure 3.9, back panel has smaller values than front panel because of the main reason that distances of back panel are always higher than front panel in laboratory because of the reflector system. So, light flux and light density decreases for the back panel. Also, relatively small reflectance rate of the mirrors and little amount of diffused radiation reaching to back panel are the other effective factors.

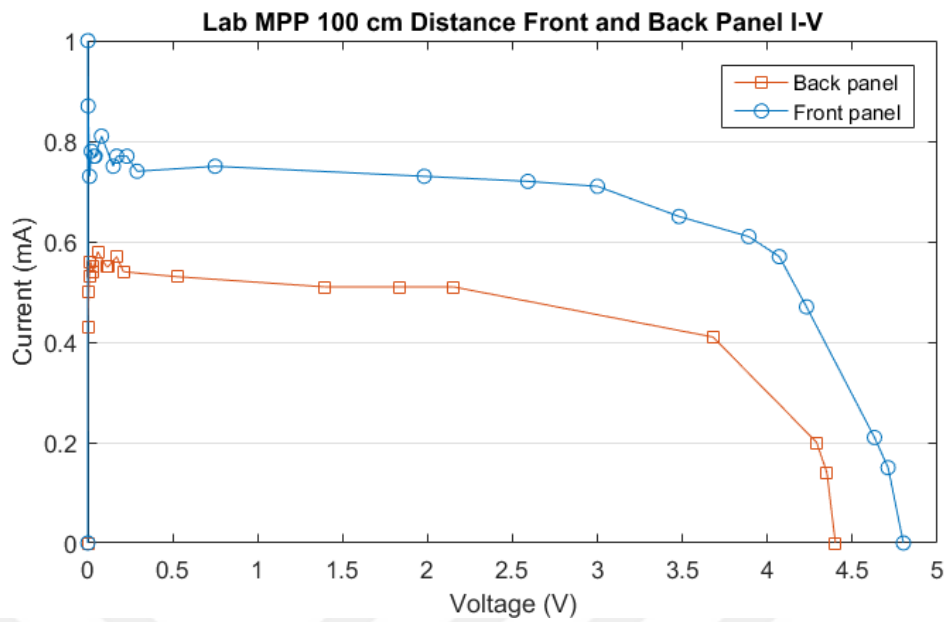


Figure 3.9 I-V graphs of front and back panels for 100 cm distance

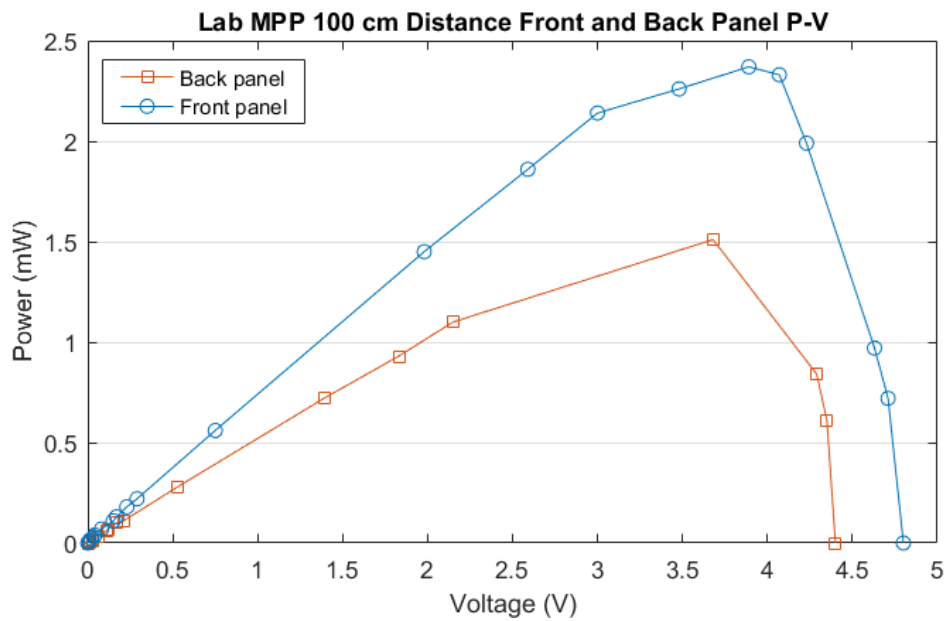


Figure 3.10 P-V graphs of front and back panels for 100 cm distance

As seen in Figure 3.10, because of the same reasons explained for Figure 3.9, power of the front panel is higher than power of the back panel. On the other hand, the main target of the system is to have high power ratios. For 100 cm measurements, the power ratio is nearly 65%. Higher power ratios are expected in real time measurements

because the effect of different distances for front and back panels does not occur in real time measurements.

3.1.3 Laboratory Simulation Measurement Values in Tables

During laboratory measurements, all zenith angles were provided to the system manually. These measurements were done for 3.6 k Ω resistors because this is the MPP resistor value or near-to-MPP value for the cases in laboratory.

The “Source Angle” values in the tables in Chapter 3.1.3 do not refer the angle between the solar system and the light source; instead, they refer the angle of the light source holder to the ground. In other words, “Source Angle” is the angle seen on the goniometer of the light source, as mentioned in Chapter 2.1.9.

Tables 3.7, 3.8, 3.9, 3.10, 3.11 and 3.12 demonstrates simulation measurements of real time done in laboratory. Angles of the light source were used to imitate positions of the sun during day hours.

Table 3.7 Lab measurement results of back-side panel: Tracking system with 30° of tilt angle

Source Angle (Degree)	Light Flux (Lx)	Voltage (Volts)	Current (mA)	Power (mW)
0	114	0.39	0.11	0.04
15	163	0.74	0.21	0.15
30	375	0.90	0.25	0.23
45	592	0.99	0.28	0.27
60	594	1.04	0.29	0.30
75	730	2.14	0.59	1.27
90	712	2.17	0.60	1.31
105	698	2.12	0.59	1.25
120	651	1.43	0.40	0.57
135	626	0.86	0.24	0.21
150	425	0.71	0.20	0.14
165	142	0.55	0.15	0.08
180	83	0.31	0.09	0.03

Table 3.8 Lab measurement results of front-side panel: Tracking system with 30° of tilt angle

Source Angle (Degree)	Light Flux (Lx)	Voltage (Volts)	Current (mA)	Power (mW)
0	337	1.02	0.28	0.29
15	703	1.94	0.54	1.05
30	954	2.39	0.66	1.59
45	1180	2.65	0.74	1.95
60	1185	2.67	0.74	1.98
75	1320	2.89	0.80	2.32
90	1289	2.85	0.79	2.26
105	1141	2.65	0.74	1.95
120	1055	2.49	0.69	1.72
135	958	2.21	0.61	1.36
150	755	1.94	0.54	1.05
165	564	1.56	0.43	0.68
180	333	0.95	0.26	0.25

Table 3.9 Lab measurement results of back-side panel: Tracking system with 45° of tilt angle

Source Angle (Degree)	Light Flux (Lx)	Voltage (Volts)	Current (mA)	Power (mW)
0	98	0.41	0.11	0.05
15	139	0.66	0.18	0.12
30	571	0.79	0.22	0.17
45	598	1.40	0.39	0.54
60	718	2.13	0.59	1.26
75	784	2.31	0.64	1.48
90	639	1.92	0.53	1.02
105	682	2.02	0.56	1.13
120	632	1.85	0.51	0.95
135	592	1.31	0.36	0.48
150	416	0.84	0.23	0.20
165	342	0.71	0.20	0.14
180	99	0.42	0.12	0.05

Table 3.10 Lab measurement results of front-side panel: Tracking system with 45° of tilt angle

Source Angle (Degree)	Light Flux (Lx)	Voltage (Volts)	Current (mA)	Power (mW)
0	426	1.21	0.34	0.41
15	638	1.82	0.51	0.92
30	802	2.10	0.58	1.23
45	903	2.37	0.66	1.56
60	1244	2.80	0.78	2.18
75	1302	2.89	0.80	2.32
90	995	2.44	0.68	1.65
105	1178	2.73	0.76	2.07
120	1144	2.71	0.75	2.04
135	1009	2.60	0.72	1.88
150	866	2.31	0.64	1.48
165	645	1.91	0.53	1.01
180	370	1.24	0.34	0.43

Table 3.11 Lab measurement results of back-side panel: Fixed system with 30° of tilt angle

Source Angle (Degree)	Light Flux (Lx)	Voltage (Volts)	Current (mA)	Power (mW)
0	90	0.33	0.09	0.03
15	104	0.43	0.12	0.05
30	109	0.53	0.15	0.08
45	123	0.57	0.16	0.09
60	142	0.58	0.16	0.09
75	420	0.80	0.22	0.18
90	713	2.56	0.71	1.82
105	398	0.82	0.23	0.19
120	122	0.53	0.15	0.08
135	105	0.48	0.13	0.06
150	96	0.45	0.13	0.06
165	85	0.32	0.09	0.03
180	76	0.28	0.08	0.02

Table 3.12 Lab measurement results of front-side panel: Fixed system with 30° of tilt angle

Source Angle (Degree)	Light Flux (Lx)	Voltage (Volts)	Current (mA)	Power (mW)
0	94	0.34	0.09	0.03
15	302	1.20	0.33	0.40
30	508	1.48	0.41	0.61
45	742	1.94	0.54	1.05
60	856	2.23	0.62	1.38
75	970	2.44	0.68	1.66
90	1050	2.81	0.78	2.20
105	950	2.38	0.66	1.57
120	836	2.19	0.61	1.33
135	783	2.01	0.56	1.12
150	567	1.68	0.47	0.78
165	370	1.21	0.34	0.41
180	143	0.40	0.11	0.04

3.1.4 Laboratory Simulation Measurement Results

Lab simulation measurements were done at a distance such that when the light source was at perpendicular position to the ground, the distance of it to solar panels was 75 cm. Also plane of the front solar panel faces the light source perpendicularly when theta is 90° in 30° tilted case. The reason of changing the angles of the light source from 0° to 180° is that real life simulations of the sunlight were achieved by this way.

In Figures 3.11 and 3.12, circle-marked lines are used for 30° tilted-tracking case, square marked lines are for 45° tilted-tracking case and diamond-marked lines show 30° tilted-fixed case values.

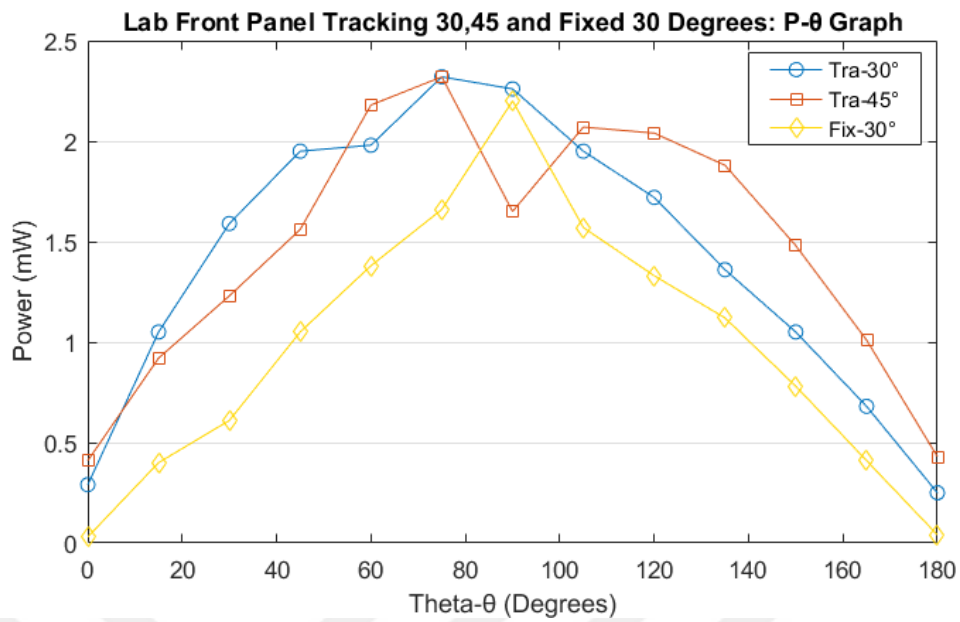


Figure 3.11 P-θ graphs of front panel for 30° tilted-tracking, 45° tracking and 30° fixed systems

Figures 3.11 and 3.12 demonstrate the effects of tracking via 30°-tilted and 30°-fixed cases. Also, the figures show the effects of changing the tilt angle of the system. Looking at Figure 3.11, the smallest values belong to the fixed 30° case. Tracking case is better than fixed case even if fixed case is 30° and tracking case is 45° as seen from the figure.

There is one drawback of 45° tracking system: When the angle is 90°, its power decreases. The reason for this case is that the light cannot reach to the front panel at 90° for 45°-tracking case. For 90°, fixed-30° becomes better than tracking-45° since it has lower incident angle but in all other cases tracking system is better than fixed case. Incident angle is the angle of coming light with the normal of the front panel.

In addition, 45°-tracking system has better results than 30°-tracking system case for smaller angles; whereas it has smaller values for higher angles.

In Figure 3.12, the values of all the cases are very small for small angles of the light source. The main reason of this case is that:

When the coming light to the panels has high incident angles, at least one of the reflectors cannot lead the light to the back panel. Also, partial shading on the back

panel occurs. As a result, output power of the back panel takes very small values for high incident angles of the coming light.

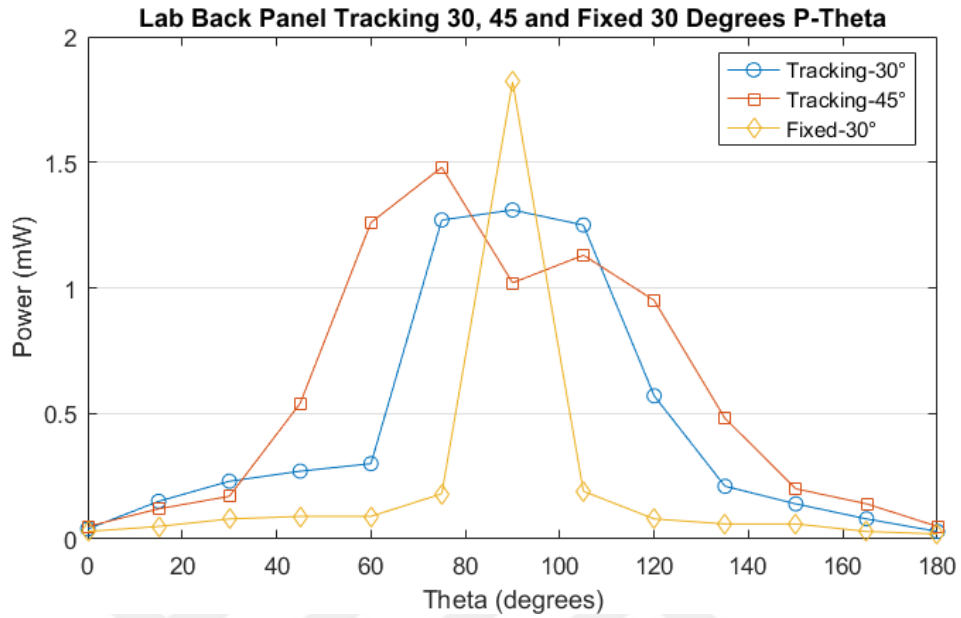


Figure 3.12 P- θ graphs of back panel for 30° tilted-tracking, 45° tracking and 30° fixed systems

In Figures 3.13 to 3.17, the circle-marked lines show values of the front panel and square-marked lines show back panel measurement values.

In addition, as seen in Figure 3.13, 3.14 and 3.15, back panel stays at very small values for small angles. The reason is the same with the case in Figure 3.12.

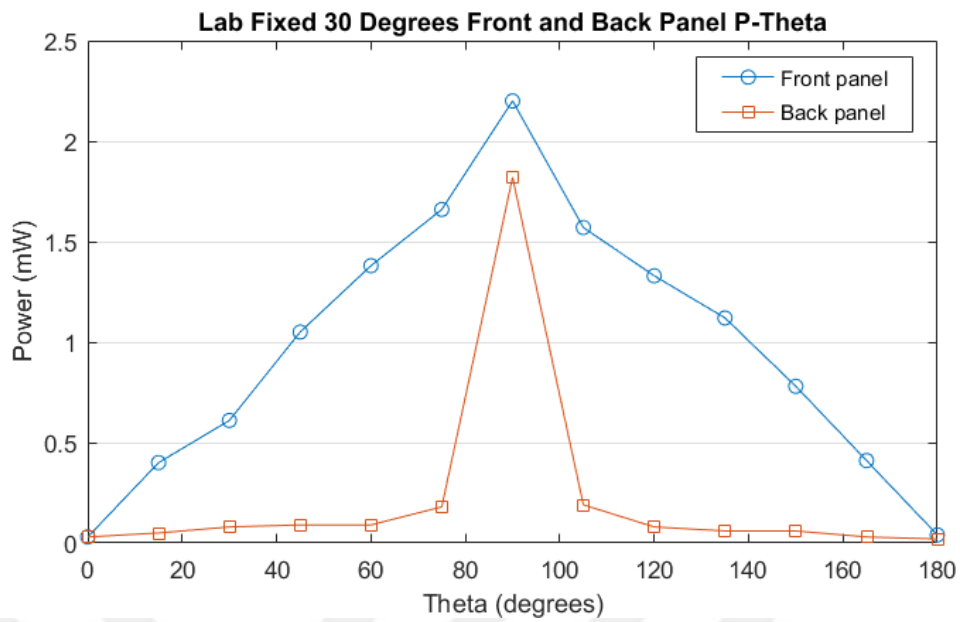


Figure 3.13 P- θ graphs of front and back panels for 30° tilted-fixed system

In Figure 3.13, when the coming light is at 90°, the power ratio of back panel to front panel is 82% for the fixed case. On the other hand, output power of the back panel drops drastically for other angles in both graphs of Figures 3.13 and 3.14. The power ratio takes the values about 60-70% in Figure 3.14 at 75°, 90° and 105° of theta.

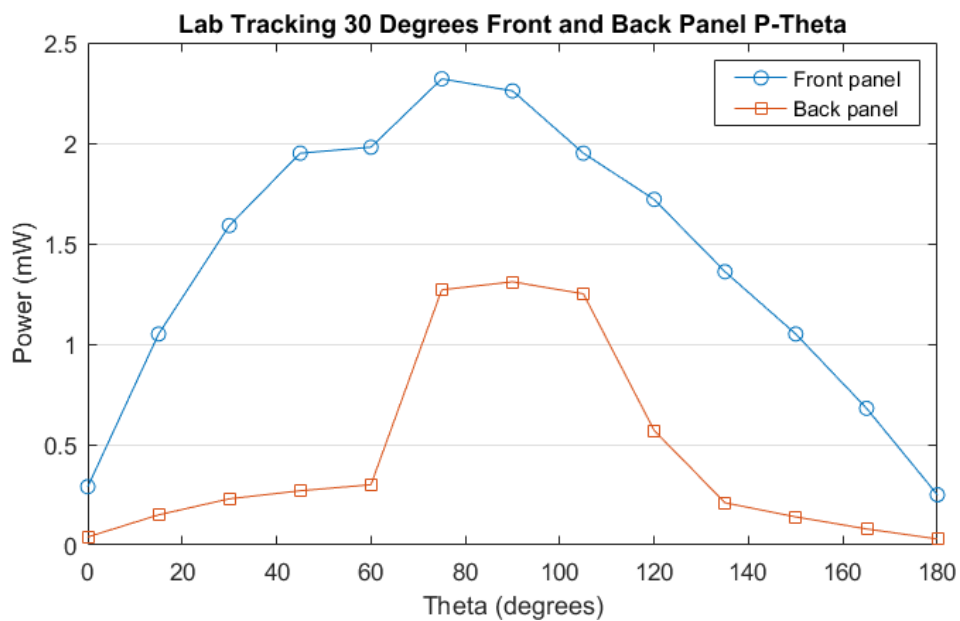


Figure 3.14 P- θ graphs of front and back panels for 30° tilted-tracking system

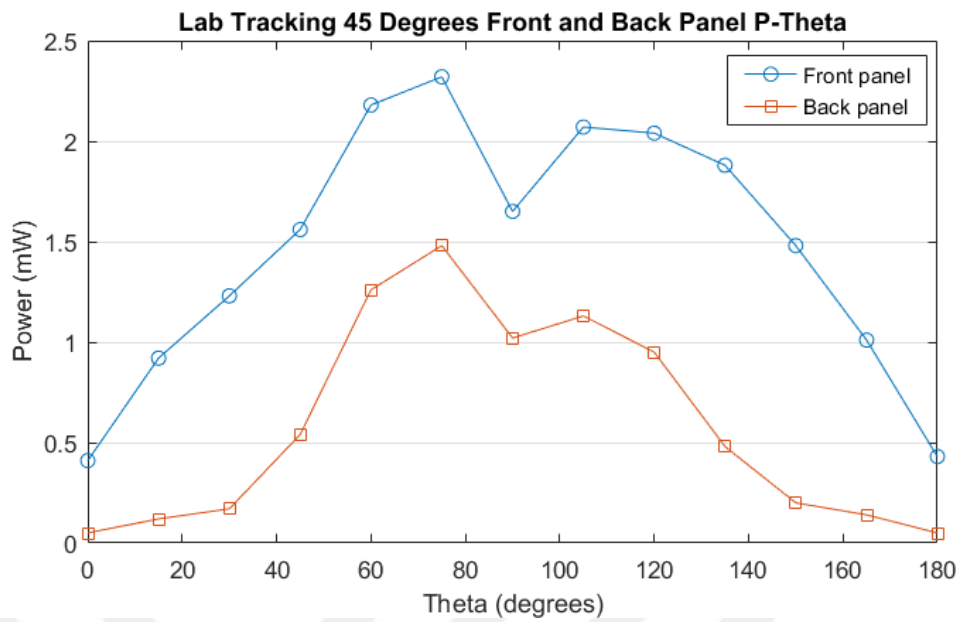


Figure 3.15 P- θ graphs of front and back panels for 45° tilted-tracking system

In Figure 3.15, similar results to 30° tilted-tracking system were obtained. The power ratio takes various values. The main reason is the incident angle of the coming light. The best power ratio is about 65% and it varies within 50-65% between the angles 60° and 120°. A considerable amount of output power was not obtained outside of these angles due to the explained reason about incident angle of coming light.

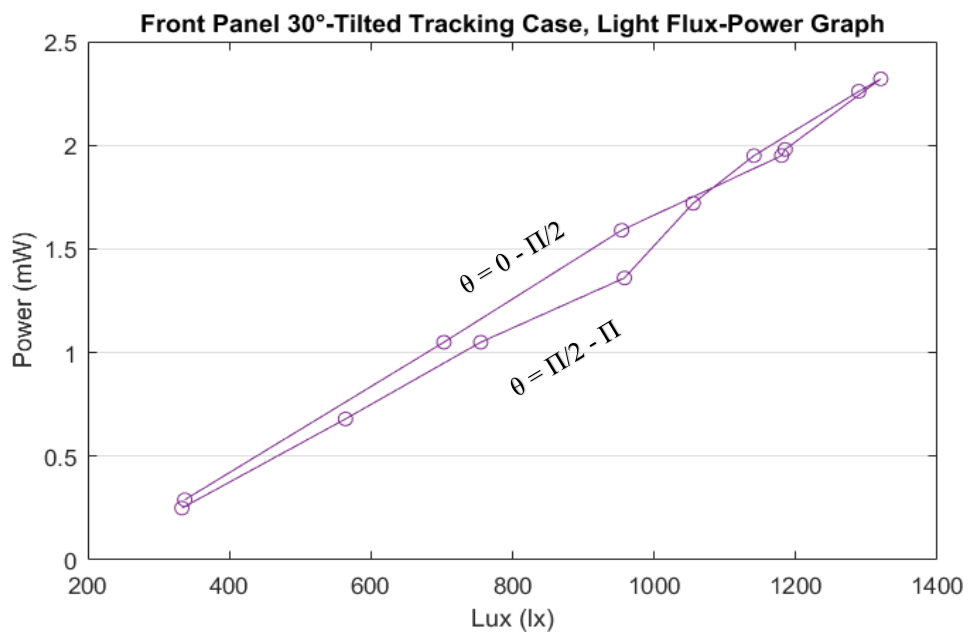


Figure 3.16 Power-Light flux graph of front panel for 30° tilted-tracking system

Figures 3.16 and 3.17 demonstrate output powers versus light fluxes of the front and back solar panels. The measurements were done from $\theta = 0^\circ$ to $\theta = 180^\circ$ with 15° -steps. The aim of these graphs is to see working performance of back panel.

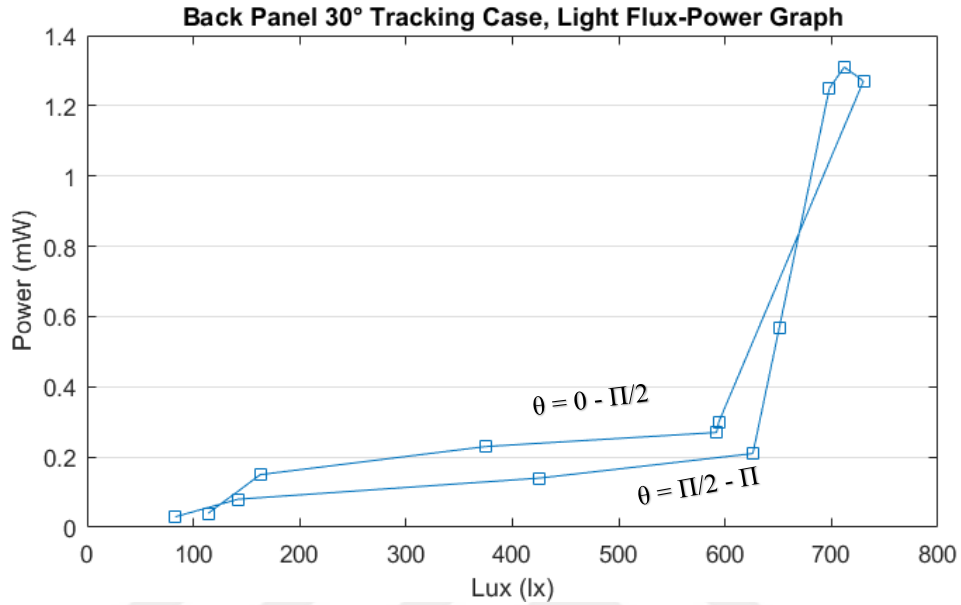


Figure 3.17 Power-Light flux graph of back panel for 30° tilted-tracking system

Normally both graphs should be linear. However, graph of the back panel is not linear. The reason is angle of incidence again. When the incoming light does not reach to the system with nearly 0° incident angle, reflectors cannot work properly or partial shading occurs. In the case of Figure 3.17, partial shading occurs because light flux is high. That means enough amounts of light reaches to the back panel. However, the back panel cannot produce sufficient electrical energy because of partial shading effect. In Figure 3.17, the back panel produces sufficient amount of power for 75° , 90° and 105° values of theta.

3.2 Real Time Measurements

During real time measurements, it was seen that real time measurement results coincide with laboratory simulation measurements in general.

Real time measurements were done in 15 Temmuz Şehitleri campus, Yıldırım Beyazıt University, Ankara, Turkey in 9th and 10th of August 2017.

For real time measurements in Chapter 3.2, all the results are given in tables firstly, then their graphs are given and the related comments are done.

3.2.1 Real Time MPP Measurement Values in Tables

Table 3.13 shows real time MPP measurement results of the back panel. The resistor values vary between 2.3Ω and $31 \text{ k} \Omega$.

Table 3.13 Real time MPP measurement values of back-side panel

R (Ω)	V (Volts)	I (mA)	P (mW)
∞ (Open Circuit)	6.67	0	0
31000	6.64	0.2	1
22000	6.62	0.3	2
9000	6.59	0.7	5
4200	6.56	1.6	10
3600	6.53	1.8	12
2700	6.53	2.4	16
1000	6.51	6.5	42
390	6.47	16.6	107
300	6.45	21.5	138
220	6.42	29.2	187
200	6.40	32.0	205
100	6.31	63.1	398
56	6.12	109.3	669
47	6.00	127.7	766
36	5.46	151.7	828
27	4.01	148.5	596
15	2.25	150.0	338
2.3	0.41	178.0	100
0 (Short Circuit)	0	180	0

There are some differences of resistor values among the tables. To obtain useful graphs for different cases, it becomes necessary to try extra resistor values for them.

Table 3.14 shows real time MPP measurement results of the front panel. The resistor values vary between 1 Ω and 31 k Ω . In total, 25 resistors were used for front panel MPP measurements.

Table 3.14 Real time MPP measurement values of front-side panel

R (Ω)	V (Volts)	I (mA)	P (mW)
∞ (Open Circuit)	6.69	0	0
31000	6.66	0.2	1
22000	6.66	0.3	2
9000	6.64	0.7	5
4200	6.63	1.6	10
3600	6.61	1.9	12
2700	6.60	2.5	16
1000	6.58	6.6	43
390	6.56	17	110
300	6.54	22	143
220	6.52	30	193
200	6.50	33	211
100	6.42	64	412
56	6.27	112	702
47	6.19	132	815
36	6.03	168	1010
27	5.85	217	1268
18.2	5.14	282	1452
17.3	4.99	288	1439
15	4.59	306	1404
13.5	4.35	322	1402
9	3.25	361	1174
7.5	2.74	365	1001
5	1.87	374	700
2.3	0.86	374	322
1	0.38	380	144
0 (Short Circuit)	0	375	0

3.2.2 Real Time MPP Measurement Results

MPP measurements were done at 12:30 in 09.08.2017, Ankara, Turkey with 30° of zenith angle given to the system. During real time and laboratory measurements, all tilt angles of the system were provided to the system manually.

In Figures 3.18 and 3.19 which are MPP measurement graphs, circle-marked lines show the front solar panel measurement results and square-marked lines show the back panel results.

Figure 3.18 has I-V graphs of front and back panels, while Figure 3.19 has P-V graphs of them.

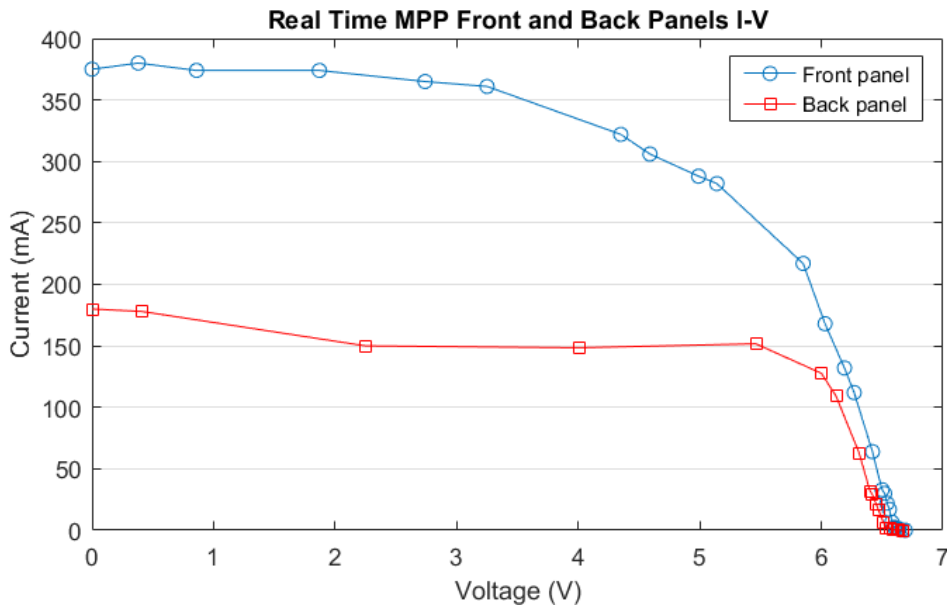


Figure 3.18 I-V graphs of front and back panels

MPP occurred at 18Ω -resistor with about 1450 mW of power for the front panel and it is at 36Ω -resistor with about 830 mW of power for the back panel.

In I-V graph of front solar panel, MPP is at $V_{MPP} = 5.14$ V and $I_{MPP} = 282$ mA. $I_{SC} = 375$ mA and $V_{OC} = 6.69$ V. So, fill factor of the front panel is %58. In the same way, MPP is at $V_{MPP} = 5.46$ V and $I_{MPP} = 152$ mA. $I_{SC} = 180$ mA and $V_{OC} = 6.67$ V for the back panel. Thus, fill factor of the back panel is about %69. The fill factor of back

solar panel is higher than the front panel. Also, both panels have sufficient levels of FF values in practice.

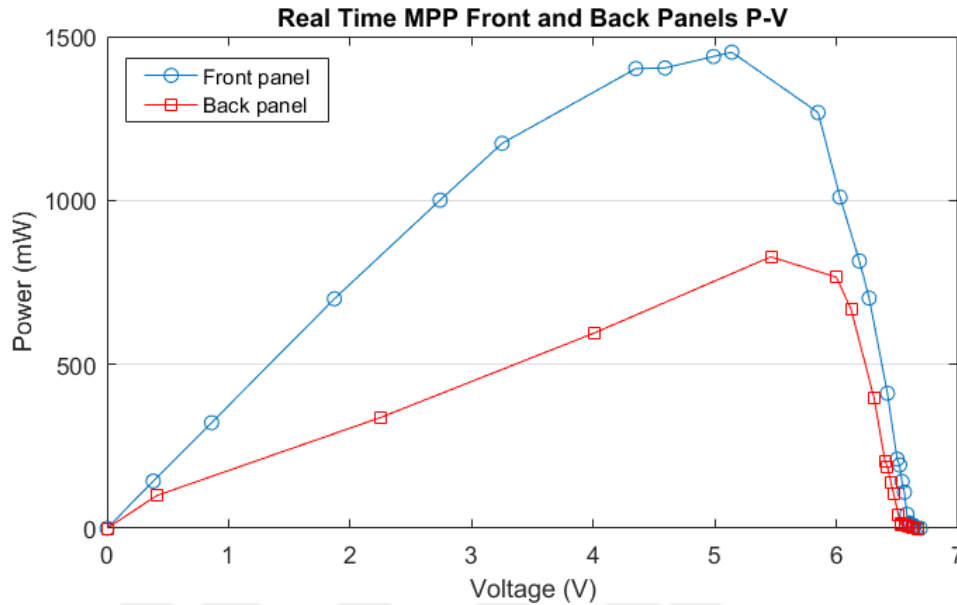


Figure 3.19 P-V graphs of front and back panels

Looking at Figure 3.19, the efficiency of the front panel can be calculated. The sunlight radiation is about 800 Wm^{-2} at noon hours in August, in general [221]. Thus, $800 \text{ Wm}^{-2} \times 0.015 \text{ m}^2 = 12 \text{ W}$ is the total light power reaching to the front panel. At MPP, the output power of the front panel is 1450 mW. Therefore, the efficiency of the front panel is $1.45 / 12 = 12\%$. Having the information that amorphous silicon solar panels have low efficiencies, this result is sufficient for the experiment.

At MPPs of two panels, the power ratio between back and front panel becomes 58%. There are some reasons under this condition. One reason is that the quality of the reflectors was found in Chapter 2.1.1 as 80% which might be increased. Another reason is that, the reflectors have equal amount of areas with the panels. Thus, any small angular change might result partial shading and the output voltage drops. Another important reason is diffused and reflected sunlight radiations which could not reach to the back panel enough.

3.2.3 Real Time Hour-Based Measurement Values in Tables

Tables from 3.15 to 3.22 have the values of real time measurements. These measurements were done hourly during daytimes. The values are averages of two-day measurements. The system was measured for four different cases: 30°-tilted (zenith) fixed system, 30°-tilted tracking system, 45°-tilted fixed system and 45°-tilted tracking system. The measurements were done as voltages; then the current and power values were calculated.

For the real time hour based measurements, energy calculations are done through summation of all the power values.

Real time measurements were done with 27Ω-resistors because MPP occurs around this value.

Table 3.15 Real time measurement values of back-side panel: Fixed system with 30° tilt angle

Hour	V (Volts)	I (mA)	P (mW)
06:00	0.28	0.01	3
07:00	0.47	0.02	8
08:00	0.61	0.02	14
09:00	1.16	0.04	50
10:00	1.47	0.05	80
11:00	3.64	0.13	491
12:00	5.02	0.19	933
13:00	3.96	0.15	581
14:00	5.52	0.20	1129
15:00	3.16	0.12	370
16:00	1.89	0.07	132
17:00	0.67	0.02	17
18:00	0.47	0.02	8
19:00	0.24	0.01	2

Table 3.16 Real time measurement values of front-side panel: Fixed system with 30° tilt angle

Hour	V (Volts)	I (mA)	P (mW)
06:00	1.14	0.04	48
07:00	2.51	0.09	233
08:00	3.12	0.12	361
09:00	5.29	0.20	1036
10:00	5.39	0.20	1076
11:00	5.55	0.21	1141
12:00	5.82	0.22	1255
13:00	5.75	0.21	1225
14:00	5.81	0.22	1250
15:00	5.77	0.21	1233
16:00	5.22	0.19	1009
17:00	3.26	0.12	394
18:00	1.10	0.04	45
19:00	0.38	0.01	5

Table 3.17 Real time measurement values of back-side panel: Tracking system with 30° tilt angle

Hour	V (Volts)	I (mA)	P (mW)
06:00	0.31	0.01	4
07:00	0.46	0.02	8
08:00	0.97	0.04	35
09:00	1.30	0.05	63
10:00	1.52	0.06	86
11:00	3.95	0.15	578
12:00	5.55	0.21	1141
13:00	4.42	0.16	724
14:00	5.91	0.22	1294
15:00	4.38	0.16	711
16:00	1.21	0.04	54
17:00	1.06	0.04	42
18:00	0.78	0.03	23
19:00	0.34	0.01	4

Table 3.18 Real time measurement values of front-side panel: Tracking system with 30° tilt angle

Hour	V (Volts)	I (mA)	P (mW)
06:00	2.18	0.08	176
07:00	4.72	0.17	825
08:00	5.49	0.20	1116
09:00	5.81	0.22	1250
10:00	5.71	0.21	1208
11:00	5.59	0.21	1157
12:00	5.84	0.22	1263
13:00	5.87	0.22	1276
14:00	5.90	0.22	1289
15:00	5.84	0.22	1263
16:00	5.85	0.22	1268
17:00	5.56	0.21	1145
18:00	4.01	0.15	596
19:00	1.63	0.06	98

Table 3.19 Real time measurement values of back-side panel: Fixed system with 45° tilt angle

Hour	V (Volts)	I (mA)	P (mW)
06:00	0.35	0.01	5
07:00	0.44	0.02	7
08:00	0.61	0.02	14
09:00	1.11	0.04	46
10:00	1.28	0.05	61
11:00	1.48	0.05	81
12:00	1.54	0.06	88
13:00	1.84	0.07	125
14:00	1.64	0.06	100
15:00	1.22	0.05	55
16:00	0.97	0.04	35
17:00	0.67	0.02	17
18:00	0.47	0.02	8
19:00	0.27	0.01	3

Table 3.20 Real time measurement values of front-side panel: Fixed system with 45° tilt angle

Hour	V (Volts)	I (mA)	P (mW)
06:00	0.71	0.03	19
07:00	1.67	0.06	103
08:00	2.64	0.10	258
09:00	5.14	0.19	979
10:00	5.35	0.20	1060
11:00	5.44	0.20	1096
12:00	5.75	0.21	1225
13:00	5.67	0.21	1191
14:00	5.75	0.21	1225
15:00	5.62	0.21	1170
16:00	4.97	0.18	915
17:00	2.60	0.10	250
18:00	0.90	0.03	30
19:00	0.45	0.02	8

Table 3.21 Real time measurement values of back-side panel: Tracking system with 45° tilt angle

Hour	V (Volts)	I (mA)	P (mW)
06:00	0.34	0.01	4
07:00	0.56	0.02	12
08:00	0.98	0.04	36
09:00	1.34	0.05	67
10:00	4.10	0.15	623
11:00	1.79	0.07	119
12:00	1.87	0.07	130
13:00	1.85	0.07	127
14:00	1.84	0.07	125
15:00	4.98	0.18	919
16:00	5.35	0.20	1060
17:00	1.08	0.04	43
18:00	0.94	0.03	33
19:00	0.42	0.02	7

Table 3.22 Real time measurement values of front-side panel: Tracking system with 45° tilt angle

Hour	V (Volts)	I (mA)	P (mW)
06:00	1.57	0.06	94
07:00	5.04	0.19	941
08:00	5.77	0.21	1233
09:00	5.86	0.22	1272
10:00	5.71	0.21	1208
11:00	5.68	0.21	1195
12:00	5.67	0.21	1191
13:00	5.73	0.21	1216
14:00	5.85	0.22	1268
15:00	5.91	0.22	1294
16:00	5.93	0.22	1302
17:00	5.83	0.22	1259
18:00	4.95	0.18	908
19:00	2.23	0.08	184

3.2.4 Real Time Hour-Based Measurement Results

Real time measurements were done hourly from 06:00 to 19:00 in 09.08.2017 and 10.08.2017, Ankara, Turkey. In real time measurements, all zenith angles were provided to the system manually.

On all the figures within Chapter 3.2.4, circle-marked lines show the front solar panel measurement results and square-marked lines show the back panel results.

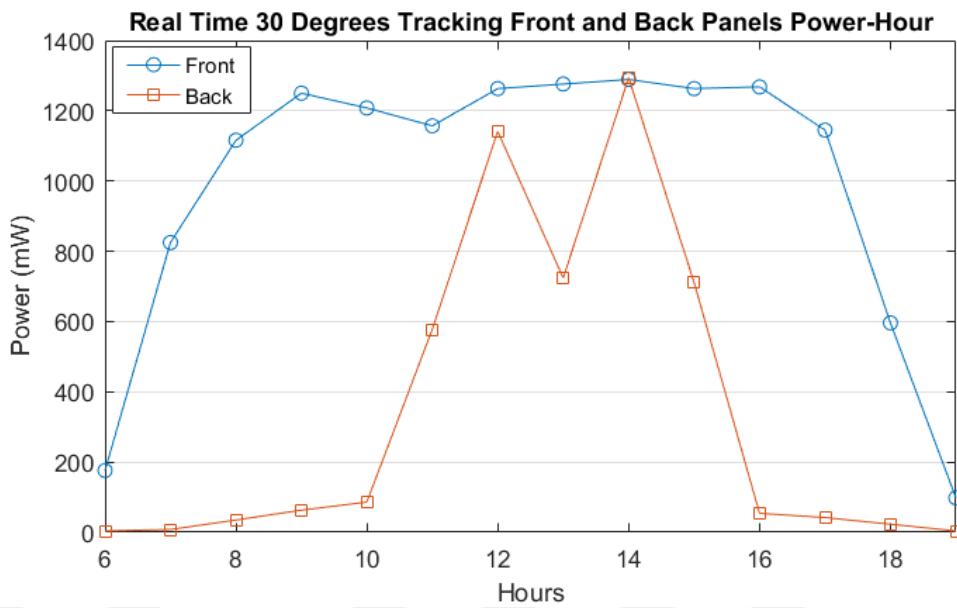


Figure 3.20 Power-Hour graphs of front and back panels for 30°-tilted tracking system

In Figure 3.20, it is seen that the back panel worked well at hours 12:00 and 14:00. At 12 am, the power ratio is 90% and it is 100% at 14:00. Thus, it is seen that the back panel provides sufficient output power under proper conditions. The same condition is seen on Figure 3.21. At 12:00 and 14:00, the back panel produces high amounts of power. The power ratio becomes 75% at 12:00 and 90% at 14:00.

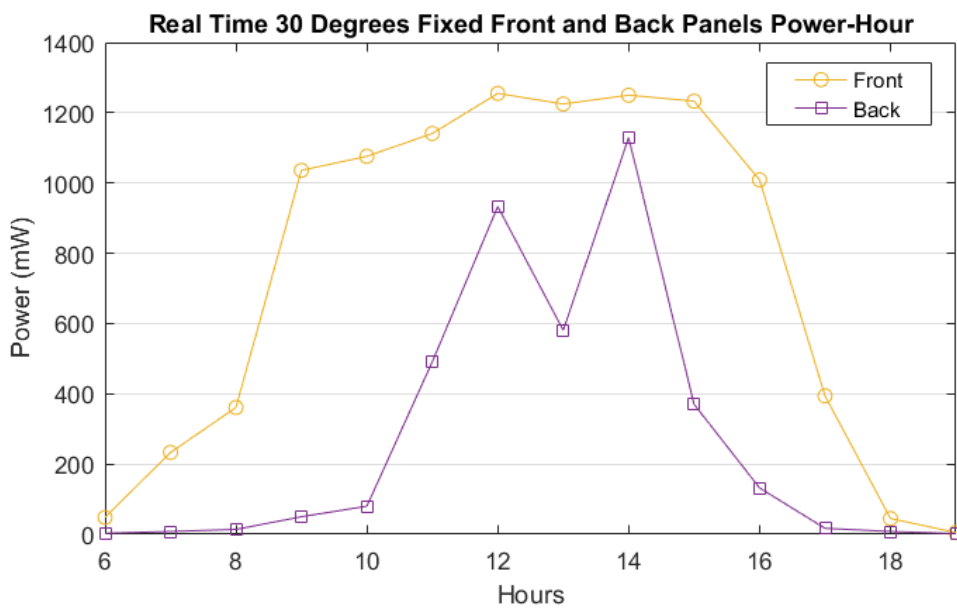


Figure 3.21 Power-Hour graphs of front and back panels for 30°-tilted fixed system

An important drawback of the experimental set up is that back solar panel does not work properly if the angle of incidence of the sunlight is away from 0° . This condition is obviously seen in the graphs in Figures 3.20, 3.21, 3.24. When the incident angle low enough, the back panel provides high amount of power and vice versa. Moreover, due to even a small diversion from 0° , back panel is affected strongly as the power reduces at 13:00 in Figures 3.20 and 3.21. Also, the back panel has low output powers for all the hours in Figure 3.25 because it cannot catch any low incident angle. In Figure 3.24 which has the results of 45° -tilted tracking system, a strange condition happens. Since the tilt angle of the system is 45° , the back panel cannot have sufficiently low incident angles at noon times, namely at 11:00, 12:00, 13:00 and 14:00. Thus, it cannot supply enough output power. On the other hand, the back panel produces considerable amounts of power at the hours which the sunlight radiance is lower, namely 10:00, 15:00 and 16:00. Also, it loses the right angle at the other hours and output power of the back panel reduces again.

There is a main reason for the case explained in the previous paragraph. The reason is “partial shading” as shown in Figure 3.22. As seen in the figure, four lines of solar cells (16 cells in total) took the sunlight but the bottom two lines (8 cells in total) could not take it. When the system does not face the sun at low incident angles near to 0° , the partial shading on back panel occurs and it cannot produce considerable amounts of power. This kind of partial shading occurs when the sunlight moves away from 0° vertically (in south-north direction).



Figure 3.22 Partial shading seen on back solar panel

On the other hand, for fixed system cases, when the sunlight deviates from being normal to the front panel horizontally (in east-west direction), the reflector system does not work properly. While one of the reflectors takes a proper angle, the other cannot take the needed angle since they are controlled together. Figure 3.23 expresses this reason visually. To sum up, vertical diversions of the sun result partial shading whereas horizontal diversions result inadequacy on the reflector system.

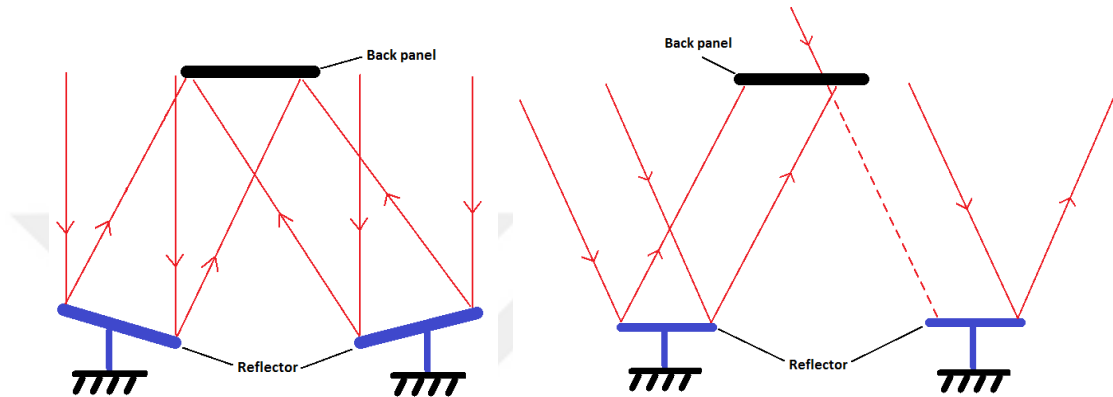


Figure 3.23 Reflector system with proper angle (left) and without proper angle (right)

In Figure 3.24, since proper angles are provided at 15:00 and 16:00, the back panel output power rises. The power ratio is 71% at 15:00 and 81% at 16:00 in Figure 3.24 for 45°-tilted tracking case, being similar to the cases in Figures 3.20 and 3.21.

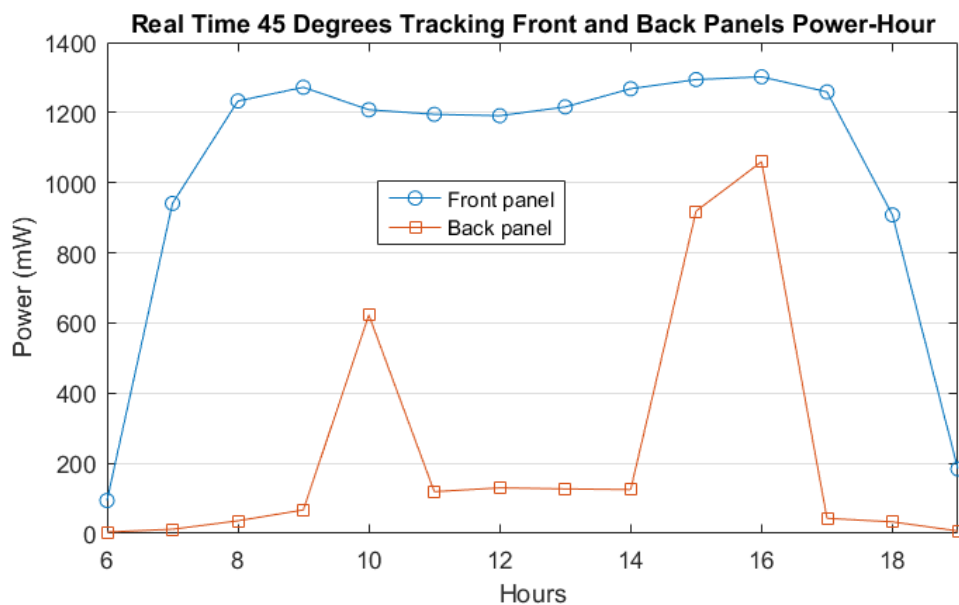


Figure 3.24 Power-Hour graphs of front and back panels for 45°-tilted tracking system

In Figure 3.25, since the back panel cannot have any angle near to 90°, it cannot give any considerable amount of output power.

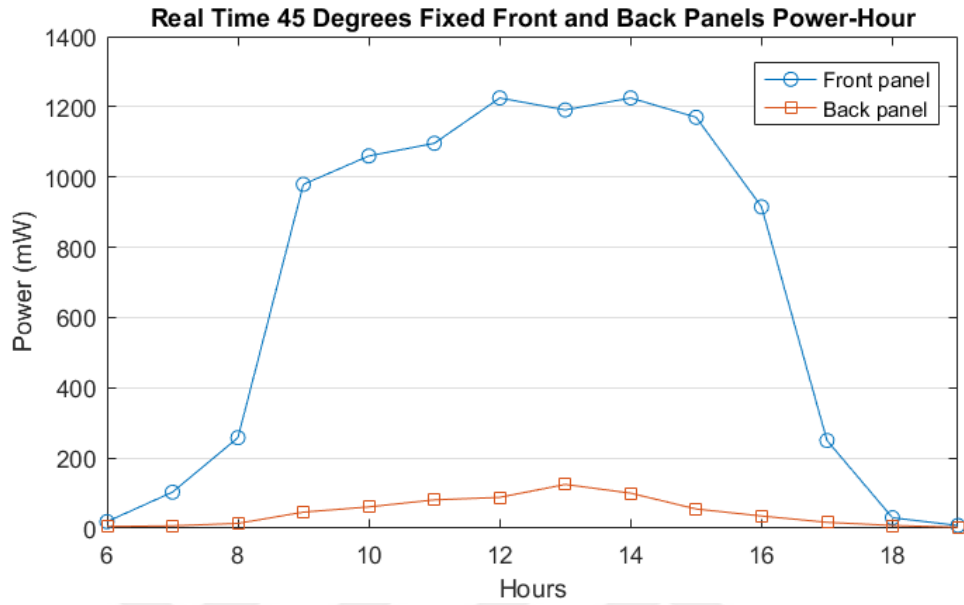


Figure 3.25 Power-Hour graphs of front and back panels for 45°-tilted fixed system

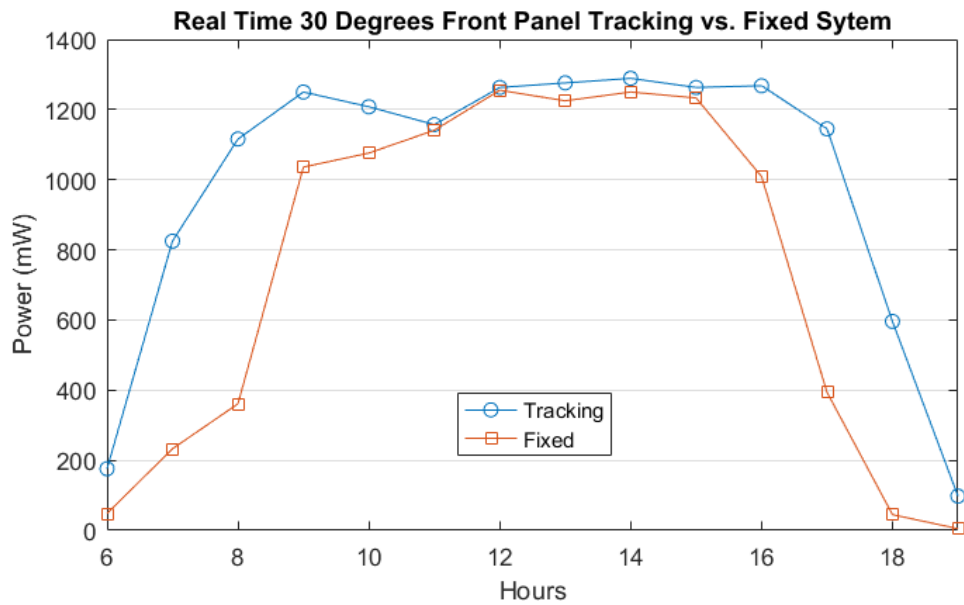


Figure 3.26 Power-Hour graphs of tracking vs. fixed systems of front panel for 30°-tilted case

In Figures 3.26 and 3.27, the effect of sun trackers is seen. While the maximum output power values are similar, the tracking systems have wider areas than the fixed ones on

both graphs of the figures. Thus, sun tracking systems provide more energy than the fixed system cases. Having the information that the energy of a power-hour graph is the area under the power line, in 30°-tilted case, the energy gain is about 35% and it is about 50% in 45°-tilted case. Therefore, high amounts of energy gains are achieved through utilizing sun tracking systems.

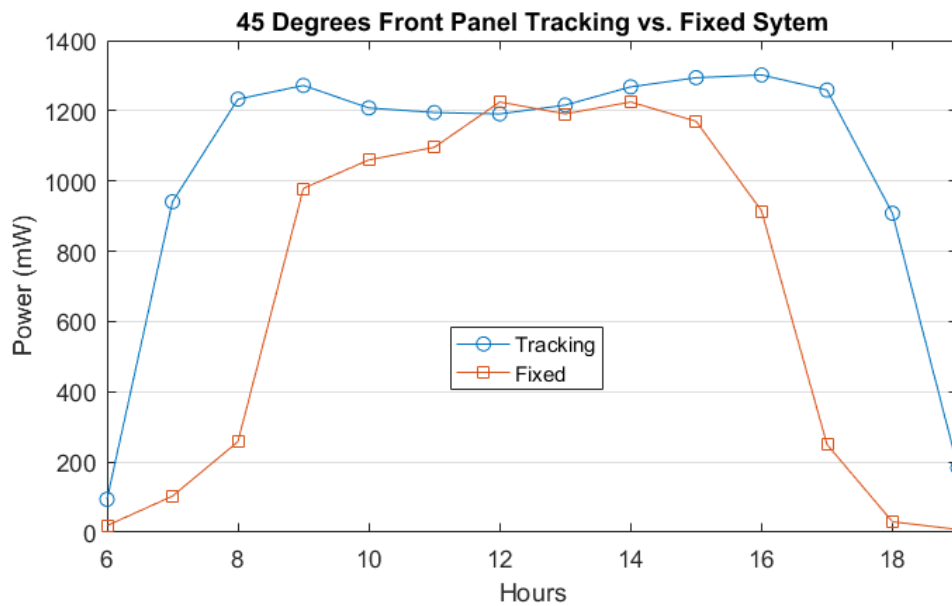


Figure 3.27 Power-Hour graphs of tracking vs. fixed systems of front panel for 45°-tilted case

In Figure 3.28, the system is with sun tracking and tilted with two different angles; 30° and 45° in south direction. There is not much difference between these two angles in Figure 3.28. However, output power values of 45°-tilted system get smaller values at noon times. The reason is that the sunlight is near to vertical to the earth; thus, 45° of tilt angle results some loss on output power at noon hours. Also, 45°-tilted system has better performance at sunset and sunrise hours because at those hours the sun has very high incident angle to the normal of the earth and 45°-tilted system has a greater projection area for the sunlight.

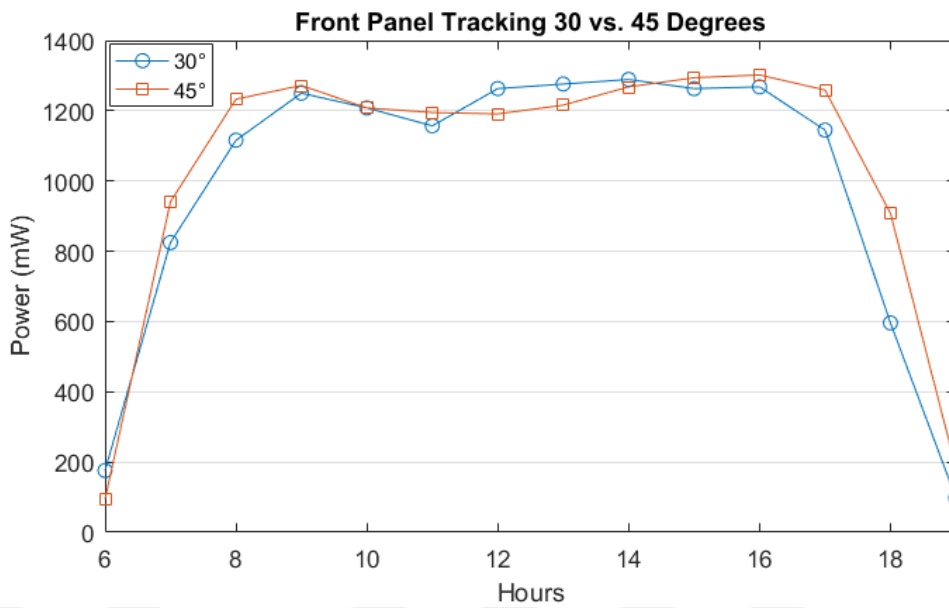


Figure 3.28 Power-Hour graphs of 30°-tilted vs. 45°-tilted tracking systems of front panel

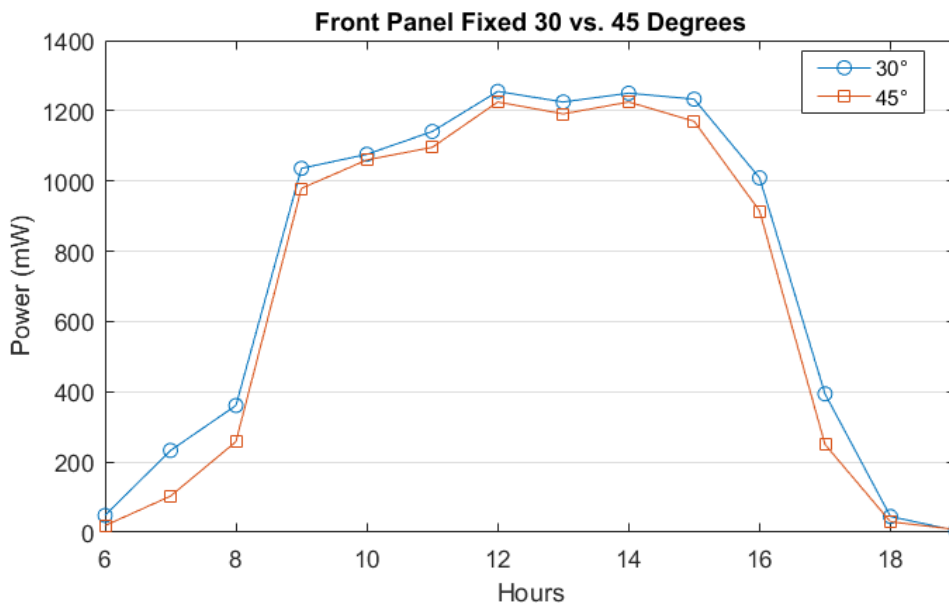


Figure 3.29 Power-Hour graphs of 30°-tilted vs. 45°-tilted fixed systems of front panel

In Figure 3.29, 30°-tilted and 45°-tilted fixed system results are given. 30°-tilted system has generally better results because it has better incident angles towards the sunlight. Computing the total energy, 30°-tilted case has about 8% of high output energy.

CHAPTER 4

DISCUSSION AND CONCLUSION

Prototype of a novel dual surface PV system with two reflectors and a single axis solar tracker was designed and constructed in this thesis study. After the system was built, the performance measurements were done in laboratory and real time. Finally, the measurement results and performance of the system were evaluated and it was seen that the dual surface PV system with sun tracker and reflectors may be used as a wholistic approach to produce electricity.

In the first part of the thesis, positions of reflectors, proper dimensions of solar panels and reflectors, number of reflectors, the sun tracking system and working principles of it, angular motion and degree of freedom of the tracker, distance between the reflectors and panels, the reflector control system, and manually configurable tilt angle of the system were designed.

After the design, the whole system was constructed. The practical difficulties were handled during the construction; such as power of the motors, voltage level of the system, power of the batteries, and diameters of pulleys and wheels.

After the construction was completed, performance measurements were done. The measurements were done in laboratory as real time simulations and was done directly as real time measurements. In general, efficiencies and fill factor values are acceptable for the cases including fixed system cases, tracking system cases, tilted cases with different angles in laboratory simulations and real time measurements.

Measurement results showed that the dual face PV system works properly under suitable conditions. In other words, when the incoming light reaches to the system with lower incident angles, the back panel produces high amounts of power with high power ratios. In other cases, namely when the incoming light reaches to the panels with higher values of incident angle, the back panel cannot produce considerable amount of power. There are two main reasons for this problem:

The first reason is partial shading. If the incoming light to the system is vertically away from being normal to the plane of front solar panel, partial shading occurs on back solar panel. Two solutions may help to improve the system against this partial shading. One solution is that using two-axis sun tracker in the system would provide zero degree of incident angle all the times. Another solution for improving the system is to use bigger reflectors. Bigger reflectors would tolerate more vertical angular motion and partial shading is retarded.

The second reason of the problem occurs when the incoming light deviates horizontally from normal of front solar panel. In case of this horizontal deviation, one of the reflectors cannot take enough light to reflect. Also, since the same pulley system stirs the reflectors, they cannot rotate independently from each other. This condition results power loss when the sunlight horizontally deviates. There are two solutions of this second reason. The first is using two-axis sun tracker like in the first reason. By this way, the sun is tracked better and the sunlight becomes normal to solar panel planes all the time. The second solution is to control the reflectors individually. Individual control of the reflectors would provide the right angle to each reflector separately for maximum production.

Another improve way for the back panel performance might be placing a mirror on the platform under the reflectors. This may provide more toleration to the sunlight both in vertical and horizontal directions.

Also, the measured power ratios between the back panel and the front panel may be increased through increasing reflector qualities. Although there are two reflectors in the system, the back panel cannot take high amounts of diffused and reflected solar radiations. Therefore, increasing reflection rates will help to increase power ratios.

To sum up, the dual surface PV system with two reflectors and a sun tracker works properly under appropriate conditions. If these suitable conditions are provided in a way, the system can be used to produce electricity in real life applications. Also, the system can be improved to tolerate wider scopes for the coming light.

REFERENCES

- [1] Joshi, A. S., Dincer, I., & Reddy, B. V., “Performance analysis of photovoltaic systems: a review”, *Renewable and Sustainable Energy Reviews*, 13(8), 1884-1897, 2009.
- [2] Johnson, G., “Plugging into the Sun”, *National Geographic*, 216(3), 28-53, 2009.
- [3] Chang J. M., Shen M. C., Huang B. J., “A criterion study of solar irradiation patterns for the performance testing of thermosyphon solar water heaters”, *Solar Energy*, 73(4):287–92, 2002.
- [4] Mathioulakis E., Belessiotis V., “A new heat-pipe type solar domestic hot water system”, *Solar Energy*, 72(1):13–20, 2002.
- [5] Madhlopa A., Mgawi R., Taulo J., “Experimental study of temperature stratification in an integrated collector-storage solar water heater with two horizontal tanks”, *Solar Energy*, 80:989–1002, 2006.
- [6] Chow T. T., He W., Ji J., Chan A. L. S., “Performance evaluation of photovoltaic–thermosyphon system for subtropical climate application”, *Solar Energy*, 81:123–30, 2007.
- [7] Ho C. D., Chen T. C., “The recycle effect on the collector efficiency improvement of double-pass sheet-and-tube solar water heaters with external recycle”, *Renewable Energy*, 31:953–70, 2006.
- [8] Lee D. W., Sharma A., “Thermal performances of the active and passive water heating systems based on annual operation”, *Solar Energy*, 81:207–15, 2007.
- [9] Pohekara S. D., Kumara D., Ramachandran M., “Dissemination of cooking energy alternatives in India—a review”, *Renewable and Sustainable Energy Reviews*, 9:379–93, 2005.

- [10] Harmim A., Boukar M., Amar M., “Experimental study of a double exposure solar cooker with finned cooking vessel”, *Solar Energy*, 82:287–9, 2008.
- [11] Buddhi D., Sharma S. D., Sharma A., “Thermal performance evaluation of a latent heat storage unit for late evening cooking in a solar cooker having three reflectors”, *Energy Conversion and Management*, 44:809–17, 2003.
- [12] Mazloumi M., Naghashzadegan M., Javaherdeh K., “Simulation of solar lithium bromide–water absorption cooling system with parabolic trough collector”, *Energy Conversion and Management*, 49:2820–32, 2008.
- [13] Youcef-Ali S., Desmons J. Y., “Influence of the aerothermic parameters and the product quantity on the production capacity of an indirect solar dryer”, *Renewable Energy*, 32:496–511, 2007.
- [14] Salihoglu N. K., Pinarli V., Salihoglu G., “Solar drying in sludge management in Turkey”, *Renewable Energy*, 32:1661–75, 2007.
- [15] Karsli S., “Performance analysis of new-design solar air collectors for drying applications”, *Renewable Energy*, 32:1645–60, 2007.
- [16] Koyuncu T., “Performance of various design of solar air heaters for crop drying applications”, *Renewable Energy*, 31:1073–88, 2006.
- [17] Elsafty A., Al-Daini A. J., “Economical comparison between a solar powered vapor absorption air-conditioning system and a vapor compression system in the Middle East”, *Renewable Energy*, 5:569–83, 2002.
- [18] Grossman G., “Solar-powered systems for cooling, dehumidification and airconditioning”, *Solar Energy*, 72(1):53–62, 2002.
- [19] Khedari J., Rawangkul R., Chimchavee W., Hirunlabh J., Watanasungsuit A., “Feasibility study of using agriculture waste as desiccant for air conditioning system”, *Renewable Energy*, 8:1617–28, 2003.

- [20] Ali C., Bacha H. B., Baccar M., Maalej A. Y., “Dynamic modelling and simulation of a new air conditioning prototype by solar energy”, *Renewable Energy*, 32:200–15, 2007.
- [21] Khattab N. M., Barakat M. H., “Modeling the design and performance characteristics of solar steam-jet cooling for comfort air conditioning”, *Solar Energy*, 73(4):257–67, 2002.
- [22] Zhou X., Yang J., Xiao B., Hou G., “Simulation of a pilot solar chimney thermal power generating equipment”, *Renewable Energy*, 32:1637–44, 2007.
- [23] Pretorius J. P., Kroger D. G., “Critical evaluation of solar chimney power plant performance”, *Solar Energy*, 80:535–44, 2006.
- [24] Chantawong P., Hirunlabh J., Zeghamati B., Khedari J., Teekasap S., Win M. M., “Investigation on thermal performance of glazed solar chimney walls”, *Solar Energy*, 80:288–97, 2006.
- [25] Karakilcik M., Dincer I., “Exergetic performance analysis of a solar pond”, *International Journal of Thermal Sciences*, 47:93–102, 2008.
- [26] Tamimi A., Rawajfeh K., “Lumped modeling of solar-evaporative ponds charged from the water of the Dead Sea”, *Desalination*, 216:356–66, 2007.
- [27] Velmurugan V., Srithar K., “Prospects and scopes of solar pond: a detailed review”, *Renewable and Sustainable Energy Reviews*, 12:2253–63, 2008.
- [28] Sencan A., Kızılkın O., Bezir N., Kalogirou S. A., “Different methods for modeling absorption heat transformer powered by solar pond”, *Energy Conversion and Management*, 48:724–35, 2007.
- [29] Garde F., Mara T., Lauret A. P., Boyer H., Celaire R., “Bringing simulation to implementation: presentation of a global approach in the design of passive solar buildings under humid tropical climates”, *Solar Energy*, 71(2):109–20, 2001.

- [30] Nordell B., Hellstrom G., “High temperature solar heated seasonal storage system for low temperature heating of buildings”, *Solar Energy*, 69(6): 511–23, 2000.
- [31] Maneewan S., Hirunlabh J., Khedari J., Zeghmami B., Teekasap S., “Heat gain reduction by means of thermoelectric roof solar collector”, *Solar Energy*, 78:495–503, 2005.
- [32] Breyer, C., & Knies, G., *Global Energy Supply Potential of Concentrating Solar Power*, Proceedings SolarPACES 2009, September 15 – 18, Berlin.
- [33] Baharwani, V., Meena, N., Dubey, A., Brighu, U., & Mathur, J., “Life Cycle Analysis of Solar PV System: A Review”, *Int J Environ Res Dev*, 4(2), 183-190, 2014.
- [34] Sherwani, A. F., & Usmani, J. A., “Life cycle assessment of solar PV based electricity generation systems: A review”, *Renewable and Sustainable Energy Reviews*, 14(1), 540-544, 2010.
- [35] Haas, R., “The value of photovoltaic electricity for society”, *Solar Energy*, 54(1), 25-31, 1995.
- [36] "Price Quotes_EnergyTrend PV", Web Address:
<http://pv.energytrend.com/pricequotes.html> , Accessed 25.12.2016.
- [37] Mellit, A., “Sizing of photovoltaic systems: a review”, *Revue des Energies Renouvelables*, 10(4), 463-472, 2007.
- [38] Fally, J., Fabre, E., & Chabot, B., “La filière photovoltaïque Polyx: état de développement et perspectives”, *Revue de l'énergie*, 37(385), 761-768, 1986.
- [39] Li, J., Chong, M., Zhu, J., Li, Y., Xu, J., Wang, P., ... & Cao, X., “35% efficient nonconcentrating novel silicon solar cell”, *Applied physics letters*, 60(18), 2240-2242, 1992.
- [40] Carlson David E., Presentation: “The Status and Outlook for the Photovoltaics Industry”, March 14, 2006, Web Address:

https://www.researchgate.net/publication/252293166_The_Status_and_Outlook_for_the_Photovoltaics_Industry , Accessed 16.02.2017.

[41] Cook, C., “The Growth of Solar Power”, Charlieonenergy, Web Address: <https://charlieonenergy.wordpress.com/2015/12/07/solar-and-moores-law/> , 2015, Accessed 18.02.2017.

[42] International Energy Agency, “Technology Roadmap: Solar photovoltaic energy”, 2010, Web Address: <http://www.iea.org/> , Accessed 20.02.2017

[43] “OpenStax CNX”, Supported by William & Flora Hewlett Foundation, Bill & Melinda Gates Foundation, 20 Million Minds Foundation, Maxfield Foundation, Open Society Foundations, and Rice University. Web Address: <http://cte-cnx-dev.cnx.org/> , <http://archive-cte-cnx-dev.cnx.org/contents/dd0537a2-fb5d-439d-8feb-bf2e50656dae@1/an-introduction-to-solar-cell-technology> , Accessed 11.02.2017.

[44] Suman, S., Khan, M. K., & Pathak, M., “Performance enhancement of solar collectors—A review”, “Renewable and Sustainable Energy Reviews”, 49, 192-210, 2015.

[45] Kalogirou, S. A., “Solar thermal collectors and applications”, “Progress in energy and combustion science”, 30(3), 231-295, 2004.

[46] Barlev, D., Vidu, R., & Stroeve, P., “Innovation in concentrated solar power”, “Solar Energy Materials and Solar Cells”, 95(10), 2703-2725, 2011.

[47] Hossain, M. S., Saidur, R., Fayaz, H., Rahim, N. A., Islam, M. R., Ahamed, J. U., & Rahman, M. M., “Review on solar water heater collector and thermal energy performance of circulating pipe”, “Renewable and Sustainable Energy Reviews”, 15(8), 3801-3812, 2011.

[48] Shukla, R., Sumathy, K., Erickson, P., & Gong, J., “Recent advances in the solar water heating systems: A review”, “Renewable and Sustainable Energy Reviews”, 19, 173-190, 2013.

- [49] Shukla, A., Buddhi, D., & Sawhney, R. L., “Solar water heaters with phase change material thermal energy storage medium: a review”, “Renewable and Sustainable Energy Reviews”, 13(8), 2119-2125, 2009.
- [50] Jaisankar, S., Ananth, J., Thulasi, S., Jayasuthakar, S. T., & Sheeba, K. N., “A comprehensive review on solar water heaters”, “Renewable and Sustainable Energy Reviews”, 15(6), 3045-3050, 2011.
- [51] Kumar, R., & Rosen, M. A., “A critical review of photovoltaic–thermal solar collectors for air heating”, “Applied Energy”, 88(11), 3603-3614, 2011.
- [52] Ho, C. K., & Iverson, B. D., “Review of high-temperature central receiver designs for concentrating solar power”, “Renewable and Sustainable Energy Reviews”, 29, 835-846, 2014.
- [53] Sharaf, O. Z., & Orhan, M. F., “Concentrated photovoltaic thermal (CPVT) solar collector systems: Part I–Fundamentals, design considerations and current technologies”, “Renewable and Sustainable Energy Reviews”, 50, 1500-1565, 2015.
- [54] Rajesh, R., & Mabel, M. C., “A comprehensive review of photovoltaic systems”, “Renewable and Sustainable Energy Reviews”, 51, 231-248, 2015.
- [55] Fthenakis, V. M., & Kim, H. C., “Photovoltaics: Life-cycle analyses”, “Solar Energy”, 85(8), 1609-1628, 2011.
- [56] SBC Energy Institute, “Solar Photovoltaic”, Web Address: <http://www.sbcenergyinstitute.com/Publications/SolarPhotovoltaic.html> , Accessed 16.02.2017.
- [57] Carlson D., Presentation: “The status and outlook for the photovoltaics industry”, BP Solar -, 2006. Braga, A. F. B., Moreira, S. P., Zampieri, P. R., Bacchin, J. M. G., & Mei, P. R., “New processes for the production of solar-grade polycrystalline silicon: A review”, “Solar energy materials and solar cells”, 92(4), 418-424, 2008.
- [58] Shah A.V., Platz R., Keppner H., “Thin-film silicon solar cells: A review and selected trends”, Solar Energy Materials and Solar Cells, 38:501-520, 1995.

[59] Dirjish, M., “What’s The Difference Between Thin-Film And Crystalline-Silicon Solar Panels?”, 2012, <http://www.electronicdesign.com/power-sources/what-s-difference-between-thin-film-and-crystalline-silicon-solar-panels> , Accessed 06.08.2017.

[60] Alchemie Limited Inc., “8 Good Reasons Why Monocrystalline Solar Panels are the Industry Standard”, <http://www.solar-facts-and-advice.com/monocrystalline.html> , Accessed 04.08.2017.

[61] “Czochralski Process and Silicon Wafers”, <https://www.waferworld.com/czochralski-process-and-silicon-wafers/> , 2016, Accessed 03.08.2017.

[62] Microchemicals GmbH, “Silicon Ingot Production: Czochralski- and Float-Zone Technique”, http://www.microchemicals.com/products/wafers/silicon_ingot_production.html , Accessed 03.08.2017.

[63] Sunpower, <http://www.sunpower.com/> , Accessed 04.08.2017.

[64] Suntech, <http://www.suntech-power.com/> , Accessed 04.08.2017.

[65] Solarcity, <http://www.solarcity.com/> , Accessed 04.08.2017.

[66] Solar Reviews, “Disadvantages of Monocrystalline solar panels”, <http://www.solarreviews.com/solar-energy/pros-and-cons-of-monocrystalline-vs-polycrystalline-solar-panels/#disadvantagesMonocrystalline> , Accessed 04.08.2017.

[67] El Chaar, L., & El Zein, N., “Review of photovoltaic technologies”, *Renewable and Sustainable Energy Reviews*, 15(5), 2165-2175, 2011.

[68] Editorial Team of Yingli Solar, “The Great Debate? Monocrystalline vs Polycrystalline Solar Panels”, <http://blog.yinglisolar.com/great-debate-monocrystalline-vs-polycrystalline-solar-panels/> , 2015; Accessed 04.08.2017.

- [69] Braga, A. F. B., Moreira, S. P., Zampieri, P. R., Bacchin, J. M. G., & Mei, P. R., “New processes for the production of solar-grade polycrystalline silicon: A review”, *Solar energy materials and solar cells*, 92(4), 418-424, 2008.
- [70] Evergreen Solar, <http://www.evergreensolar.com/> , Accessed 04.08.2017.
- [71] Manna, T. K., Mahajan, S. M., “Nanotechnology in the development of photovoltaic Cells”, In: *Proceedings of the international conference on clean electrical power*, p. 379–86, 2007.
- [72] <https://evergreensolar.com/> , Accessed 04.08.2017.
- [73] Dornberger, E., “Tiny spheres with a big effect”, *Innovations*, Wacker Co. internal newsletter, 2005.
- [74] Williams, E., “Global Production Chains and Sustainability”, United Nation University, Tokyo, Japan, 147pp, 2000.
- [75] Solar Quotes, Peacock Media Group, “Monocrystalline vs Polycrystalline Solar Panels”, <https://www.solarquotes.com.au/panels/photovoltaic/monocrystalline-vs-polycrystalline/> , Accessed 05.08.2017.
- [76] Carlson, D. E., Wronski, C. R., “Amorphous silicon solar cell”, *Applied Physics Letters*, 28:671, 1976.
- [77] Markvart, T. (Ed.), “Solar electricity” (Vol. 6), John Wiley & Sons, 2000.
- [78] Green, M. A., Hishikawa, Y., Warta, W., Dunlop, E. D., Levi, D. H., Hohl-Ebinger, J., & Ho-Baillie, A. W., “Solar cell efficiency tables (version 50)”, *Progress in Photovoltaics: Research and Applications*, 25(7), 668-676, 2017.
- [79] Yurdakoş, E. B., “The production of silicon-based solar panel for application in energy charge workstations”, M.Sc. Thesis, Dokuz Eylül University, 2015.
- [80] Lyden, S., & Haque, M. E., “Maximum Power Point Tracking techniques for photovoltaic systems: A comprehensive review and comparative analysis”, *Renewable and Sustainable Energy Reviews*, 52, 1504-1518, 2015.

- [81] Verma, D., Nema, S., Shandilya, A. M., & Dash, S. K., “Maximum power point tracking (MPPT) techniques: Recapitulation in solar photovoltaic systems”, *Renewable and Sustainable Energy Reviews*, 54, 1018-1034, 2016.
- [82] Jordehi, A. R., “Maximum power point tracking in photovoltaic (PV) systems: A review of different approaches”, *Renewable and Sustainable Energy Reviews*, 65, 1127-1138, 2016.
- [83] Ramli, M. A., Twaha, S., Ishaque, K., & Al-Turki, Y. A., “A review on maximum power point tracking for photovoltaic systems with and without shading conditions”, *Renewable and Sustainable Energy Reviews*, 67, 144-159, 2017.
- [84] Ram, J. P., Babu, T. S., & Rajasekar, N., “A comprehensive review on solar PV maximum power point tracking techniques”, *Renewable and Sustainable Energy Reviews*, 67, 826-847, 2017.
- [85] Gupta, A., Chauhan, Y. K., & Pachauri, R. K., “A comparative investigation of maximum power point tracking methods for solar PV system”, *Solar Energy*, 136, 236-253, 2016.
- [86] Skaaland, Å., Ricke, M., Wallevik, K., Strandberg, R., Imenes, A. G., “Potential and Challenges for Building Integrated Photovoltaics in the Agder Region”, Report: Prosjekt/FoU-report nr. 6/2011, ISSN: 0808-5544, Press: Kai Hansen, 4626 Kristiansand, January 2011.
- [87] Salas, V., Olias, E., Barrado, A., & Lazaro, A., “Review of the maximum power point tracking algorithms for stand-alone photovoltaic systems”, *Solar energy materials and solar cells*, 90(11), 1555-1578, 2006.
- [88] McEvoy, A., Markvart, T., Castañer, L., Markvart, T., & Castaner, L. (Eds.), “Practical handbook of photovoltaics: fundamentals and applications”, Elsevier, 2003.
- [89] National Instruments, “Part II – Photovoltaic Cell I-V Characterization Theory and LabVIEW Analysis Code”, 2012, <http://www.ni.com/white-paper/7230/en/> , Accessed 07.08.2017.

- [90] Abdelhalim Zekry, ResearchGate, "Why is the Fill Factor of Solar Cells low?", https://www.researchgate.net/post/Why_is_the_Fill_Factor_of_Solar_Cells_low , Accessed 07.08.2017.
- [91] Anyaka, B. O., Ahiabuike D. C., Mbunwe M. J., "Improvement of PV Systems Power Output Using Sun-Tracking Techniques", *International Journal of Computational Engineering Research*, 3 (9): 80–98, 2013.
- [92] Wieder, S., "An Introduction to Solar Energy for Scientists and Engineers", Wiley, 1982.
- [93] Attar, M. Z., "Enhancement of an Electronic Solar Tracking System", *International Journal of Energy Engineering*, 4(1), 5-9, 2014.
- [94] Roth P., Georgiev A., Boudinov H., "Cheap two-axis sun following device", *Energy Conversion and Management*, 46:1179–92, 2005.
- [95] Ai B., Shen H., Ban Q., Ji B., Liao X., "Calculation of the hourly and daily radiation incident on three step tracking planes", *Energy Conversion and Management*, 44:1999–2011, 2003.
- [96] Mumba J., "Development of a photovoltaic powered forced circulation grain dryer for use in the tropics", *Renewable Energy*, 6(7):855–62, 1995.
- [97] Pavel Y. V., Gonzalez H. J., Vorobiev Y. V., "Optimization of the solar energy collection in tracking and non-tracking PV solar system", In: *Proceedings of the 1st international conference on electrical and electronics engineering, ICEEE*; p. 310–4, 2004.
- [98] Helwa N. H., Bahgat A.B.G., Shafee A.M.R.E., Shenawy E.T.E., "Maximum collectable solar energy by different solar tracking systems", *Energy Sources*, 22:23–4, 2000.
- [99] Chicco G., Schlabbach J., Spertino F., "Performance of grid-connected photovoltaic systems in fixed and sun-tracking configurations", *Conference: Power Tech, 2007 IEEE Lausanne*, 677-682, 2007.

- [100] Shaltout M.A.M., Ghttas A., Sabry M., “V-trough concentrator on a PV full tracking system in a hot desert climate”, *Renewable Energy*, 6(5–6):527–32, 1995.
- [101] Baltas P., Tortoreli M., Russell P. E., “Evaluation of power output for fixed and step tracking PV arrays”, *Solar Energy*, 37(20):147–63, 1986.
- [102] Stern M., Duran G., Fourer G., Mackamul K., Whalen W., Loo M. V., et al., “Development of a low-cost integrated 20-kW-AC solar tracking sub-array for grid connected PV power system applications”, Final technical report, NRELISR- 520-2475 9, National Renewable Energy Laboratory, A National Laboratory of the U.S. Department of Energy Managed by Midwest Research Institute for the U.S. Department of Energy; June 1998.
- [103] Nann S., “Potential for tracking PV systems and V-troughs in moderate climates”, *Solar Energy*, 45(6):385–93, 1990.
- [104] Michaelides I. M., Kalogirou S. A., Chrysis I., Roditis G., Hadjiyianni A., Kambezidis H.D., et al., “Comparison of performance and cost effectiveness of solar water heaters at different collector tracking modes in Cyprus and Greece”, *Energy Conversion and Management*, 40:1287–303, 1999.
- [105] Mitton, S., “The Cambridge Encyclopedia of Astronomy”, 1st ed. London: Prentice-Hall of Canada, 1977.
- [106] Keefe, R., “Solar Cell Efficiency”, Successful Endeavours Pty Ltd., 2013, Web Address: <http://www.successful.com.au/blog/2013/11/02/solar-cell-efficiency/> , Accessed 28.02.2017.
- [107] Jordehi, Rezaee A., "Maximum power point tracking in photovoltaic (PV) systems: A review of different approaches", *Renewable and Sustainable Energy Reviews*, 65: 1127-1138, 2016.
- [108] Liu Y-H., Chen J-H., Huang J-W., “A review of maximum power point tracking techniques for use in partially shaded conditions”, *Renewable Sustainable Energy Reviews*, 41:436–53, 2015.

- [109] Ishaque K., Salam Z., “A review of maximum power point tracking techniques of PV system for uniform insolation and partial shading condition”, *Renewable Sustainable Energy Reviews*, 19:475–88, 2013.
- [110] Ishaque K., Salam Z., “A comprehensive MATLAB Simulink PV system simulator with partial shading capability based on two-diode model”, *Solar Energy*, 85:2217–27, 2011.
- [111] Abdalla I., Corda J., Zhang. L., "Multilevel DC-link inverter and control algorithm to overcome the PV partial shading", *IEEE Transactions on Power Electronics*, 28.1: 14-18, 2013.
- [112] Kok S. T. & Saad Mekhilel., “Modifed Incremental Conductance MPPT Algorithm to Mitigate Inaccurate Responses under Fastchanging Solar Irradiation Level.” *Solar Energy*, 101: 33–342, 2014.
- [113] Ünlü M., Çamur S., & Arifoğlu B., “A new maximum power point tracking method for PV systems under partially shaded conditions”, In *Power Engineering, Energy and Electrical Drives (POWERENG)*, 2013 Fourth International Conference on (pp. 1346-1351), IEEE. 2013, May.
- [114] Rodrigo P., Fernández E. F., Almonacid F., Pérez-Higueras P. J., and Perez H., “A Simple Accurate Model for the Calculation of Shading Power Losses in Photovoltaic Generators”, *Solar Energy*, 93:322–333, 2013.
- [115] Kouchaki, A., Iman-Eini H., Asaei B., “A New Maximum Power Point Tracking Strategy for PV Arrays under Uniform and Non-uniform Insolation Conditions”, *Solar Energy*, 91: 221–232, 2013.
- [116] Dadjé A., Djongyang N., Kana J. D., & Tchinda R., “Maximum power point tracking methods for photovoltaic systems operating under partially shaded or rapidly variable insolation conditions: a review paper”, *International Journal of Sustainable Engineering*, 9(4), 224-239, 2016.
- [117] Mertens, K., “Figures from the Textbook Photovoltaics”, <http://www.textbook-pv.org/figures.html> , Accessed 07.08.2017.

- [118] “How different angles of incidence of solar rays impact the performance of a solar cell”, All Science Fair Projects, http://www.all-science-fair-projects.com/print_project_1091_96 , Accessed 28.02.2017.
- [119] Racharla, S., Rajan, K., “Solar tracking system—a review”, *International Journal of Sustainable Engineering*, 1-10, 2017.
- [120] Rockwell Automation, “Solar Tracking Application.” A Rockwell Automation White Paper: 1–8, 2009.
- [121] Clifford M. J., Eastwood D., “Design of a novel passive solar tracker”, *Solar Energy*, 77:269–80, 2004.
- [122] Poulek V., “Testing the new solar tracker with shape memory alloy actors”, *Conference Record of the Twenty Fourth, IEEE Photovoltaic Specialists Conference*, 1:1131–3, 1994.
- [123] Radajewski, W., “Water-driven solar tracking mechanism”, *Energy in Agriculture* 6, 167–176, 1987.
- [124] McCluney, R., “Passive optical solar tracking system”, *Applied Optics* 22, 3433–3439, 1983.
- [125] Mousazadeh, H., Keyhani, A., Javadi, A., Mobli, H., Abrinia, K., & Sharifi, A., “A review of principle and sun-tracking methods for maximizing solar systems output”, *Renewable and sustainable energy reviews*, 13(8), 1800-1818, 2009.
- [126] Al-Atrash H., Batarseh I., Rustom K., “Effect of measurement noise and bias on hillclimbing MPPT algorithms”, *IEEE Trans Aerosp Electron Syst*, 46(2):745–60, 2010.
- [127] Safari A., Mekhilef S., “Simulation and hardware implementation of incremental conductance MPPT with direct control method using cuk converter”, *IEEE Trans Ind Electron*, 58(4):1154–61, 2011.

- [128] Wu T., Chang C., Chen Y., “A fuzzy-logic-controlled single-stage converter for PV powered lighting systems applications”, *IEEE Trans Ind Electron*, 47(2):287–96, 2000.
- [129] Femia N., Granozio D., Petrone G., Vitelli M., “Predictive & adaptive MPPT perturb and observe method”, *IEEE Trans Aerosp Electron Syst*, 43(3):934–50, 2007.
- [130] Hiyama T., Kitabayashi K., “Neural network based estimation of maximum power generation from PV module using environmental information”, *IEEE Trans Energy Convers*, 12(3):241–6, 1997.
- [131] Hiyama T., Kouzuma S., Imakubo T., “Identification of optimal operating point of PV modules using neural network for real time maximum power tracking control”, *IEEE Trans Energy Convers*, 10(2):360–7, 1995.
- [132] Dorofte C., Borup U., Blaabjerg F., “A combined two-method MPPT control scheme for grid-connected photovoltaic systems”, *European Conference in Power Electronics and Applications*, pp. 1–10, 2005.
- [133] Mutoh N., Ohno M., Inoue T., “A method for MPPT control while searching for parameters corresponding to weather conditions for PV generate systems”, *IEEE Trans Ind Electron*, 53(4):1055–65, 2006.
- [134] Mutoh N., Ohno M., Inoue T., “A control method to charge series-connected ultra-electric double-layer capacitors suitable for photovoltaic generate systems combining MPPT control method”, *IEEE Trans Ind Electron*, 54(1):374–83, 2007.
- [135] Syafaruddin, Karatepe E., Hiyama T., “Artificial neural network-polar coordinated fuzzy controller based maximum power point tracking control under partially shaded conditions”, *IET Renew Power Gen*, 3(2):239–53, 2009.
- [136] Khare, A., & Rangnekar, S., “A review of particle swarm optimization and its applications in solar photovoltaic system”, *Applied Soft Computing*, 13(5), 2997-3006, 2013.

- [137] Liu, Y. H., Huang, S. C., Huang, J. W., & Liang, W. C., "A particle swarm optimization-based maximum power point tracking algorithm for PV systems operating under partially shaded conditions", *IEEE Transactions on Energy Conversion*, 27(4), 1027-1035, 2012.
- [138] Ishaque, K., & Salam, Z., "A deterministic particle swarm optimization maximum power point tracker for photovoltaic system under partial shading condition", *IEEE transactions on industrial electronics*, 60(8), 3195-3206, 2013.
- [139] Ishaque, K., Salam, Z., Shamsudin, A., & Amjad, M., "A direct control based maximum power point tracking method for photovoltaic system under partial shading conditions using particle swarm optimization algorithm", *Applied Energy*, 99, 414-422, 2012.
- [140] Miyatake, M., Veerachary, M., Toriumi, F., Fujii, N., & Ko, H., "Maximum power point tracking of multiple photovoltaic arrays: A PSO approach", *IEEE Transactions on Aerospace and Electronic Systems*, 47(1), 367-380, 2011.
- [141] Pandey, S., Wu, L., Guru, S. M., & Buyya, R., "A particle swarm optimization-based heuristic for scheduling workflow applications in cloud computing environments", "Advanced information networking and applications (AINA)", 2010 24th IEEE international conference on (pp. 400-407). IEEE, April 2010.
- [142] Ahmed, J., & Salam, Z., "A Maximum Power Point Tracking (MPPT) for PV system using Cuckoo Search with partial shading capability", *Applied Energy*, 119, 118-130, 2014.
- [143] Wang, J., Jiang, H., Wu, Y., & Dong, Y., "Forecasting solar radiation using an optimized hybrid model by Cuckoo Search algorithm", *Energy*, 81, 627-644, 2015.
- [144] Ahmed, J., & Salam, Z., "A soft computing MPPT for PV system based on Cuckoo Search algorithm", *Power Engineering, Energy and Electrical Drives (POWERENG)*, 2013 Fourth International Conference on (pp. 558-562). IEEE, May 2013.

- [145] Shi, J. Y., Xue, F., Qin, Z. J., Zhang, W., Ling, L. T., & Yang, T., “Improved Global Maximum Power Point Tracking for Photovoltaic System via Cuckoo Search under Partial Shaded Conditions”, *Journal of Power Electronics*, 16(1), 287-296, 2016.
- [146] Miyatake, M., Inada, T., Hiratsuka, I., Zhao, H., Otsuka, H., & Nakano, M., “Control characteristics of a fibonacci-search-based maximum power point tracker when a photovoltaic array is partially shaded”, *Power Electronics and Motion Control Conference, 2004. IPEMC 2004. The 4th International (Vol. 2, pp. 816-821). IEEE, August 2004.*
- [147] Ramaprabha, R., Balaji, M., & Mathur, B. L., “Maximum power point tracking of partially shaded solar PV system using modified Fibonacci search method with fuzzy controller”, *International Journal of Electrical Power & Energy Systems*, 43(1), 754-765, 2012.
- [148] Ramaprabha, R., Mathur, B., Ravi, A., & Aventhika, S., “Modified Fibonacci search based MPPT scheme for SPVA under partial shaded conditions”, *Emerging Trends in Engineering and Technology (ICETET), 2010 3rd International Conference on (pp. 379-384). IEEE, November 2010.*
- [149] Ahmed, N. A., & Miyatake, M., “A novel maximum power point tracking for photovoltaic applications under partially shaded insolation conditions”, *Electric Power Systems Research*, 78(5), 777-784, 2008.
- [150] Bione J., Vilela O. C., Fraidenraich N., “Comparison of the Performance of PV Water Pumping Systems Driven by Fixed, Tracking and V-trough Generators”, *Solar Energy*, 76 (2): 703–711, 2004.
- [151] Tudorache, Tiberiu, Oancea C. D., Kreindler L., “Performance Evaluation of a Solar Tracking PV Panel”, *Bucharest Scientific Bulletin, Series C: Electrical Engineering* 74 (1): 3–10. ISSN: 1454-234x, 2012.
- [152] Hon, Snehal P., Kolte M. T., “FPGA Based Standalone Solar Tracking System”, *International Journal of Scientific and Research Publications*, 3 (10): 1–5, 2013.

- [153] Dhanabal, R., Bharathi V., Ranjitha R., Ponni A., Deepthi S., Mageshkannan P., “Comparison of Efciciencies of Solar Tracker Systems with Static Panel Single Axis Tracking System and Dual Axis Tracking System with Fixed Mount”, *International Journal of Engineering and Technology (IJET)*, 5 (2): 1925–1933, 2013. ISSN: 0975-4024
- [154] Heredia I. L., Moreno J. M., Magalhaes P. H., Cervantes R., Que´me´re´ G., Laurent O., “Inspira’s CPV sun tracking (concentrator photovoltaics)”, Springer, p. 221–51, 2007.
- [155] Zogbi R., Laplaze D., “Design and construction of a sun tracker”, *Solar Energy*, 33(3/4):369–72, 1984.
- [156] Rumala S-S. N., “A shadow method for automatic tracking”, *Solar Energy*, 37(3):245–7, 1986.
- [157] Lynch W. A., Salameh Z. M., “Simple electro-optically controlled dual-axis sun tracker”, *Solar Energy*, 45(2):65–9, 1990.
- [158] Konar A., Mandal A. K., “Microprocessor based automatic sun-tracker”, *IEE Proceedings Part A Physical Science Measurement and Instrumentation Management and Education Reviews*, 138(4):237–41, 1991.
- [159] Koyuncu B., Balasubramanian K., “A microprocessor controlled automatic suntracker”, *IEEE Transactions on Consumer Electronics*, 37(4):913–7, 1991.
- [160] Hamilton S. J., “Sun-tracking solar cell array system”, Bachelor of Engineering Thesis Division of Electrical Engineering. Department of Computer Science & Electrical Engineering, University of Queenzland; October 1999.
- [161] Zeroual A., Raoufi M., Ankrim M., Wilkinson A. J., “Design and construction of a closed loop sun-tracker with microprocessor management”, *Solar Energy*, 19(4):263–74, 1998.
- [162] Kalogirou S. A., “Design and construction of a one-axis sun-tracking”, *Solar Energy*, 57(6):465–9, 1996.

- [163] Khalifa A-J. N., Al-Mutawalli S. S., “Effect of two-axis sun tracking on the performance of compound parabolic concentrators”, *Energy Conversion and Management*, 39(10):1073–9, 1998.
- [164] Abouzeid M., “Use of a reluctance stepper motor for solar tracking based on a programmable logic array (PLA) controller”, *Renewable Energy*, 23: 551–60, 2001.
- [165] Abdallah S., Nijmeh S., “Two axes sun tracking system with PLC control”, *Energy Conversion and Management*, 45:1931–9, 2004.
- [166] Contreras A., Garcia J., Gonzalez C., Martinez E., “Portable solar tracker”, Final Presentation, May 08, 2006. URL: <http://engineering.utsa.edu>
- [167] Lakeou S., Ososanya E., Latigo B. O., Mahmoud W., Karanga G., Oshumare W., “Design of a low-cost digital controller for a solar tracking photo-voltaic (PV) module and wind turbine combination system”, In: 21st European PV Solar Energy Conference, Dresden/Germany, September 2006.
- [168] Hatfield P., “Low cost solar tracker”, Bachelor of Electrical Engineering Thesis, Department of Electrical and Computer Engineering, Curtin University of Technology; October 2006.
- [169] Jinayim T., Arunrungrasmi S., Tanitteerapan T., Mungkung N., “Highly efficient low power consumption tracking solar cells for white LED-based lighting system”, *International Journal of Electrical Computer and Systems Engineering*, 1(2):1307–5179, 2007.
- [170] Aiuchi K., Yoshida K., Onozaki M., Katayama Y., Nakamura M., Nakamura K., “Sensor-controlled heliostat with an equatorial mount”, *Solar Energy*, 80:1089–97, 2006.
- [171] Gagliano S., Savalli N., Tina G., Pitrone N., “Two-axis sun tracking system: design and simulation”, In: *Eurosun 2006*, 2006.
- [172] Palavras I., Bakos G. C., “Development of a low-cost dish solar concentrator and its application in zeolite desorption”, *Renewable Energy*, 3:2422–31, 2006.

- [173] Rumyantsev V. D., Concentrator Photovoltaics, Chapter: “Terrestrial concentrator PV systems”, p. 151–74, 2007. URL: <http://www.springerlink.com/content/r7244751j441832v/>
- [174] Abdallah S., “The effect of using sun tracking systems on the voltage–current characteristics and power generation of flat plate PV”, Energy Conversion and Management, 45:1671–9, 2004.
- [175] Rosell J. I., Vallverdu X., Lecho M. A., Ibanez M., “Design and simulation of a low concentrating PV/thermal system”, Energy Conversion and Management, 46:3034–46, 2005.
- [176] Huang B. J., Sun F. S., “Feasibility study of one-axis three positions tracking solar PV with low concentration ratio reflector”, Energy Conversion and Management, 48:1273–80, 2007.
- [177] Edwards B. P., “Computer based sun following system”, Solar Energy, 21:491–6, 1978.
- [178] Davies P.A., “Sun tracking mechanism using equatorial and ecliptic axes”, Solar Energy, 50(6):487–9, 1993.
- [179] AL-Jumaily K. E. J., AL-Kaysi M. K. A., “The study of the performance and efficiency of flat linear Fresnel lens collector with sun tracking system in Iraq”, Renewable Energy, 14(14):41–8, 1998.
- [180] Nuwayhid R. Y., Mrad F., Abu-Said R., “The realization of a simple solar tracking concentrator for university research applications”, Renewable Energy, 24:207–22, 2001.
- [181] Blanco-Muriel M., Alarcon-Padilla D. C., Lopez- Moratalla T., Lara-Coira M., “Computing the solar vector”, Solar Energy, 70(5):431–41, 2001.
- [182] Alata M., Al-Nimr M. A., Qaroush Y., “Developing a multipurpose sun tracking system using fuzzy control”, Energy Conversion and Management, 46:1229–45, 2005.

- [183] Canada J., Utrillas M. P., Lozano J. A. M., Pedros R., Amo J. L. G., Maj A., “Design of a sun tracker for the automatic measurement of spectral irradiance and construction of an irradiance database in the 330–1100 nm range”, *Renewable Energy*, 32:2053–68, 2007.
- [184] Aliman O., Daut I., Isa M., Adzman M. R., “Simplification of sun tracking mode to gain high concentration solar energy”, *American Journal of Applied Sciences*, 4(3):171–5, 2007.
- [185] Abdallah S., Badran O. O., “Sun tracking system for productivity enhancement of solar still”, *Desalination*, 220:669–76, 2008.
- [186] Khlaichom P., Sonthipermpon K., “Optimization of solar tracking system based on genetic algorithms”, 3rd Conference of the Energy Network of Thailand, May 2007. <http://www.thaiscience.info/>
- [187] Poulek V., Libra M., “New bifacial solar trackers and tracking concentrators”, 2007. <http://www.solar-trackers.com>
- [188] Poulek V., Libra M., “A very simple solar tracker for space and terrestrial applications”, *Solar Energy Materials & Solar Cells*, 60:99–103, 2000.
- [189] Karimov KhS., Saqib M. A., Akhter P., Ahmed M. M., Chatthad J. A., Yousafzai S. A., “A simple photo-voltaic tracking system”, *Solar Energy Materials & Solar Cells*, 87:49–59, 2005.
- [190] Poulek V., Libra M., “New solar tracker”, *Solar Energy Materials and Solar Cells*, 51:113–20, 1998.
- [191] Hession P. J., Bonwick W. J., “Experience with a sun tracker”, *Solar Energy*, 32(1):3–11, 1984.
- [192] Saxena A.K., Dutta V., “A versatile microprocessor based controller for solar tracking”, New Delhi, India: Photovoltaic Laboratory, Centre for Energy Studies, Indian Institute of Technology, p. 1105–9, 1990.

- [193] Durisch W., Urban J., Smestad G., “Characterization of solar cells and modules under actual operating conditions”, WREC, In: Proceedings of the WREC-IV world renewable energy congress, p. 359–66, 1996.
- [194] Ajay K., Nagaraju J., “Micro-controller based sun tracker for line focus concentrating collectors”, Journal of the Solar Energy Society of India, 13(1&2):1–8, 2003.
- [195] Luque-Heredia I., Gordillo F., Rodriguez F., “A PI based hybrid sun tracking algorithm for photovoltaic concentration”, In: Proceedings of the 19th European PV solar energy conference and exhibition, 2004.
- [196] Georgiev A., Roth P., Olivares A., “Sun following system adjustment at the UTFSM”, Energy Conversion and Management, 45:1795–806, 2004.
- [197] Roth P., Georgiev A., Boudinov H., “Cheap two-axis sun following device”, Energy Conversion and Management, 46:1179–92, 2005.
- [198] Roth P., Georgiev A., Boudinov H., “Design and construction of a system for sun tracking”, Renewable Energy, 29:393–402, 2004.
- [199] Bakos G. C., “Design and construction of a two-axis sun tracking system for parabolic trough collector (PTC) efficiency improvement”, Renewable Energy, 31:2411–21, 2006.
- [200] Rubio F. R., Ortega M. G., Gordillo F., Lopez-Martinez M., “Application of new control strategy for sun tracking”, Energy Conversion and Management, 48:2174–84, 2007.
- [201] Pickard, W. F., Shen, A. Q., & Hansing, N. J., “Parking the power: Strategies and physical limitations for bulk energy storage in supply–demand matching on a grid whose input power is provided by intermittent sources”, “Renewable and Sustainable Energy Reviews”, 13(8), 1934-1945, 2009.
- [202] Sukhatme, K., & Sukhatme, S. P., “Solar energy: principles of thermal collection and storage”, Tata McGraw-Hill Education, 1996.

- [203] Schoenung, S. M., Eyer, J. M., Iannucci, J. J., & Horgan, S. A., "Energy storage for a competitive power market", "Annual review of energy and the environment", 21(1), 347-370, 1996.
- [204] Dell, R. M., & Rand, D. A. J., "Energy storage—a key technology for global energy sustainability", "Journal of Power Sources", 100(1), 2-17, 2001.
- [205] Schainker, R. B., "Executive overview: energy storage options for a sustainable energy future", In Power Engineering Society General Meeting, 2004. IEEE (pp. 2309-2314). IEEE, June, 2004.
- [206] Van der Linden, S., "Bulk energy storage potential in the USA, current developments and future prospects", "Energy", 31(15), 3446-3457, 2006.
- [207] Ibrahim, H., Ilinca, A., & Perron, J., "Energy storage systems-characteristics and comparisons", "Renewable and sustainable energy reviews", 12(5), 1221-1250, 2008.
- [208] Aliexpress, Universal Solar Panel Charging Regulator, <https://www.aliexpress.com> , Accessed 03.08.2017.
- [209] <https://www.direnc.net/12v-10rpm-90c-reduktorlu-motor-9675> , Accessed 03.08.2017.
- [210] Weisstein, E. W., "Spherical Coordinates", MathWorld--A Wolfram Web Resource. <http://mathworld.wolfram.com/SphericalCoordinates.html> , Accessed 29.07.2017.
- [211] Weisstein, E. W., "Cylindrical Coordinates", MathWorld, <http://mathworld.wolfram.com/CylindricalCoordinates.html> , Accessed 29.07.2017.
- [212] https://vwww.org/sites/default/files/imagecache/large/images/Cylindrical_coordinate_system.svg.png , Accessed 29.07.2017.
- [213] <http://www.seos-project.eu/modules/laser-rs/images/coordinates-spherical.png> , Accessed 29.07.2017.
- [214] <http://cdselectronics.com/kits/solartracker.htm> , Accessed 30.07.2017

- [215] <https://engmousaalkaabi.blogspot.com.tr/2015/05/solar-tracker-circuit.html> , Accessed 30.07.2017.
- [216] <http://www.alldatasheet.com/datasheet-pdf/pdf/17871/PHILIPS/LM324.html> , Accessed 05.08.2017.
- [217] <http://www.alldatasheet.com/> , Accessed 06.08.2017.
- [218] <http://www.mextechin.com/?product=digital-lux-meter-model-lx-1010b> , Accessed 06.08.2017.
- [219] http://articulo.mercadolibre.cl/MLC-435468340-luxometro-lx1010b-de-alta-precision-_JM , Accessed 03.08.2017.
- [220] Electromagnetic Spectrum, Introduction to Remotes Sensing, Humboldt State University, http://gsp.humboldt.edu/olm_2015/Courses/GSP_216_Online/lesson1-2/spectrum.html , Accessed 03.08.2017.
- [221] ÇAĞLAR, A., Yamali, C., Baker, D. K., & KAFTANOĞLU, B., “Measurement of solar radiation in Ankara, Turkey”, *Isi Bilimi ve Teknigi Dergisi/Journal of Thermal Science & Technology*, 33(2), 2013.
- [222] Berkeley University, Lecture slides, Web address: http://bccp.berkeley.edu/o/Academy/workshop08/08%20PDFs/Inv_Square_Law.pdf , Accessed 13.08.2017.

CURRICULUM VITAE

PERSONAL INFORMATION

Name Surname: Mustafa Latif ÇOBANKAYA

Date of Birth: 05.05.1988

Phone: +90 541 525 45 99

E-mail: latifcobankaya@gmail.com



EDUCATION

Highschool: Özel Büyükkoyuncu Fen Lisesi

Bachelor of Science: İhsan Doğramacı Bilkent University

WORK EXPERIENCE

Research Assistant in Yıldırım Beyazıt University, 2015-...

TOPICS OF INTEREST

- Solar Systems
- Sun Tracking Systems
- Optoelectronics
- Materials Science